UNIVERSIDADE FEDERAL DE PERNAMBUCO
CENTRO DE TECNOLOGIA E GEOCIÊNCIAS
DEPARTAMENTO DE GEOLOGIA
PROGRAMA DE PÓS-GRADUAÇÃO EM GEOCIÊNCIAS

CAIO CEZAR GARNIER BRAINER

GEOLOGIA, PETROLOGIA E GEOQUÍMICA DE GRANITOS A DUAS MICAS E BIOTITA GRANITOS NA PROVÍNCIA BORBOREMA: CONTRIBUIÇÃO AO CONHECIMENTO DA OROGÊNESE BRASILIANA

Recife
2021

CAIO CEZAR GARNIER BRAINER

GEOLOGIA, PETROLOGIA E GEOQUÍMICA DE GRANITOS A DUAS MICAS E BIOTITA GRANITOS NA PROVÍNCIA BORBOREMA: CONTRIBUIÇÃO AO CONHECIMENTO DA OROGÊNESE BRASILIANA

Dissertação apresentada ao Programa de Pós-Graduação em Geociências da Universidade Federal de Pernambuco, como requisito parcial para obtenção do título de Mestre em Geociências. Área de concentração: Geoquímica, Geofísica e Evolução Crustal.

Orientadora: Profª Drª Ignez de Pinho Guimarães

Coorientador: Prof. Dr. Adejardo Francisco da Silva Filho

Recife

2021

Catalogação na fonte:
Bibliotecário Carlos Moura, CRB-4 / 1502

B814g Brainer, Caio Cezar Garnier.
Geologia, petrologia e geoquímica de granitos a duas micas e biotita granitos na Província Borborema: contribuição ao conhecimento da orogênese Brasiliana. / Caio Cezar Garnier Brainer. – 2021.
123 f.: il.

Orientadora: Profa. Dra. Ignez de Pinho Guimarães.
Coorientador: Prof. Dr. Adejardo Francisco da Silva Filho.
Dissertação (mestrado) – Universidade Federal de Pernambuco. CTG. Programa de Pós-Graduação em Geociências, 2021.
Inclui referências, apêndice e anexos.

1. Geociências. 2. Granitos peraluminosos. 3. Província Borborema. 4. Termobarometria. 5. Geoquímica. 6. Geocronologia. I. Guimarães, Ignez de Pinho (orientadora). II. Silva Filho, Adejardo Francisco da (coorientador). III. Título.

550 CDD (22. ed.)

UFPE
BCTG/2022-237

CAIO CEZAR GARNIER BRAINER

GEOLOGIA, PETROLOGIA E GEOQUÍMICA DE GRANITOS A DUAS MICAS E BIOTITA GRANITOS NA PROVÍNCIA BORBOREMA: CONTRIBUIÇÃO AO CONHECIMENTO DA OROGÊNESE BRASILIANA

Dissertação apresentada ao Programa de Pós-Graduação em Geociências da Universidade Federal de Pernambuco, Centro de Tecnologia e Geociências, como requisito para a obtenção do título de Mestre em Geociências. Área de concentração: Geoquímica, Geofísica e Evolução crustal.

Aprovado em: 07/07/ 2021.

BANCA EXAMINADORA

_____

Profª Drª Ignez de Pinho Guimarães (Orientadora)
Universidade Federal de Pernambuco - UFPE

_____

Prof. Dr. Sérgio Pacheco Neves (Examinador Interno)
Universidade Federal de Pernambuco – UFPE

_____

Profª Drª Maria de Lourdes da Silva Rosa (Examinadora Externa)
Universidade Federal de Sergipe – UFS

Esta dissertação é dedicada a todos aqueles que acreditaram em mim, até quando eu duvidei.

AGRADECIMENTOS

Agradeço a CAPES pelo financiamento fornecido através da bolsa de estudos e ao CNPq pelo financiamento das análises e tornar este projeto possível.

Agradeço aos meus orientadores, Professora Ignez e Professor Adejardo, por todo o acompanhamento e disponibilidade durante o mestrado assim como toda paciência (A Professora Ignez que o diga).

Agradeço a todos os professores e colegas do departamento pela ajuda e troca de conhecimentos dispensada, aos amigos do grupo de pesquisa (GEG), a Jefferson pela companhia ao longo de todos os campos, Zé pela ajuda com o inglês e a Douglas.

Aos caros amigos que me acompanham desde a graduação, A Bianca, Gisely e Lais (Valeu pela ajuda com o Abstract!).

Um agradecimento especial para minha mãe Patrícia e minha avó Zuleide, que embora não entendam nada do que estudo sempre me motivaram a acreditar em mim mesmo, a meu pai Paulo e ao meu falecido avô Aluízio, que sempre contribuíram para minha permanência na universidade.

RESUMO

Leucogranitos peraluminosos são rochas tidas como características de ambientes colisionais, sendo considerados como produtos oriundos de fusão parcial da crosta continental. A presença de leucogranitos peraluminosos abrange todos os setores da Província Borborema, estando em maior quantidade na Subprovíncia Sul. O pluton Quipapá, situado no domínio Pernambuco – Alagoas, é caracterizado como um leucogranito a duas micas, formado essencialmente por quartzo, k-feldspato, plagioclásio, muscovita e biotita. A química mineral do pluton Quipapá é caracterizada por cristais de muscovita de caráter primário, biotita peraluminosa e rica na molécula annita. Dados termobarométricos apontam para uma cristalização em temperaturas < 800 °C e pressões variando entre 4 a 7,8 Kbar, indicando alojamento em níveis crustais rasos e sob baixa fugacidade de oxigênio. Geoquimicamente as rochas são caracterizadas como peraluminosas, ferrosas e álcali-cálcicas formadas através de fusão por desidratação de muscovita em rochas metapelíticas. Os dados U-Pb em zircão indicam uma idade de cristalização de 641 ± 5 Ma associada ao estágio compressional da orogênese Brasiliana no domínio Pernambuco – Alagoas, tendo shear heating como a provável fonte de calor para sua gênese. O pluton Mamanguape, localizado na subprovíncia central, também é caracterizado como um leucogranito a duas micas. É caracterizado como um granito peraluminoso, de caráter ferroso e assinatura álcali - cálcica, com idade de cristalização de 574 ± 2 Ma obtida por U-Pb em zircão e valores εHf variando entre +1,5 e -13,7 com idades TDM entre 1,4 a 2,2 Ga indicando uma possível mistura de material crustal Paleoproterozóico com material mantélico juvenil. A compilação e comparação dos dados petrográficos, geoquímicos e geocronológicos dos diversos plutons leucograníticos presentes em todos os setores da Província Borborema apontam para um grupo coeso de rochas de caráter peraluminoso, majoritariamente ferroso e variando entre álcali-cálcicas a cálcio-alcalinas com temperaturas < 800 °C. Os aspectos petrogenéticos apontam para fontes heterogêneas, com protólitos variando de metapelitos e metagrauvacas. Os diferentes intervalos de idade apontam para os diferentes estágios da orogênese Brasiliana – Pan-Africana, abrangendo desde o pico do estágio contracional.

Palavras chave: granitos peraluminosos; Província Borborema; termobarometria; geoquímica; geocronologia.

ABSTRACT

The peraluminous leucogranites rocks are characteristic of collisional environments, being considered as products derived from partial melting of the continental crust. The presence of peraluminous leucogranites covers all sectors of the Borborema Province, being found in greater quantity in the Southern Subprovince. The Quipapá pluton, located in the Pernambuco-Alagoas Domain, is characterized as a two micas leucogranite, formed essentially by quartz, k-feldspar, plagioclase, muscovite, and biotite. The mineral chemistry of the Quipapá pluton is characterized by muscovite crystals as a primary character, and peraluminous biotite enriched in the annite molecule. Thermobarometric data points to crystallization at temperatures below 800° C and pressures ranging from 4 to 7.8 Kbar, indicating accommodation in shallow crustal levels and under low oxygen fugacity. Geochemically, the rocks are characterized as peraluminous, ferrous, and alkali-calcium formed through melting by dehydration of muscovite in metapelites rocks. The U-Pb data in zircon indicates a crystallization age of 641 ± 5 Ma associated with a compressional stage of the Brasiliano orogenesis in the Pernambuco-Alagoas domain, having the shear heating as the probable source of heat for its genesis. The Mamanguape pluton, located in the central subprovince, is also characterized as a two-mica leucogranite whose mineralogy is similar to the various peraluminous leucogranites of the Borborema Province. It is characterized as a peraluminous granite of ferrous character and alkali-calcium signature, with a crystallization age of 574 ± 2 Ma obtained by U-Pb in zircon, and εHf values varying between +1.5 and -13.7, and TDM ages between 1.4 to 2.2 Ga indicating a possible mixture of Paleoproterozoic crustal material with juvenile mantle material. The compilation and comparison of the petrographic, geochemical, and geochronological data of the various leucogranites plutons existent in all sectors of the Borborema Province point to a cohesive group of peraluminous rocks, mostly ferrous, ranging from alkali-calcium to calcium-alkaline with temperatures <800° C. Petrogenetic aspects point to heterogeneous sources, with protoliths varying from metapelites and metagraywackes. The different age ranges point to different stages of the Brasiliano-Pan-African orogenesis, encompassing from the peak of the contractional stage to the transcurrent stage.

Keywords: peraluminous leucogranites; Borborema Province; thermobarometry; geochemistry; geochronology.

LISTA DE FIGURAS

SUMÁRIO

1 INTRODUÇÃO

1.1 GRANITOS E SUAS CLASSIFICAÇÕES

Os granitos são as rochas mais abundantes na crosta continental superior (WEDEPOHL, 1991), sendo caracterizados em um sentido amplo como rochas plutônicas constituídas majoritariamente por quartzo, K-feldspato e plagioclásio.

Diversos são os processos presentes na literatura responsáveis pela origem de rochas de composição granítica, sendo os principais: Fusão parcial de rochas da crosta continental (JOHANNES; HOLTZ, 1996; STEVENS; CLEMENS, 1993), cristalização fracionada originada através de magmas basálticos primários (BOWEN, 1948) e mistura entre magmas crustais e mantélicos (PITCHER, 1993; YOUNG, 2003).

Diversos são os esquemas que ao longo dos anos que tentam caracterizar as rochas graníticas de acordo com seu conteúdo mineralógico ou petrográfico, a exemplo da classificação QAP (STRECKEISEN, 1976), baseada nas proporções volumétricas de quartzo, plagioclásio e K feldspato, ou em seus aspectos geoquímicos (eg. BARBARIN, 1999; CHAPPELL, B. W.; WHITE, 1974; FROST et al., 2001; KILPATRICK; ELLIS, 1992; LOISELLE; WONES, 1979; WHITE, 1979).

A norma CIPW proposta por (CROSS et al., 1902) foi uma das primeiras metodologias utilizada para caracterizar rochas ígneas com base em suas composições químicas.

Utilizando esquemas químicos desprovidos de relações petrogenéticas ou tectônicas Frost et al., (2001), utilizou relações como Fe* (FeOt/FeOt+MgO), $Na_2O + K_2O – CaO$ (MALI) e o índice de saturação em alumina (ISA) corrigido para apatita utilizando as razões moleculares [Al/(Ca – 1,67P + Na + K)] para subdividir os granitos entre: (**a**) ferrosos e magnesianos; (**b**) cálcicos, cálcio-alcalinos, álcali-cálcicos e alcalinos; (**c**) peraluminosos, metaluminosos e peralkalinos.

Um dos primeiros esquemas para classificação petrogenética foi proposto por Chappell e White (1974) baseado em aspectos mineralógicos, geoquímicos e aspectos de campo, dividindo os granitos em dois tipos: Tipo I e tipo S. Os granitoides do tipo I e S foram caracterizados como sendo originados através de fontes contrastantes e características distintas (Tab. 1). De acordo com as observações de Chappell e White (1974), os granitos do tipo I são caracterizados geoquimicamente como sendo relativamente sódicos, metaluminosos e apresentando uma ampla variação em seu teor de SiO_2 enquanto os granitoides do tipo S seriam relativamente potássicos, peraluminosos e com teor de SiO_2 restrito a altos valores.

Tabela 1 – Divisão dos granitos entre Tipo-I e Tipo-S originalamente apresentada por Chappell e White (1974)

Tipo - I	**Tipo - S**
Sódio relativamente alto, Na_2O > 3,2% nas variedades felsicas e < 2,2% nas mais máficas	Sódio relativamente Baixo, Na_2O < 3,2% em rochas com K_2O com valores aproximados de 5%, caindo para 2,2% em rochas com 2% de K2O
Razão Molar Al_2O_3/Na_2O+K_2O+CaO < 1,1	Razão Molar Al_2O_3/Na_2O+K_2O+CaO > 1,1
Diopsidio CIPW normativo ou < 1% de coríndon normativo	Coríndon normativo > 1%
Ampla variação composicional (variando entre máfica e felsica)	Composições restritas a altos teores de SiO_2
Variações intra elementos regulares no interior dos plutons; diagramas com variação linear ou não linear	Diagramas com variações irregulares

Chappel e White (1974)

Um outro tipo de granitoide foi proposto por Loiselle e Wones (1979), chamado de granitos tipo A, relacionados a magmatismo em zonas de rift ou no interior de blocos continentais estáveis e sendo caracterizados geoquimicamente como relativamente potássicos, apresentando altas razões de $FeO_t/(FeO_t+MgO)$, teores elevados de HFSE e ETR (com exceção de Eu).

Dois outros tipos de granitos foram adicionados posteriormente a classificação SIMA, sendo os granitos do tipo M e C. Os granitos tipo M foram descritos por White (1979) como sendo granitos oriundos de fontes mantélicas, especificamente crosta oceânica subductada, com características geoquímicas de ambiente de arco (ALONSO-PEREZ; MÜNTENER; ULMER, 2009) através de processos de diferenciação enquanto os granitos tipo C, ou charnockiticos ígneos, foram descritos como por Kilpatrick e Ellis (1992) como granitoides distintos possuindo alto teor de K_2O, TiO_2, P_2O_5, elementos litófilos de raio grande (LILE) e baixos teores de CaO.

Barbarin (1999) propôs uma classificação baseada em aspectos mineralógicos, petrográficos e relação com ambientes geodinâmicos, identificando seis tipos de granitos distintos: granitos peraluminosos com muscovita (**MPG**), biotita granitos peraluminosos com cordierita (**CPG**), granitoides cálcio-alcalinos ricos em K (**KCG**), granitoides cálcio-alcalinos com anfibólio (**ACG**), granitoides toleiticos de arco e de dorsal oceânica (**ATG e RTG**), granitoides alcalinos e peralcalinos **(PAG)** (Tab. 2).

Tabela 2 – Tabela relacionando os tipos petrogenéticos, suas origens e ambientes geodinâmicos

Granitóides		Origem	Ambiente geodinâmico
Granitos peraluminosos com muscovita	**MPG**	**Origem crustal**	**Colisão continental**
Granitos peraluminosos com cordierita	**CPG**	Granitoides peraluminosos	
Granitoides cálcio-alcalinos ricos em K	**KPG**	**Origem mista (Crosta + Manto)**	**Regimes transicionais**
Granitoides cálcio-alcalinos com anfibólio	**ACG**	Granitoides metaluminosos e calcio-alcalinos	**Subducção**
Granitoides toleiticos de arco	**ATG**	**Origem mantélica**	
Granitoides de dorsal oceânica	**RTG**		**Expansão oceânica ou domeamento continental e rifteamento**
Granitoides alcalinos e peralcalinos	**PAG**	Granitoides toleiticos, alcalinos e peralcalinos	

Barbarin (1999)

1.2 LEUCOGRANITOS PERALUMINOSOS

Os leucogranitos peraluminosos são rochas caracterizadas como típicas de orógenos colisionais (BARBARIN, 1996, 1999; NABELEK, 2019). Este grupo de rochas apresentam minerais que muitas vezes são considerados como característicos como muscovita, biotita, granada, cordierita, turmalina, coríndon e topázio (CLARKE, 1981).

Ao longo dos anos receberam diversas nomenclaturas, sendo classificados inicialmente como granitos Tipo-S por Chappel e White (1974) e relacionados a fontes sedimentares ou supracrustais (CHAPPEL;WHITE, 1984). Barbarin (1996, 1999) nomeou os granitos peraluminosos em orógenos colisionais como **MPG** e **CPG** baseado na abundancia de muscovita primária ou cordierita (Tab. 2). De acordo Barbarin (1996, 1999) **MPGs** constituem um grupo de granitos ricos em muscovita primária e pequena quantidade de minerais máficos como biotita, raramente apresentando enclaves máficos, restitos micáceos e xenólitos das rochas encaixantes, já os **CPGs** são constituídos por granitos ricos em biotita com presença de minerais máficos como cordierita que podem ocorrer alteradas para muscovita secundária e uma maior proporção de enclaves máficos devido a pequena participação de material mantélico em sua gênese.

De acordo com Frost et al., (2001) leucogranitos compõem um grupo distinto de granitoides peraluminosos (ASI>1), altos valores de SiO_2 (>70%), variando entre a série ferrosa e magnesiana, e com natureza variando de cálcica a alcalina. Para alguns autores como Holtz e Johannes, (1991) a grande variação composicional apresentada por leucogranitos peraluminosos reflete os diferentes protólitos assim como pelas diferentes condições de anatexia. A gênese destes tipos de rocha é frequentemente associada a fusão parcial de litologias crustais (SYLVESTER, 1998; PATIÑO DOUCE; HARRIS, 1998; PATIÑO DOUCE, 1999) através de fusão por desidratação de muscovita (PETÖ, 1976; SPEAR, 1993), biotita (LE BRETON; THOMPSON, 1988) e fusão de muscovita em presença de H_2O (PATIÑO DOUCE; HARRIS, 1998; WEINBERG; HASALOVÁ, 2015).

Patiño Douce (1999) considerou leucogranitos peraluminosos como sendo representantes de magmas oriundos de fontes puramente crustais, formados através de fusão por desidratação de muscovita ou biotita.

1.3 MODELOS TÉRMICOS E ASPECTOS GEODINÂMICOS

A gênese de magmas leocráticos e peraluminosos é frequentemente associada a fusão parcial de rochas metassedimentares em ambientes colisionais. Diversos modelos térmicos são propostos para a origem deste tipo de magmatismo, sendo o principais: (1) Influxo de H_2O; (2) Fusão parcial por descompressão; (3) Litologias com alta produção de calor radiogênico e (4) *Shear heating.*

O influxo de H_2O provoca o rebaixamento das temperaturas da curva do solidus, induzindo ao processo de fusão parcial. De acordo com Weinberg e Hasalová (2015) há diversas mecanismos sob os quais H_2O interage com litologias férteis, sendo elas: (1) Magmas ricos em H_2O liberando fluidos tardi magmáticos em seu processo de cristalização (ANNEN; SPARKS, 2002); (2) Liberação de H_2O de magmas ricos para litologias “secas”; (3) Migração de fluidos provenientes de litologias sofrendo desidratação subsolidus para litologias acima da curva de solidus hidratado (WHITE, R. W.; STEVENS; JOHNSON, 2011) e (4) Percolação advinda de rochas ricas em H_2O sob falhas de empurrão para rochas mais quentes em níveis crustais mais rasos (LE FORT et al., 1987). Em ambientes colisionais fusão por influxo de H_2O geralmente tendem a ocorrer quando rochas de temperaturas mais altas são sobrepostas a rochas mais frias, estas últimas sofrendo desidratação cujos fluidos ascendentes tendem a induzir fusão parcial nas rochas superiores.

Fusão parcial nas porções superiores da crosta continental podem ser induzidas através da descompressão e rápida exumação de rochas infracrustais com temperaturas elevadas, as quais foram soterradas a profundidades superiores a 45 Km durante espessamento crustal e somente após 40 Ma de relaxamento térmico como demonstrado por Nabelek e Liu (2004) em suas modelagens. Thompson e Connolly (1995) apresentam resultados semelhantes, em seu modelo rochas metapelíticas irão sofrer fusão parcial através de desidratação de micas quando soterradas em profundidades superiores a 58 Km.

Soterramento profundo de litologias com produção anômala de calor radiogênico podem induzir fusão parcial nas porções superiores da crosta (HUERTA; ROYDEN; HODGES, 1998). Nabelek e Liu (2004) através de modelagens matemáticas demonstrou que soterramenta de litologias com produção de calor radiogênico mais realísticas (2 $\mu W\ m^{-3}$) somente podem gerar fusão parcial após 50 Ma de soterramento em níveis inferiores da crosta.

Com relação a *shear heating* ou *strain heating*, diversos autores (LELOUP et al., 1999; NABELEK, 2019; NABELEK; LIU, 1999, 2004; NABELEK; LIU; SIRBESCU, 2001; NABELEK; WHITTINGTON; HOFMEISTER, 2010) apresentaram modelos de geração de magmas leucograniticos em orógenos colisionais como consequência da resposta térmica das rochas produzida devido a deformação. A elevação de temperatura em zonas de cisalhamento de escalas litosféricas podem induzir fusão parcial na base da crosta, o que promove injeção de magmas que também irão contribuir para o aumento de temperatura em porções superiores da crosta (LELOUP et al., 1999). Embora haja um equívoco quanto ao *shear heating* ser localizado nas zonas de cisalhamento, de acordo com Nabelek (2019), *shear heating* ocorre com qualquer rocha sob deformação, estando situadas ou não nas proximidade de falhas ou zonas de cisalhamento.

1.4 APRESENTAÇÃO E OBJETIVOS

A presente dissertação é constituída por uma coletânea de artigos submetidos em periódicos internacionais, sendo esta o pré requisito para a obtenção do título de Mestre em Geociências, na área de concentração Geoquímica, Geofísica e Evolução Crustal do Programa de Pós-Graduação em Geociências da Universidade Federal de Pernambuco (UFPE).

O primeiro artigo desta coletânea, submetido ao *Journal of South American Earth Sciences* intitulado *EARLY EDIACARAN TWO MICAS GRANITES MARKING THE BRASILIANO OROGENY CONTRACTIONAL STAGE IN THE PEAL DOMAIN, NE BRAZIL*, consiste na caracterização petrológica do pluton Quipapá através da química mineral,

geoquímica e geocronologia. O trabalho apresenta novas informações sobre os granitos que marcam o ínicio do estágio contracional no Domínio Pernambuco – Alagoas.

O segundo artigo, intitulado *PETROGENESIS OF EDIACARAN LEUCOGRANITES IN THE BORBOREMA PROVINCE, NE BRAZIL: U-Pb ZIRCON GEOCHRONOLOGICAL, GEOCHEMICAL AND Lu-Hf ISOTOPIC DATA CONSTRAINTS* e submetido ao periódico *Brazilian journal of Geology* aborda os aspectos petrológicos e isotópicos do pluton Mamanguape assim como analisa os aspectos geoquímicos e geocronológicos dos diversos leucogranitos peraluminosos e biotita granitos presentes na Província Borborema.

1.5 LOCALIZAÇÃO

A principal área de estudada está localizada na região nordeste do Brasil (Fig. 1a) próxima ao limite entre os estados de Pernambuco e Alagoas, abrangendo os municípios de Quipapá, Jurema e São benedito do Sul. Nesta região, que participa das cartas geológicas Garanhuns (SC-24-X-B-V) e Palmares (SC-25-V-A-VI) foram estudados em etapas de campo os plutos Quipapá e Jurema (Fig. 1b). A segunda área estudada está situada no município de Mamanguape, Paraíba, na folha Guarabira (SB-25-Y-A-V) (Fig. 1b), porém desta região foram utilizados dados previamente adquiridos.

Figura 1 – (a) Localização das áreas de estudo, (b) Localização ampliada das áreas de estudo com destaque para as cartas geológicas regionais.

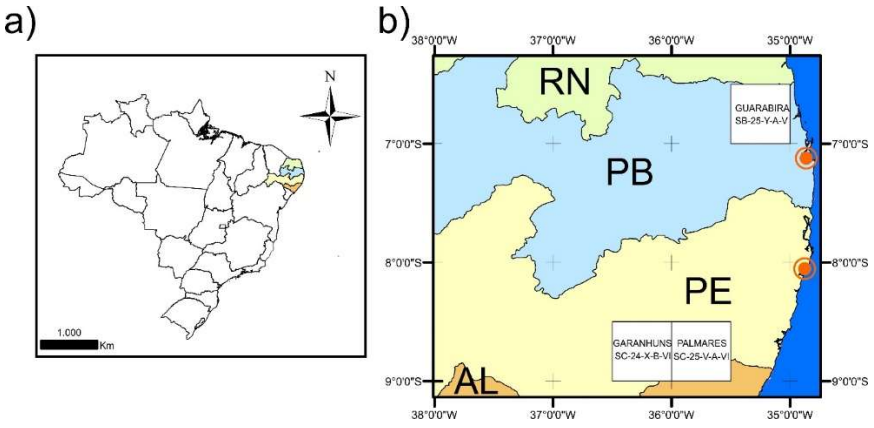

Fonte: Autor

2 MATERIAIS E MÉTODOS

2.1 REVISÃO BIBLIOGRÁFICA

O levantamento bibliográfico realizado ao início da pesquisa teve como objetivo a análise e compilação dos aspectos geológicos, geoquímicos e geocronológicos dos leucogranitos peraluminosos situados em toda a Província Borborema e o contexto tectônico nos quais estão relacionados durante a evolução Neoproterozóica/Brasiliana. Em conjunto a isso foi realizada uma análise bibliográfica acerca dos principais processos relacionados a gênese e evolução de leucogranitos peraluminosos assim como os contextos tectônicos relacionados com este tipo de magmatismo.

Em preparações pré trabalho de campo foram realizadas análises nas folhas Garanhuns (SC-24-X-B-V) e Palmares (SC-25-V-A-VI) em escala de 1:100000 da CPRM, o modelo digital de terreno das regiões e as imagens gamaespectométricas, com o intuito de reconhecimento prévio dos aspectos litológicos e estruturais.

2.2 ETAPAS DE CAMPO

Foram realizadas três etapas de campo entre 2019 e 2020 com o objetivo de adquirir amostras e novos dados sobre geologia das regiões estudadas. Durante o trabalho de campo foram utilizados instrumentos de navegação como bússola, GPS, mapas geológicos regionais e mapa pré trabalho de campo, e materiais para análise petrográfica macroscópica e coleta das amostras (Lupa, imã, canivete e martelo).

2.3 PETROGRAFIA

As amostras coletadas nos plutons Quipapá e Mamanguape que foram selecionadas para a confecção de lâminas petrográficas polidas após uma minunciosa descrição macroscópica foram preparadas no laboratório de laminação da Universidade Federal de Pernambuco (UFPE) e em laboratórios de confecção comercial (GEOLAB). Uma descrição petrográficas detalhada das lâminas foi realizada no Laboratório de Microscopia Ótica da UFPE com o uso de microscópio óptico de luz transmitida, os minerais opacos identificados foram analisados no microscópio de luz refletida do Laboratório de Estudos Metalogenéticos Aplicados da UFPE.

2.4 QUIMICA MINERAL

As seções polidas selecionadas para análises de química mineral, foram enviadas para o laboratório de microssonda eletrônica da Universidade de Brasília (UNB), sendo analisadas em uma microssonda eletrônica JEOL modelo JXA-8230 equipada com cinco espectrômetros WDS e um EDS sob voltagem de aceleração de 15Kv e diâmetro de 10 nÄ.

2.5 LITOGEOQUÍMICA

As preparação das amostras para análises químicas de rocha total foram feitas no Laboratório de Preparação de Amostras do NEG-LABISE na UFPE através de britagem, quarteamento e pulverização em moinho de disco.

Os procedimentos analíticos laboratoriais foram realizados por um espectrômetro de emissão atômica por plasma acoplado indutivamente (ICP-AES) para os elementos maiores e por espectrômetro de massa por plasma acoplado indutivamente (ICP-MS) nos laboratórios ALS na Austrália.

2.6 GEOCRONOLOGIA U-Pb

A preparação das amostras foi realizada no NEGLABISE através da pulverização das rochas selecionadas, e separação através de métodos magnéticos (imãs de Nd e separador FRANTZ) e gravimétricos (Bromofórmio). Os zircões foram separados e selecionados com o auxílio de lupa binocular e preparado um *mount*. As análises U-Pb em zircão foram realizadas no Laboratório de Geoquímica Isotópica da Universidade Federal de Ouro Preto (UFOP) – Setor de Isótopos Radiogênicos após seleção dos pontos (núcleos/bordas) em imagens CL obtidas via microssonda eletrônica de varredura (MEV) em um JEOL 6510. Os dados foram U-Pb obtidos através de ablação a laser por um espectrômetro de massa com setor de campo duplamente focalizado (LA-SF-ICP-MS) Element 2 Thermo Finnigan com um sistema de laser Photon-Machines 193nm acoplado, com diâmetro do feixe do laser de 30 μm.

2.7 ISÓTOPOS Lu-Hf

As análises isotópicas para Lu-Hf também foram realizadas no laboratório de Geoquímica Isotópica da UFOP, de acordo com a metodologia de Matteini et al., (2010) através

de um espectrômetro de massa com fonte de plasma indutivamente acoplada via ablação laser (LA-ICP-MS) utilizando feixes de 40 μm que foram sobrepostos aos de feixes de 30 μm utilizados para as análises U-Pb, ou no mesmo núcleo/borda previamente analisado.

3 GEOLOGIA REGIONAL

A Província Borborema, definida por Almeida et al., (1981) ocupa a maior parte do nordeste do Brasil abrangendo uma área de aproximadamente 450.000 km². É limitada ao norte e a oeste pela Bacia do Parnaíba, ao sul pelo Cráton São Francisco e ao leste pelas bacias costeiras. A Província Borborema representa a parte ocidental de um cinturão localizado na parte noroeste/central de Gondwana (Fig. 1a) formada através da convergência e colisão entre os crátons Oeste da África, Congo-São Francisco e Amazônico durante o Ediacarano ca. 600 Ma. Correlações entre a Província Borborema e os cinturões Pan Africanos são apresentadas em diversos trabalhos (CABY, 1989; CASTAING et al., 1994; CAXITO, F. de A. et al., 2020; BRITO NEVES; CORDANI, 1991; BRITO NEVES; VAN SCHMUS; FETTER, 2002; GANADE et al., 2016; JARDIM DE SÁ, 1984; KALSBEEK et al., 2013; NEVES, 2003; TOTEU et al., 1994, 2001).

De acordo com VAN SCHMUS; KOZUCH; BRITO NEVES, (2011) a estruturação atual da Província Borborema pode ser subdividida em três grandes sub províncias utilizando como limites as zonas de cisalhamento Patos e Pernambuco, dessa forma: a subprovíncia norte, localizada na região ao norte da zona de cisalhamento de Patos; subprovíncia Transversal entre a zona de cisalhamento Patos e a zona de cisalhamento de Pernambuco; e subprovíncia sul, que corresponde a região ao sul da zona de cisalhamento Pernambuco (Fig. 1b).

Figura 2 – (a) Reconstrução preé-drift da América do Sul – África (NEVES et al., 2015); (b) Mapa da Província Borborema com subdivisões propostas por Van Schmus et al., (2011). ND: Domínio Norte; CD: Domínio Central; SD: Domínio Sul

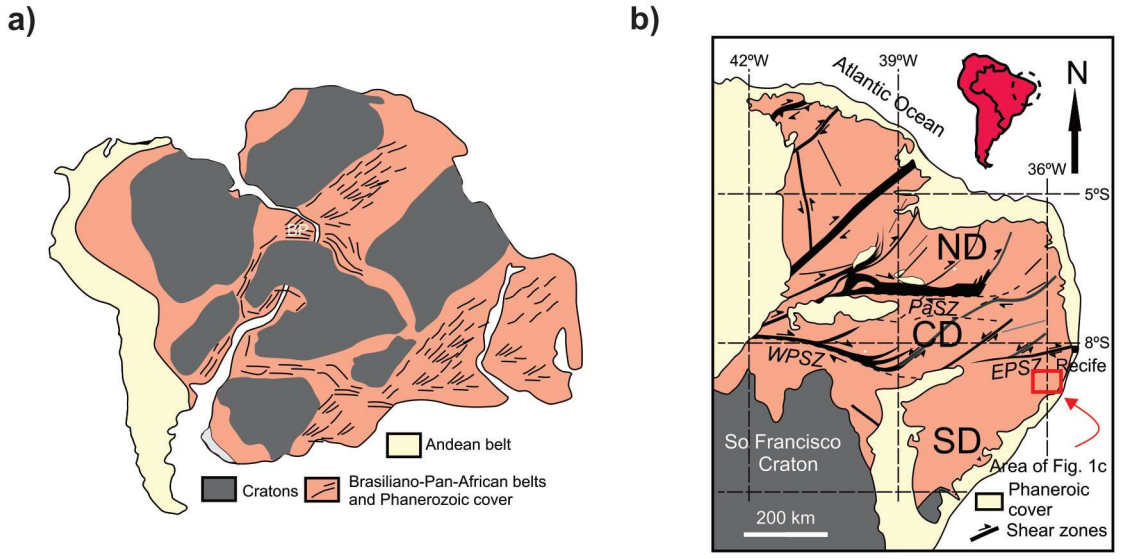

Fonte: Neves et al., (2015)

As características geológicas e estruturais de Província Borborema podem ser sumarizadas em um embasamento paleoproterozoico constituído de gnaisses e migmatitos (1,98 ~ 2,2 Ga) (VAN SCHMUS et al., 1995; VAN SCHMUS; KOZUCH; DE BRITO NEVES, 2011), englobando pequenos blocos arqueanos 3,4-3,1 Ga (DANTAS et al., 1998, 2004; VAN SCHMUS et al., 1995), sequências supracrustais deformadas e metamorfizadas (BRITO NEVES et al., 2001; SANTOS et al., 2010; GUIMARÃES et al., 2012; SANTOS, 1995), além de plutons graníticos neoproterozoicos tonianos a ediacaranos (FERREIRA et al., 2011; FERREIRA; SIAL; JARDIM DE SÁ, 1998; GUIMARÃES et al., 2011; GUIMARÃES et al., 2004; SIAL, 1986; SILVA FILHO et al., 2016) e extensas zonas de cisalhamento de caráter transcorrente e direção NE-SW e E-W, algumas apresentando possíveis continuações com as zonas de cisalhamento do continente Africano (CABY, 1989; CASTAING et al., 1994; CAXITO et al., 2020; OLIVEIRA, E. P. et al., 2006; VAN SCHMUS et al., 2008; VAUCHEZ et al., 1995).

O contexto geodinâmico da província Borborema durante o neoproterozóico é amplamente debatido. Diversos modelos tem sido apresentados, baseados em colagem de terrenos distintos (NEVES et al., 1995; SANTOS, 1995; SANTOS. et al., 2018) em ciclos de Wilson com abertura e fechamento de pequenos oceanos (CAXITO et al., 2014, 2016; GANADE DE ARAUJO; WEINBERG; CORDANI, 2014; OLIVEIRA, Elson P.; WINDLEY; ARAÚJO, 2010) e modelos baseados em derformação e retrabalhamento crustal intracontineltal (NEVES, 2003, 2011, 2015)

O modelo de Santos (1995) propõe que a estruturação atual da província Borborema é resultado de uma colagem de terrenos tectono – estratigráficos distintos durante o neoproterozóico (Toniano - Ediacarano). Neves (2003) sugeriu um modelo tectônico intracontinental no qual a Província Borborema permaneceu como um único grande segmento crustal desde o paleoproterozóico, consistindo essencialmente de retrabalhamento crustal intracontinental. Modelos baseados em um ciclo de Wilson completo foram propostos por Caxito et al., (2014,2016) e Oliveira et al., (2010), com fases convergentes entre o PEAL e o Craton São Francisco ocorrendo entre 630-620 Ma e 630-617 Ma, respectivamente. Ganade de Araujo, Weinberg e Cordani (2014) propõem que a evolução Neoproteróica da Província Borborema como sendo resultado de dois processos colisionais distintos, tendo um processo ocorrido no intervalo de 620 - 610 Ma entre o bloco Paraíba e o embasamento da BP e outro em ca. 590 com a colisão entre Cráton São Francisco e a BP.

O pluton Quipapá, foco principal desta dissertação está localizado no domínio Pernambuco – Alagoas (PEAL), limitado ao norte pela zona de cisalhamento Pernambuco e ao

sul pelo domínio Sergipano. É constituído por rochas meta Vulcano-sedimentares e ortognaisses migmatizados. Através de um mapeamento isotópico Sm-Nd Silva Filho et al., (2014) subdividiu esse domínio em três subdomínios: Garanhuns, Palmares e Agua Branca. O pluton Quipapá ocorre intrudindo as rochas metassedimentares do subdomínio Garanhuns.

O pluton Mamanguape por sua vez, está localizado na subprovíncia central, situada entre as zonas de cisalhamento Patos e Pernambuco. Esta subprovíncia é subdividida nos terrenos ou domínios (SANTOS, 1995; SANTOS; MEDEIROS, 1999; VAN SCHMUS; KOZUCH; DE BRITO NEVES, 2011): Piancó – Alto Brígida (PAB), Alto Pajeú (AP), Alto Moxotó (AM) e Rio Capibaribe (RC). A área no qual o pluton Mamanguape está situado, o domínio Alto Pajeú, que é constituído por sequências metassedimentares e sequencias metavulcanosedimentares intrudidas por granitos Ediacaranos (LEITE et al., 2000).

4 ARTIGO 1 – EARLY EDIACARAN TWO-MICA GRANITES MARKING THE CONTRACTIONAL STAGE OF THE BRASILIANO OROGENY IN THE PERNAMBUCO-ALAGOAS DOMAIN, NE BRAZIL

Brainer, C.C.G.[1]; Guimarães, I.P.[1]; Silva Filho, A.F.[1]; Lima, J.V.[1]; Amorim, J.V.A.[2]

[1]Geosciences Post Graduation Programme - Pernambuco Federal University, Brazil
[2]School of Earth Sciences - University of Western Australia, Australia

ABSTRACT

The two-mica granitoids intrude metasedimentary rocks of the Pernambuco-Alagoas Domain in the Southern subprovince of the Borborema Province. They comprise biotite (<8 %) - muscovite (>10 %), ferroan, alkali-calcic leucogranites. Zircon, apatite, and opaque minerals are the accessory phases. Most of the muscovite grains show high Na, Ti, Alt, and low Si (3.08–3.10 apfu) contents, being considered primary muscovite. Biotite grains have high Fe and Al, and low Mg contents, and Fe# (FeOt/FeOt + MgO) values ranging from 0.68 to 0.79, typical of biotite crystallized from peraluminous magmas. Plagioclase grains show compositional variation within the albite to low oligoclase fields (Ab94An05Or01 - Ab88An11Or01), and the K-feldspar crystals have composition ranging from Or97Ab03 to Or92Ab08. Thermobarometric data point out crystallization at temperatures < 800 ◦C and pressures ranging from 4.2 to 5.0 kbar. High Rb/Ba, Rb/Sr ratios, CaO/Na2O < 0.3, and negative correlation between Rb/Sr with Ba and Sr contents suggest that the studied granitoids magmas were formed by partial melting of metasedimentary sources, through muscovite and biotite dehydration. Shear heating appears to be the main heating source, but radioactive heat and previous basalt underplating could also contribute to increase the crustal temperature. The best candidate to the source of the studied granitoids is the Palmares Sequence metasedimentary rocks, due to similar Nd isotopic signature. Magma evolution was dominated by fractional crystallization of K-feldspar, apatite, ilmenite, and small amount of biotite, under low to middle fO2 (between 0 and + 1 Δ QFM) conditions. The crystallization age, ca. 630 Ma for the studied granitoids, is likely correlated to the peak of the high-T regional metamorphism, that was associated with the contractional stage of the Brasiliano Orogeny.

KEYWORDS: Two-mica granites. Borborema Province. Thermobarometry. Geochemistry. Geochronology.

4.1. INTRODUCTION

Granites are common rocks in the upper continental crust and can be formed in most tectonic settings. Granite generation provides important clues regarding the tectonic regime and crustal evolution processes (Pitcher, 1993). Since granitic rocks show a great diversity of composition, sources, and evolutionary processes, granite genesis is one of the most debated subjects among petrologists. Peraluminous two-mica leucogranites, commonly referred to as S-type granites (Chappell and White, 1974, 2001), are usually described as generated via partial melting of continental crust (eg. Vielzeuf and Montel, 1994; Gardien et al., 1995; Patiño Douce and Harris, 1998). They are prevalent in orogenic belts associated with medium- to high-grade metasedimentary rocks (Nabelek, 2020) and can provide important clues for the growth and reworking/recycling of continental crust.

In the Borborema Province, NE Brazil, the Brasiliano Orogeny (630–540 Ma) was characterized by intense magmatism (Sial, 1986; Ferreira et al., 1998; Brito Neves et al., 2003; Guimarães et al., 2004, 2011; Ferreira et al., 2011; Silva Filho et al. 2014, among others) and large-scale shear zones. Peraluminous leucogranite magmatism occurs in all subprovinces of the Borborema Province. In the Northern subprovince, the granites constitute expressive intrusions of topaz, tourmaline, muscovite leucogranite in the Ceará Central domain, and rare two-mica leucogranite plutons in the Rio Grande do Norte domain. In the Transversal subprovince, they form dyke swarms with less than 6% of modal biotite and have garnet and muscovite as accessory phases. According to Ferreira et al. (1998), the Pernambuco-Alagoas domain has a high incidence of two-mica leucogranite intrusions.

In this work, we present and discuss the mineral chemistry, whole-rock geochemical, and geochronological data from two-mica granites, described in the literature as Quipapá and Jurema plutons, intruded in the Pernambuco-Alagoas Domain, to constrain their crystallization conditions, possible sources, and tectonic setting in the context of the Brasiliano Orogeny.

4.2. REGIONAL CONTEXT

The Borborema Province occupies most of Northeastern Brazil. It is limited to the north and to the west by the Parnaíba basin, to south by the São Francisco Craton, and to east by the

marginal basins. In pre-rift reconstructions (Fig. 1a), the Borborema Province represents an orogenic belt localized in the northwestern-central part of Western Gondwana due to the convergence and collision of West Africa, Congo-São Francisco and Amazonia cratons during the Ediacaran, ca. 600 Ma, Brasiliano–Pan-African Orogeny (Van Schmus et al., 2008; references therein). A plethora of studies attempting correlations between the Borborema Province and Pan-African has been done (Caby et al., 1989; Jardim de Sá, 1984; Toteu et al., 1994, 2001; Brito Neves and Cordani, 1991; Castaing et al., 1993; Trompette, 1997; Brito Neves et al., 2002; Neves, 2003; Kalsbeek et al. 2013, Ganade de Araújo et al., 2016, Caxito et al., 2020). However, the intense deformation, displacement and juxtaposition of distinct domains, the lack of reliable paleomagnetic data, and the patchy distribution of geochronological and geochemical data, leave many gaps concerning the tectonic evolution of the province and its paleogeography.

The Borborema Province comprises: (1) gneiss-migmatite Paleoproterozoic basement (1.98–2.20 Ga) and minor Archean blocks (Van Schmus et al., 1995, 2011; Dantas et al., 1998, 2004, 2013); (2) Neoproterozoic supracrustal sequences (Brito Neves et al., 2001; Santos et al., 2010; Guimarães et al., 2012; Neves et al., 2020); (3) Neoproterozoic magmatism (Tonian to Ediacaran), mostly granitic, (Sial, 1986; Ferreira et al., 1998, 2015; Brito Neves et al., 2003; Guimarães et al., 2004, 2012, 2016; Silva Filho et al., 2016; Neves et al., 2020; among others). The whole Borborema Province is cut by large transcurrent shear zones of NE-SW and E-W trending, with possible continuation in the African continent (Caby, 1989; Casting et al., 1994; Trompette, 1994; Oliveira et al., 2006; Van Schmus et al., 2008; Caxito et al., 2020; Toteu et al., 2001).

Two large shear zones, the E-W-trending Patos and Pernambuco, divided the Borborema Province into three domains (Van Schmus et al., 1995, 2008) or subprovinces (Van Schmus et al., 2011): Northern to the North of Patos shear zone; Transversal between Patos and Pernambuco shear zones and Southern, to the South of the Pernambuco shear zone (Fig. 1b). Each subprovince was divided into domains (Van Schmus et al., 2008). The study area is in the Pernambuco-Alagoas domain of the Southern subprovince (Fig. 1c). However, the Patos shear zone, represents late - stage (ca. 565 Ma) structure of the Brasiliano Orogeny (Viegas et al., 2014; Archanjo et al., 2021), and does not separate distinct blocks. Thus, the terms subprovince and domains, are used here, only as descriptive terms.

The tectonic evolution of the Borborema Province during the Cryogenian-Ediacaran (Brasiliano Orogeny) has been subjected to a long-standing debate. Santos (1996) proposed a model involving accretion of allochthonous terranes during the Neoproterozoic (Tonian and

Ediacaran). The model was followed by many authors (eg., Santos et al., 2000, 2010; Brito Neves et al., 2000; Santos et al., 2017, 2018). In contrast, Neves (2003) proposed an intracontinental orogenic setting with small amount of oceanic crust consumption (Neves, 2003; Neves et al., 2006), in agreement with the suggestion of a continuous basement among the proposed terranes since the Paleoproterozoic (Mariano et al., 2001; Guimarães and Brito Neves, 2004; Neves et al., 2006; references therein). Furthermore, a model consisting of a complete Wilson cycle with rifting, followed by subduction of large oceanic realms and a subsequent collision was also proposed (Oliveira et al., 2010; Caxito et al., 2014; 2020; among others). However, the lack of well-characterized Cryogenian-Ediacaran sutures across the Borborema Province hinder application of this model. Alternatively, Ganade de Araújo et al. (2014) proposed the existence of marginal subduction zones and reworking in an intracontinental setting at the core of the Borborema Province.

Ganade de Araujo et al. (2014) proposed a model to the Neoproterozoic evolution of the Borborema Province (620–570 Ma), which involved two distinct collisional events: 1) Collision between the Parnaiba block (forefront of the Amazonas-West Africa Craton) and the old basement of the Borborema Province, took place at ca. 620–610 Ma, along the west Gondwana Orogen, on the west side of the Borborema Province; 2) Collision between the Borborema Province and the São Francisco Craton at ca. 590–580 Ma, along the Sergipano Orogen. According to Caxito et al. (2016), the collision between the São Francisco Craton (lower plate) and the Pernambuco-Alagoas Domain (PEAL) (upper plate) ca. 620–590 Ma, was responsible for crustal thickening, deformation, metamorphism, melt generation and intrusion of syn-collisional two-mica granites, corresponding to the Rajada orthogneiss protolith at ca. 610 Ma (Brito Neves et al., 2015). However, as pointed out by Caxito et al. (2020), diachronism of events appears to be a rule during the Cryogenian-Ediacaran evolution of the Borborema Province, while convergence was taking place in some areas, others were under extension, transcurrence or collision.

Figura 3 – Figure 1 – a) Pre-drift reconstruction of South América – Africa (Neves et al., 2015); (b) Borborema Province map with the subdivisions proposed by Van Schmus et al., (2011) (c) Simplified geologic map of the studied area. RCSZ: Rio da Chata shear zone, RSZ: Ribeirão shear zone.

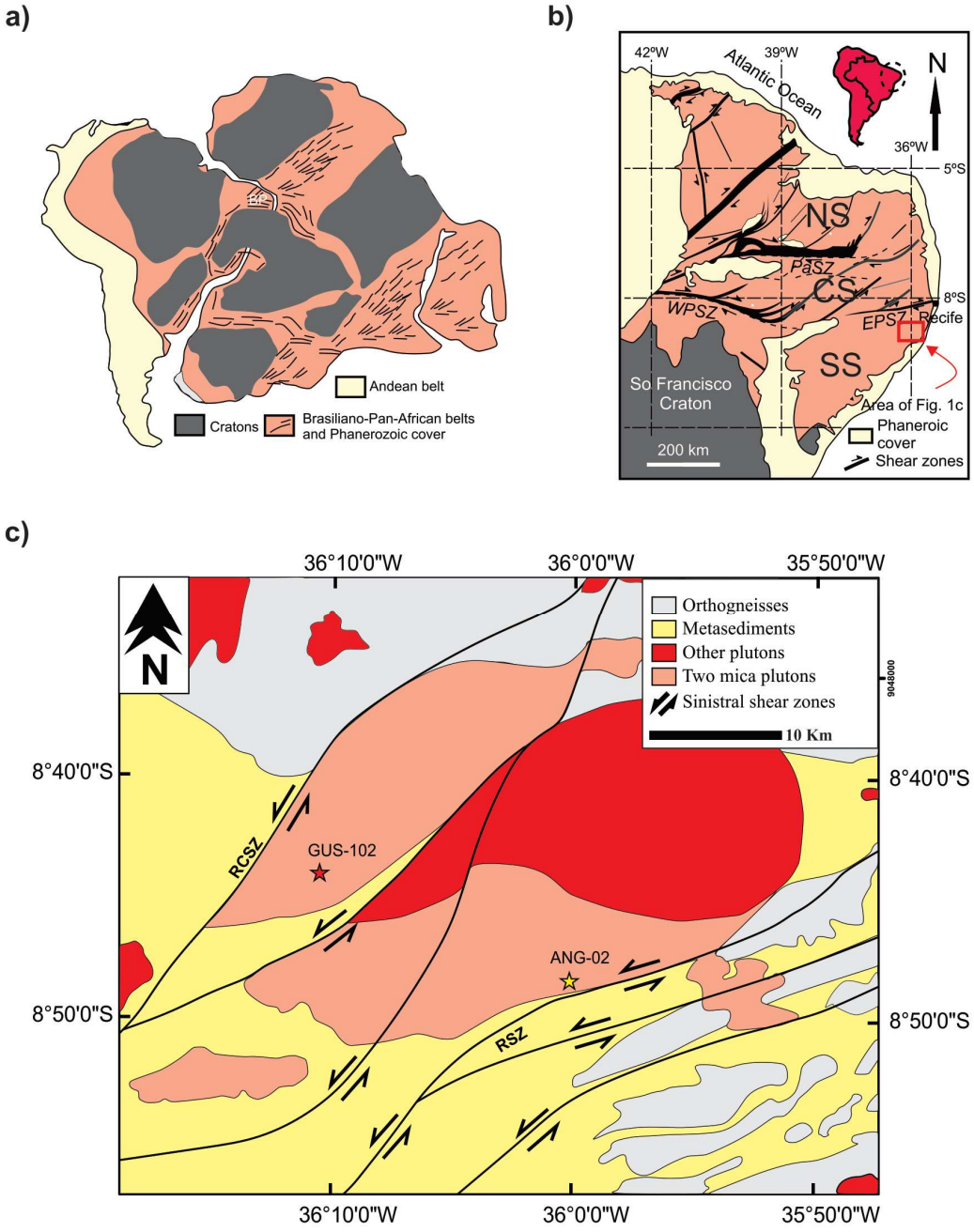

The eastern part of the PEAL has the largest number of Ediacaran intrusions than other Borborema Province domains. The supracrustal sequences comprise garnet biotite gneisses, quartzites and calc-silicate rocks and amphibolite, described as comprising the Cabrobó Complex (Santos, 1996; Medeiros, 1998). The Belem do São Francisco Complex consists of migmatized orthogneisses with composition ranging from granite to tonalite. Silva Filho et al.

(2014), divided the PEAL domain into three crustal subdomains based on Sm-Nd isotopic data: Garanhuns, Água Branca and Palmares. The Quipapá Pluton intrudes rocks of the Garanhuns crustal subdomain.

4.3. LOCAL GEOLOGY AND PETROGRAPHY

The studied granitoids are referred in the literature as Quipapá and Jurema pluton. However, no field and petrographic distinctions are available for which the studied granitoids are going to be referred as the Quipapá granites.

The Quipapá granites form an elongated body with the main axes trending E-W and NE-SW respectively, intruded in migmatized biotite-gneisses and schists of the Palmares metasedimentary rocks, between the Ribeirão and Rio da Chata shear zones (Fig. 1c). The granitoids are medium- to fine-grained, equigranular to slightly porphyritic, felsic syenogranites in composition, with biotite as the main mafic mineral phase. In macroscale, two petrographic facies are distinguished by the modal percentage of biotite ± white mica. The late facies is characterized by < 3% of modal biotite, modal muscovite ~ 7%, lack or rare zircon grains, whereas in the other facies, biotite comprises 6 to 7%, and muscovite 10% to 12% of the modal compositions. Polygonal country rocks xenoliths are common, suggesting that the melts were not generated by in situ partial melting.

Figura 4 – Figure 2 – Petrographic aspects of the Quipapa granites (a) Quartz crystals (Qtz) with lobate texture and sericitized plagioclase; (b) K - feldspars (Kf) phenocrysts with flame perthite texture and myrmekite; (c) Deformed muscovite crystal (Ms); (d) Biotite (Bt) and Muscovite (Ms) crystals associated with anhedral opaque minerals.

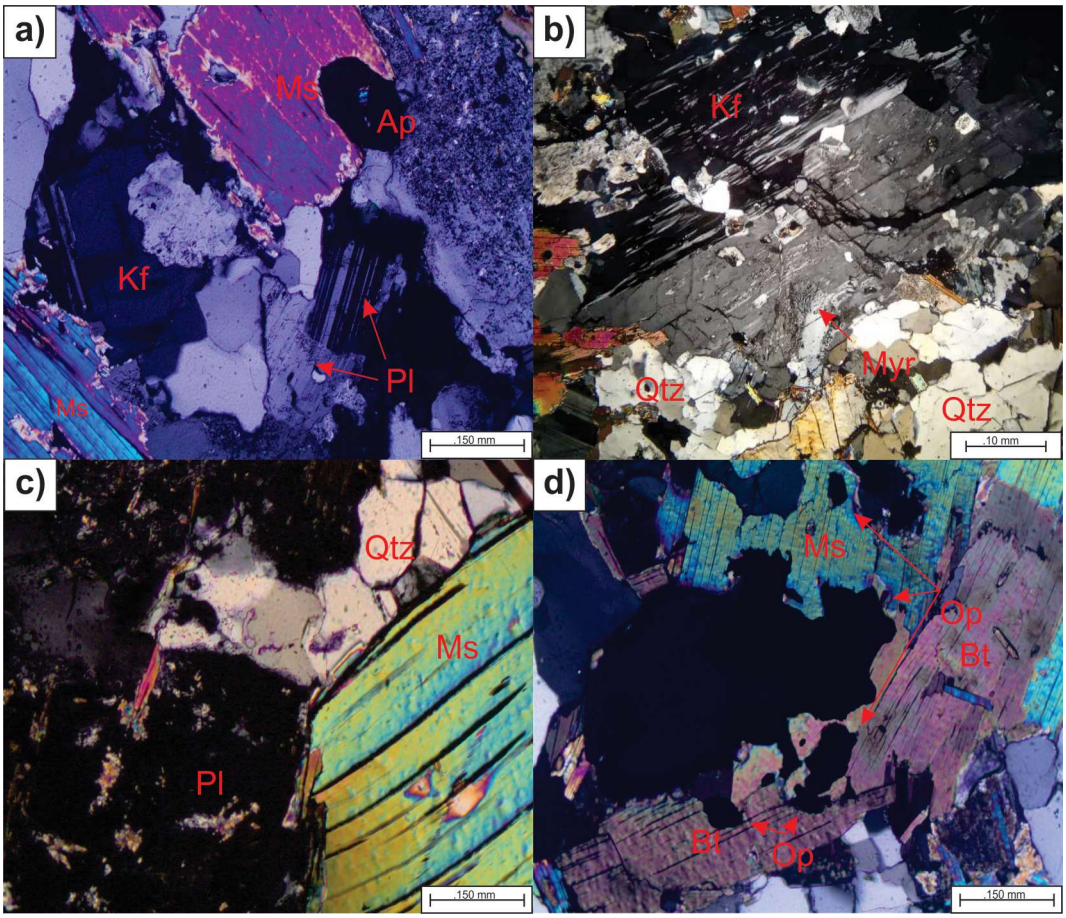

Quartz forms anhedral fractured crystals, showing strong undulose extinction and irregular contacts (Figs, 2a e 2b). It suggests recrystallization by grain boundary migration under high-temperature conditions (Hirth and Tullis, 1992). Microcline phenocrysts (1 to 1.5 cm long) and perthite exsolutions form subhedral set in a seriate matrix comprising anhedral crystals. The presence of flame perthite (Fig. 2b) suggests deformation under greenschist-amphibolite facies conditions (Pryer and Robin, 1995, 1996). Plagioclase crystals are subhedral and frequently show alteration to sericite (Fig. 2c). Muscovite forms large euhedral to subhedral crystals, in association with small euhedral to subhedral biotite crystals (Figs. 2c, 2d). Biotite inclusions are also found in muscovite. The accessory minerals comprise zircon as inclusions in biotite, euhedral apatite crystals and small subhedral to anhedral opaque minerals associated with biotite (Fig. 2d).

4.4. MINERAL CHEMISTRY

4.4.1. INTRODUCTION

Quantitative chemical electron probe microanalyses were carried out using the JEOL JXA-8230 Super Probe model, with five Wavelength Dispersive Spectrometers (WDS), from the Electron Microprobe Laboratory, University of Brasilia. Systematic WDS analysis were obtained for muscovite, biotite, plagioclase, alkali feldspar and opaque minerals in four representative samples. Operating conditions were 15 kV accelerating voltage, with a beam current of 10 nA and probe diameters of 3 mm for all minerals except plagioclase (5 mm). Count times on peak and background were 10s and 5s, respectively. Synthetic and natural mineral standards were used for the analysis.

4.4.2. WHITE MICA

Seventeen white mica flakes were analyzed, and representative compositions are shown in Table A1. Most of the analyzed white mica flakes have high-TiO_2 contents (>1%), being classified as primary muscovite in the Ti-Mg-Na ternary diagram, proposed by Miller et al. (1981), with only few of them, falling in the field of secondary muscovite (Fig. 3). The Si contents range within the 3.08–3.28 apfu interval, which according to Rieder et al., (1998) are muscovite (values ranging from 3.0 to 3.1 apfu) and phengite (3.1–3.5 apfu) according to Tappert et al. (2013). In the M^{2+} – Al – Si ternary diagram (Monier, 1986), the studied white micas fall in the solid solution along the muscovite-caledonite join (Fig. 4), suggesting phengitic substitution $[Al^{VI}, Al^{IV} \Leftrightarrow (M^{2+})^{VI}, Si^{IV}]$.

Figura 5 – Figure 3 –. Ternary diagram proposed by Miller et al., (1981) for distinction between primary and secondary muscovite.

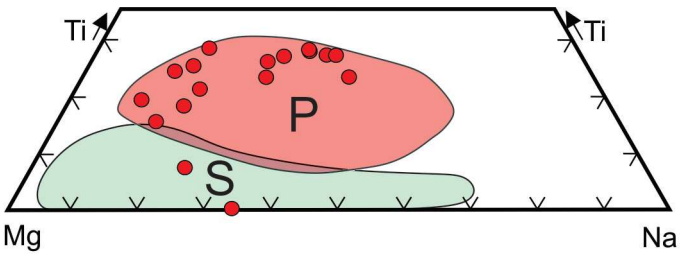

Figura 6 – Figure 4 –. Composition of micas on M^{2+} – Al_t – Si diagram (Monier et al., 1986). All Fe is assumed as Fe^{2+}.

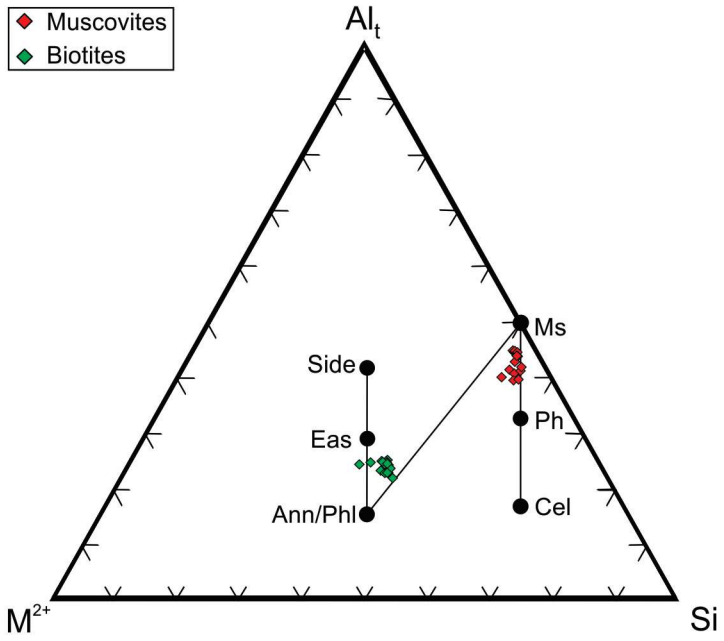

4.3. BIOTITE

A total of 20 spot analyses were done in biotite crystals, and values are given in Table A2. The biotite crystals plot in primary and primary re-equilibrated in the 10*TiO_2 – FeOt – MgO ternary diagram (Fig. 5a) of Nachit et al. (2005). Re-equilibrated biotite can be generated by fluid-oversaturation in highly fractionated granite, during the late or subsolidus stages of crystallization (Stussi and Cuney, 1996).

The analyzed biotite shows (Fe/Fe+Mg) ratios ranging between 0.68–0.79. It is Al- and Fe-rich, and Mg-poor (Fig. 5b). According to Abdel Raman (1994), such compositions are typical of biotite from peraluminous granitic suites (Fig. 5c and 5d).

Figura 7 – Figure 5 – (a) Ternary diagram FeOt – 10*TiO_2 – MgO for discrimination between primary (**A**), re equilibrated primary (**B**) and secondary (**C**) biotite (Nachit et al., (1985); (b) Al_t versus Fe# diagram proposed by Nachi et al., (1985); (c) and (d) diagrams proposed by Abdel Raman (1994) for discrimination between biotite from peraluminous (**P**), alkaline (**A**) and calc-alkaline (**C**) magmas

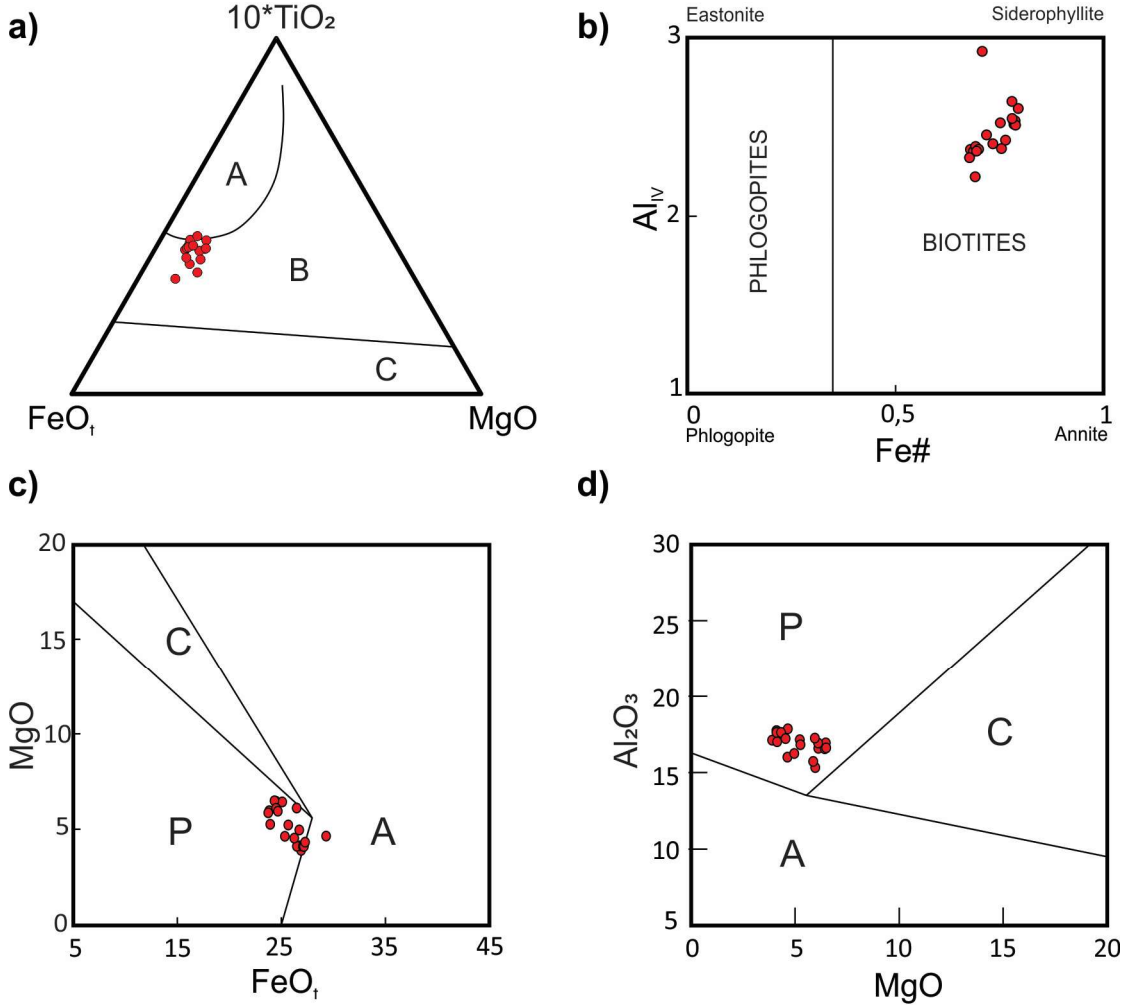

4.4.4. FELDSPARS

Thirty-two feldspar grains were analyzed. Representative compositions of plagioclase and K-feldspar are shown in Tables A3 and A4, respectively. The plagioclase is albite-rich, showing homogeneous composition ranging from ($Ab_{94}An_{05}Or_{01}$) to ($Ab_{89}An_{11}Or_{00}$), while the K-feldspar has compositions ranging from $Or_{97}Ab_{03}$ to $Or_{92}Ab_{08}$ (Fig. 6).

Figura 8 – Figure 6. Ternary classification of feldspars from Deer et al. (1992)

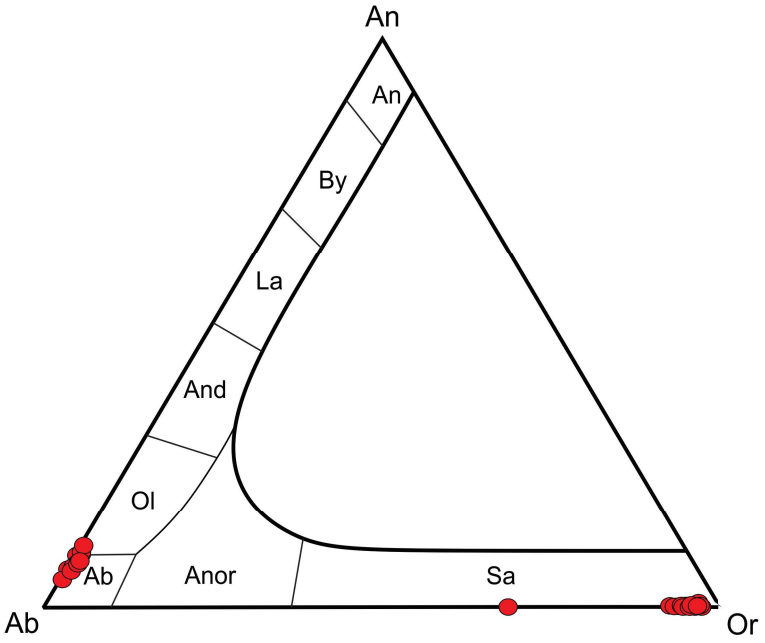

4.4.5. OPAQUE MINERALS

Opaque minerals form isolated subhedral crystals. Five grains were analyzed, and the results are shown in Table A5. In the Fe_2O_3 - TiO_2 - FeO ternary diagram (Buddington & Lindsley, 1964), the analyzed opaque minerals are essentially ilmenite (Fig. 7).

Figura 9 – Figure 7. Ternary classification diagram for oxides proposed by Buddinton and Lindsley (1964)

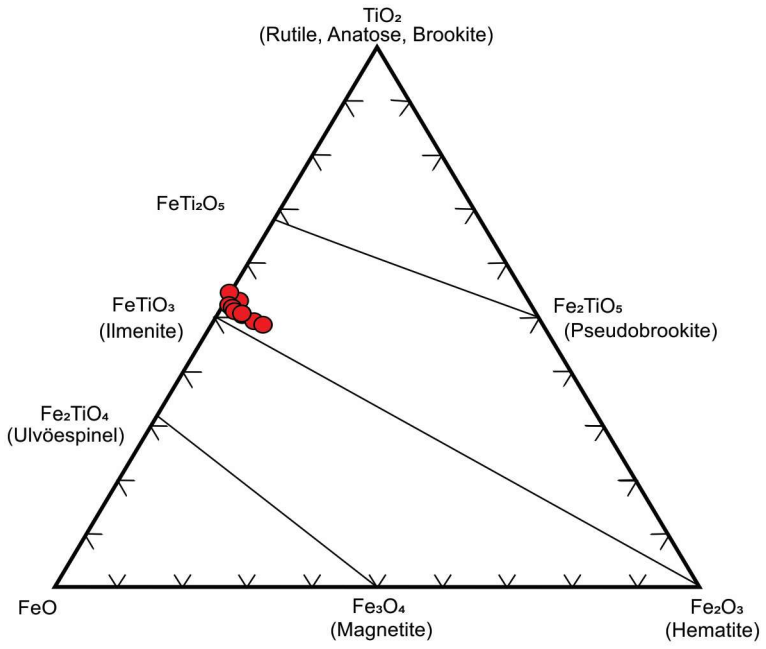

4.5. CRYSTALLIZATION CONDITIONS

4.5.1. TEMPERATURE

The crystallization temperature for the Quipapá granites was constrained using the zircon saturation geothermometer, proposed by Watson and Harrison (1983) [ln DZr =12900/T(ºK) - 0:85*(M-1) - 3.80], subsequently modified by Boehnke et al. (2013), [In DZr = 10108 ± 32)/T(K) - (1.16 ± 0.15) (M - 1) - (1.48 ± 0.09)], the apatite saturation geothermometer (Harrison and Watson, 1984; Pichavant et al., 1992), and the Thermocalc software (Holland and Powell, 1998, 2011).

The zircon saturation thermometer is based on the zircon solubility in crustal melts, which is dominantly controlled by temperature and composition. At pressures less than 25 kbar, zircon solubility is not affected by water contents, while oxygen fugacity has little influence (Boehnke et al., 2013). The Watson and Harrison (1983) and Boehnke et al. (2013) thermometers used the cationic ratio values for the M parameter [(Na + K + 2Ca)/(Al*Si)] between 0.9 to 1.7. The typical peraluminous granites have M ~1.3 and zircon solubilities ranging from ~ 100 ppm, with dissolved Zr at 750 °C, to 1330 ppm with dissolved Zr at 1020°C (Watson and Harrison, 1983). The calculated temperature varied from 731 to 825 °C using the Watson and Harrison (1983) calibration, whereas values ranged between 677–794 °C, average using the Boehnke et al. (2013) calibration. According to Siegél et al. (2018), the presence of inherited zircon grains (xenocrysts), as the case of the Quipapá granitoids, can yield higher liquidus. However, the average temperature (743 ± 43°C) obtained using the Thermocalc software (Holland and Powell, 1998, 2011) is like the average temperature (747 ºC) obtained using zircon saturation thermometer with the calibration of Boehnke et al. (2013). The temperatures calculated using apatite saturation geothermometer proposed by Pichavant et al. (1992), range between 621–736 °C.

4.5.2. PRESSURE

Massome and Schreyer (1987) used the muscovite composition and crystallization temperature to define the pressure in which primary muscovite crystallized. Hence, the apatite saturation temperatures were chosen to calculate the pressure, as they are consistent with the estimated temperatures for the primary muscovite stability. According to Massome and

Schreyer (1987), the muscovite barometer is dependent on the muscovite Si content and temperature. Using muscovite crystals without phengitic substitution i.e., those with Si between 3.08-3.10 apfu, the pressure values obtained using the Massome and Schreyer (1987) barometer for the crystallization of the Quipapá granitoids varied from 4.2 to 5.0 kbar, suggesting emplacement in depths within the 15.5 to 18.5 km interval. An average pressure of 7.0 ± 1.4 kbar was defined using the software Thermocalc (Holland and Powell, 1998, 2011), for the emplacement of the Quipapá granitoids. However, this value is unlikely, due to the set of incomplete reactions resulted by the small number of mineral phases in the studied granitoids.

4.5.3. OXYGEN FUGACITY

The oxygen fugacity (fO_2) during the crystallization of granitic magmas depends on the magma composition. The FeO/Fe_2O_3 ratio is an important factor controlling the magmatic fractionation and the stability of the Fe-bearing minerals.

Biotite compositions from the studied granites suggest fO_2 near the FMQ oxygen buffer when plotted on Fe/(Fe+Mg) vs Al_t diagram of Anderson et al. (2008) (Fig. 8), i.e., crystallization under low fO_2 conditions, which is corroborated by the presence of modal ilmenite.

Figura 10 – Figure 8. Fe/(Fe + Mg) diagram comparing biotite compositions from plutons of magnetite and ilmenite series and approximated values of fO_2 compared to FMQ buffer (Anderson et al., 2008)

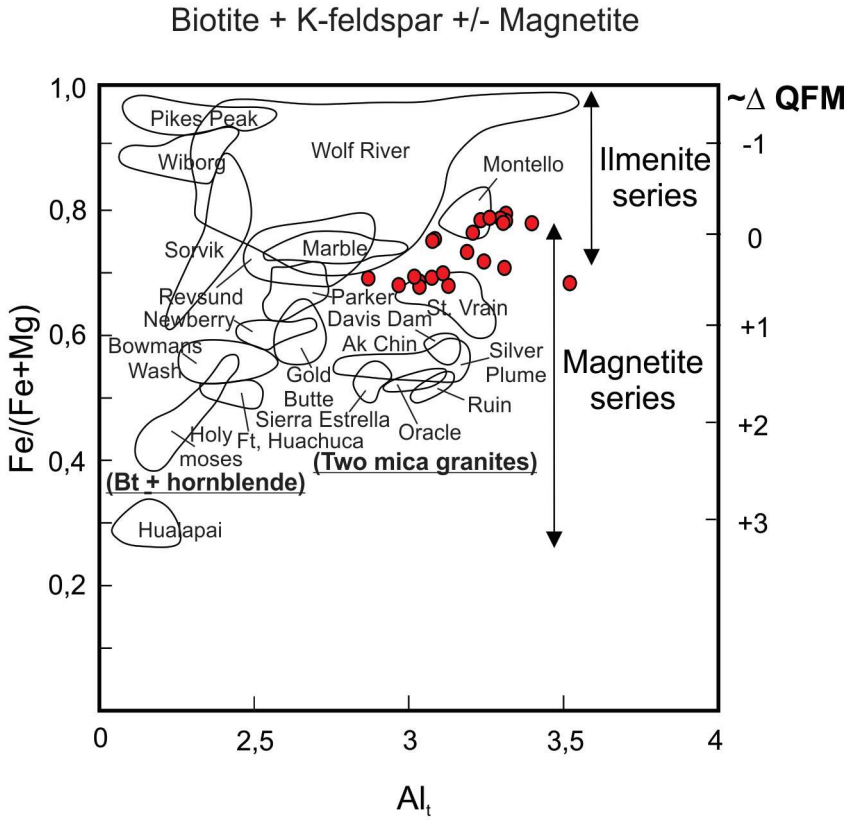

4.6. GEOCHRONOLOGICAL DATA

4.6.1 Introduction

U-Pb isotopic analyses were performed on zircon grains using a Thermo-Fisher Neptune high-resolution multicollector ICP-MS coupled with a New Wave laser ablation system, in the geochronology laboratory at the University of Brasília.

The sample was initially crushed and sieved, and the heavy minerals were concentrated using gravimetric and magnetic methods. Zircon grains were handpicked using a binocular microscope. Selected grains were mounted on epoxy resin for LA-MC-ICP-MS isotope ratio acquisition. The data reduction followed Bühn et al. (2009) and Matteini et al. (2010) procedures. Only coherent interval analyses were chosen to avoid signal mixed ages. The internal GJ standard zircon (Jackson et al., 2004) was used to normalization. The age calculations were performed using in-house-developed Excel worksheets. Common ^{204}Pb was

monitored using the ^{202}Hg and (^{204}Hg + ^{204}Pb) masses. Concordia diagram and weighted average ages were calculated using the IsoplotR (Vermeesch, 2018).

The crystallization age of the studied leucogranites is based on U-Pb zircon ages of two samples:

4.6.2 Sample GUS-102

It was collected in the west part of the intrusion (the so-called Jurema Pluton). Zircon grains were extracted from a coarse- to medium-grained two-mica leucogranite. Most of the zircon grains are subhedral to euhedral, bi-pyramided, equant to elongate, with length/width ratios ranging from 1:1 to 1:5, and many inclusions. Significantly older inherited cores were recorded as well as overgrowths (Fig. 9a). Oscillatory zoning was recorded in many grains, most in the grain rims. Thirty-five zircon grains were analyzed (Table A6). However, most of the results were discarded due to high discordance related to high common Pb (Fig. 9b). Most inheritance, recorded in the grain cores, show $^{207}Pb/^{206}Pb$ ages ranging from 1.7 to 2.1 Ga and in a concordia, plot define an upper intercept age of 1978 ± 4 Ma (Fig. 9c), interpreted as the as the crystallization age of zircon xenocrysts from the Quipapá Granite.

Nine concordant younger grains defined two cluster. One cluster comprises four spots analyzed in the core, and Th/U ratios ranging from 0.21 to 0.83, defining a concordia age of 641 ± 5 Ma, with a MSWD = 1.9 (Fig. 9d). This age is like that obtained by Silva Filho et al. (submitted) for sample ANG-02 in the east part of the intrusion and can be interpreted as the crystallization age of the studied granitoids. The other three spots located in the rim, showing Th/U ratios ranging from 0.1 to 0.32, defined an age of 581 ± 6 Ma (Fig. 9d) with a low MSDW (0.061). However, this age is like that reported by Neves et al. (2012) for the high-K, calc-alkaline, syn-transcurrent granites of the Panelas Pluton, which makes contacts with the Quipapá granites.

4.6.3 Sample ANG-02

The sample from the eastern part of the intrusion (the so-called Quipapá Pluton), was analyzed by SHRIMP (Silva Filho et al., submitted). This sample was collected from a coarse-grained, leucocratic, equigranular two-mica ± garnet syenogranite (Silva Filho et al., 2007), close to the Ribeirão shear zone (Fig. 1). The analyzed zircon grains defined a concordia age of 631 ± 5 Ma, interpreted as the granitoids crystallization age. $^{206}Pb/^{238}U$ ages of 598 ± 11 Ma,

566 ± 7 Ma, and 587 ± 7 Ma were obtained in the grain rims by Silva Filho et al. (submitted) and interpreted as metamorphic ages produced by the Ribeirão shear zone activity, and the emplacement of the adjacent syn-transcurrent Panelas pluton, ca. 580 Ma (Neves et al., 2012).

Figura 11 – Figure 9. (a) Cathode Luminescence (CL) imagens for representative zircon grains of sample GUS-102 (b) All the analyzed zircon grains on Concordia diagram (c) Discordia diagram for crystallization age of Paleoproterozoic inherited zircon grains (d) Concordia diagram for Neoproterozoic magmatic zircon grains of sample GUS-102.

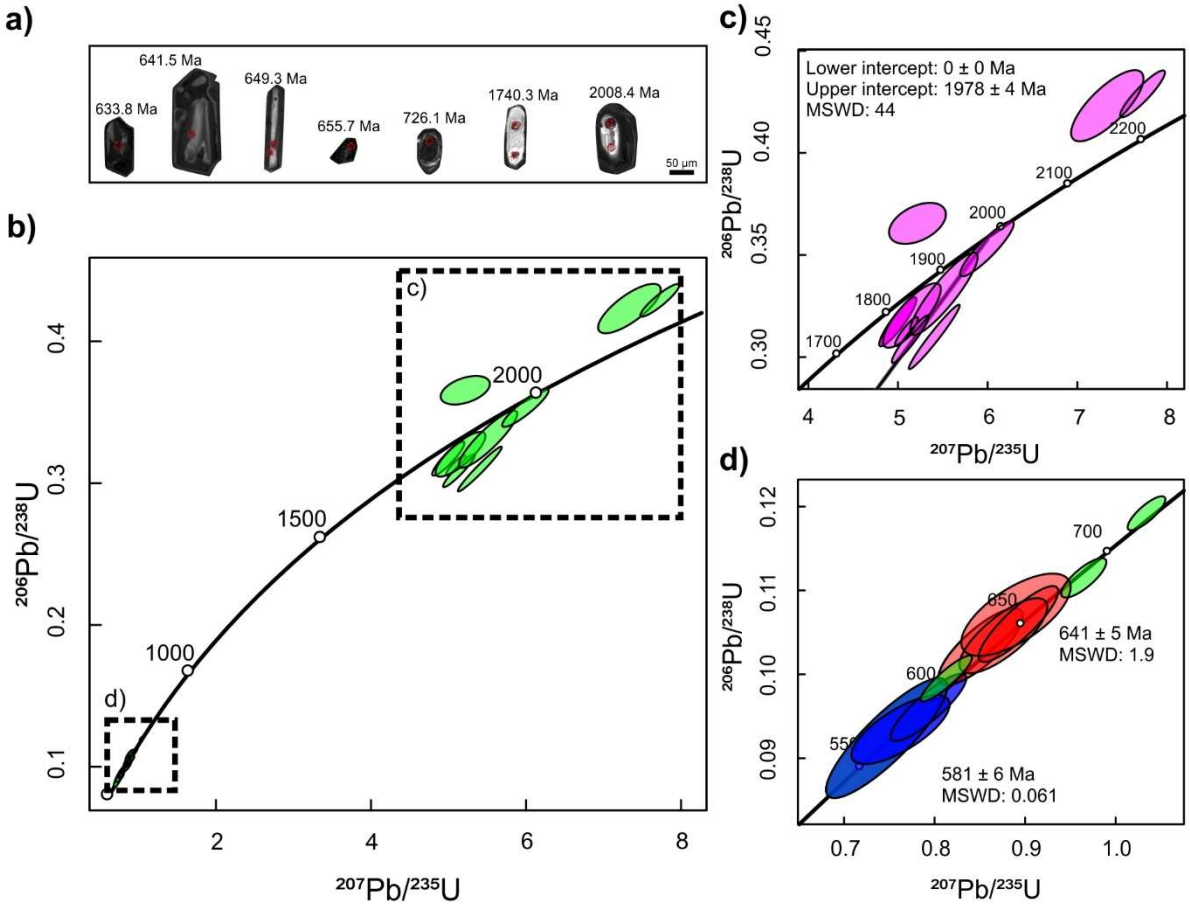

4.7. WHOLE ROCK GEOCHEMISTRY

The Quipapá granites are Si-rich (SiO_2 = 70.8–75 wt. %, Table A7), weakly to strongly peraluminous, showing alumina saturation index (ASI = [molar $Al_2O_3/(Na_2O+K_2O+CaO)$]) ranging from 1.07 to 1.38 (Fig 10a) and a general increase in ASI with SiO_2 content. They have high total alkalis ($Na_2O + K_2O$) content (7.8 to 9.26 wt. %), K_2O/Na_2O ratios between 1.4–2.2, and low CaO (0.52–1.43 wt. %) content. According to the classification of Frost et al. (2001),

the Quipapá granites are ferroan, with FeOt/(FeOt+MgO) ratios > 0.8 (Fig 10b), and alkalic-calcic when plotted in the modified alkali lime index ($K_2O + Na_2O - CaO$) versus SiO_2 diagram (Fig. 10c).

Figura 12 – Figure 10. (a) Shand's index for the Quipapa granites; (b) $FeO_t/FeO_t + MgO$ versus SiO_2 with fields after Frost et al. (2001); (c) Modified alkali-lime (MALI) diagram (Forst et al., 2001).

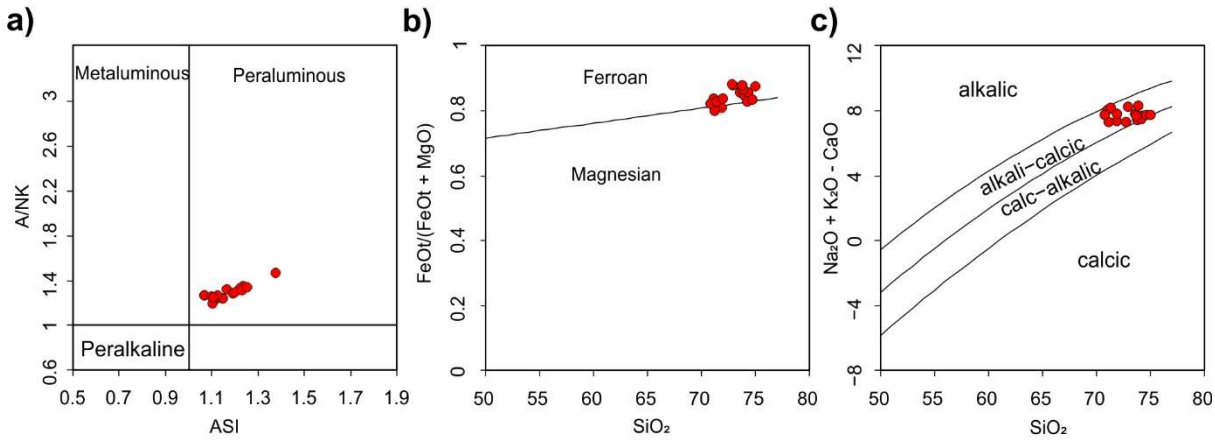

On binary SiO_2 vs. major and trace element variation diagrams (Fig. 11), the studied granitoids show a general decrease in K_2O, MgO, Fe_2O_3t, CaO, TiO_2, decrease in P_2O_5 during the late stage of crystallization, whereas Al_2O_3 contents are relatively constant, suggesting K-feldspar, ± biotite, apatite and ± ilmenite fractionation during the magmatic evolution.

Figura 13 – Figure 11. Diagrams of major elements vs SiO_2 for the Quipapá granites.

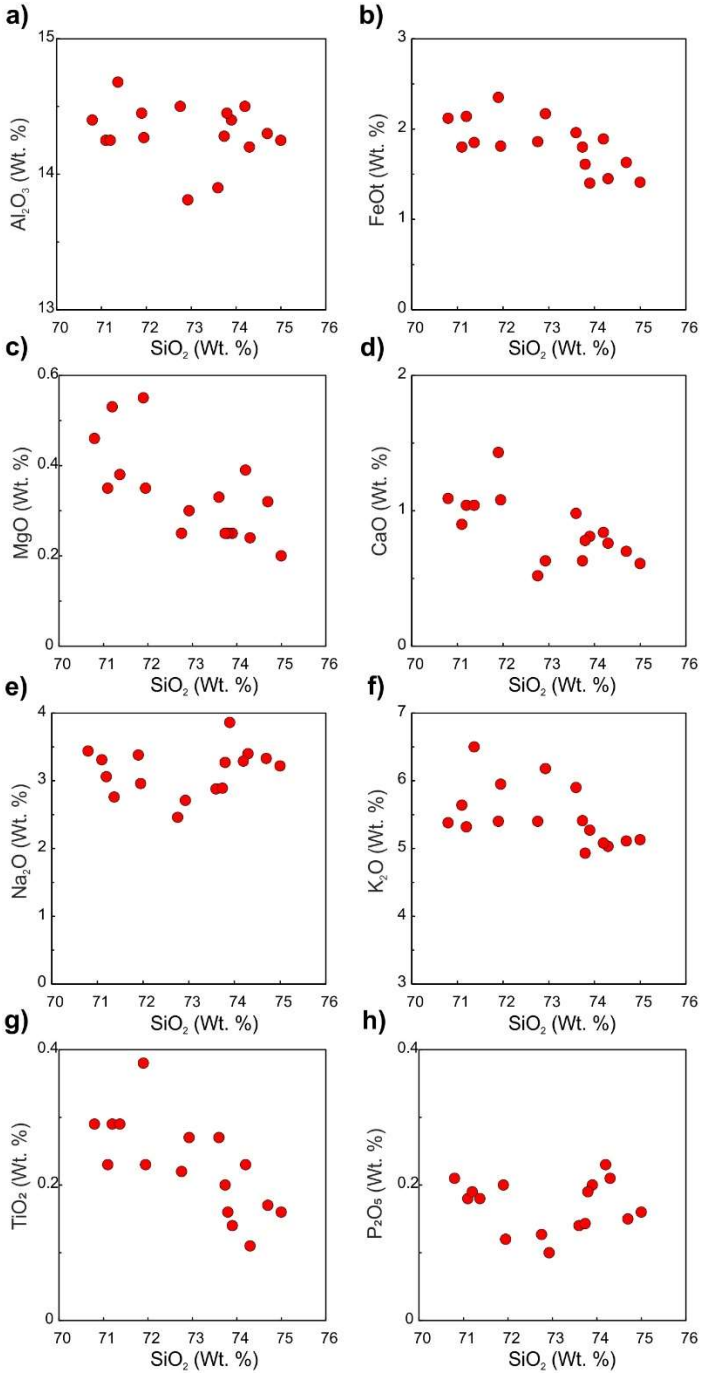

The Quipapá granites show fractionated chondrite normalized REE patterns (Nakamura, 1974), characterized by higher contents of light rare earth elements (LREE) relative to heavy

rare earth elements (HREE) (Fig. 12a), with $(Ce/Yb)_N$ ratios ranging between 16.9 and 83.2, and deep negative Eu anomalies, with Eu/Eu* ratios varying from 0.26 to 0.51, suggesting K-feldspar fractionation or plagioclase in the residue. Moreover, the spidergrams normalized to the values suggested by Thompson et al. (1982), show enrichment of large ion lithophile elements (LILE) and depletion in high field strength elements (HFSE), characterized by notable negative Ti, Sr, Ba and less pronounced Nb and Ta anomalies (Fig. 12b).

Figura 14 – Figure 12. (a) REE patterns normalized to the chondrite values of Nakamura (1974); (b) Spidergrams normalized to the values suggested by Thompson (1982).

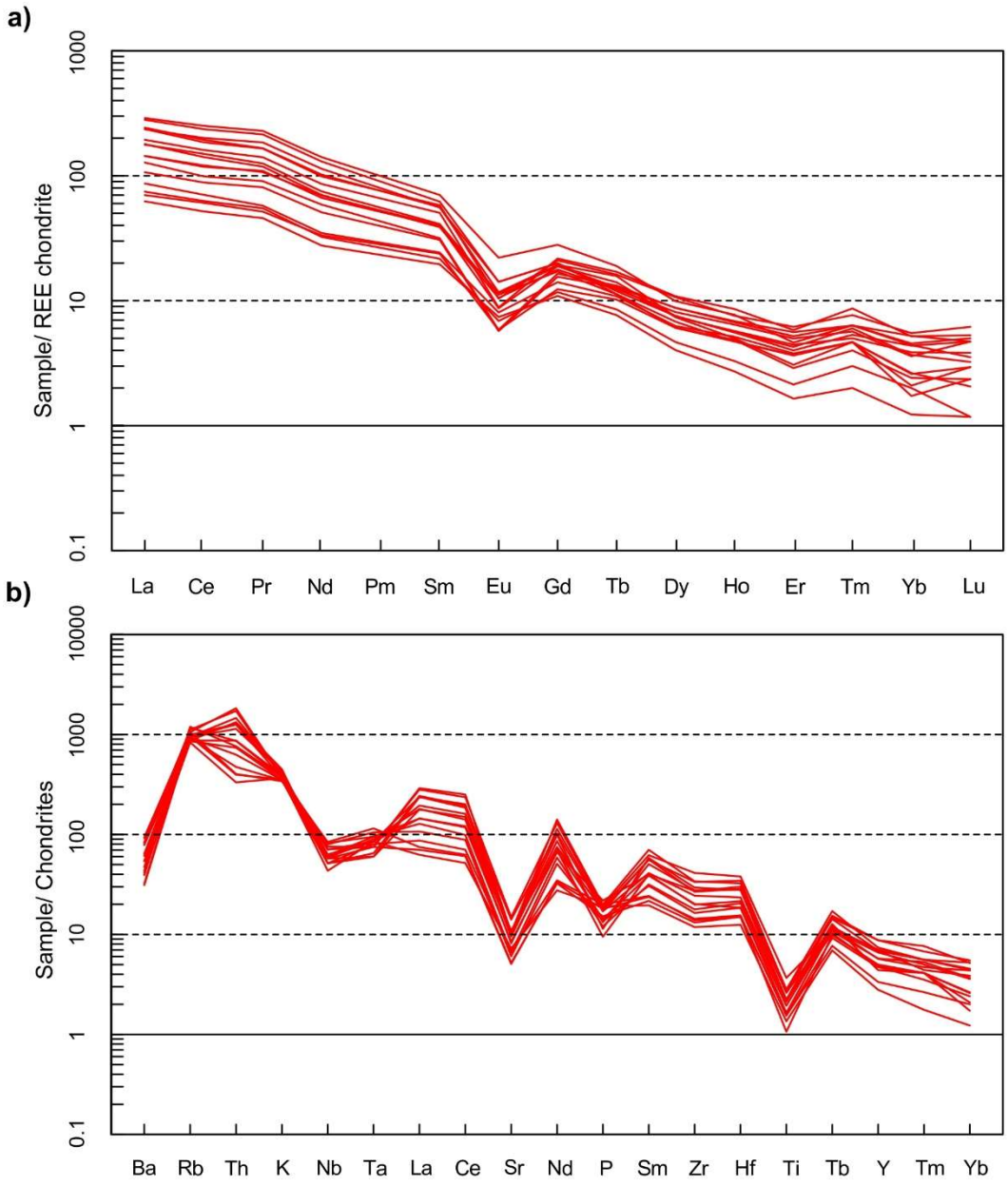

4.8. DISCUSSION

4.8.1. CRYSTALLIZATION CONDITIONS

The mean crystallization temperature obtained in the Quipapá granites samples (747 °C) using the zircon saturation is < 800 ºC and considered a valid estimate of the liquidus temperature. The low temperatures range are commonly related to many inherited zircon grains (Miller et al., 2003). The presence of many Paleoproterozoic inherited zircon grains within the Quipapá granites is confirmed by U-Pb geochronological data. The temperatures (621–736°C) obtained using apatite saturation geothermometer (Pichavant et al., 1992) are consistent with the stable mineral assembly recorded in the studied granites. They are interpreted as the solidus temperature.

The crystallization pressure of the Quipapá granites (4.2–5.0 kbar) was constraint using the geobarometer proposed by Massome and Schreyer (1987), composition of large flakes of muscovite without phengitic substitutions and crystallization temperature obtained by the apatite saturation geothermometer. The obtained pressures values suggest that the Quipapá granitoids crystallized in middle crust at depths of 15.5 to 18.5 km, under fO_2 conditions near the FMQ oxygen buffer.

4.8.2. HEATING SOURCES, MAGMA GENERATION AND EVOLUTION

Peraluminous granites, specifically two-mica leucogranites, are common in collisional orogens. They have mineralogical assemblages characterized by primary muscovite, garnet, tourmaline, and small amount of biotite (Clarke, 1981).

Peraluminous magmas are originated via partial melting of the continental crust, at relatively low temperatures when water is supplied by dehydration reactions (Gardien et al., 1995) or volatile influx at the source region (Ebadi and Johannes, 1991; Weinberg and Hasalova, 2015). However, at dry conditions, high temperatures (760–850 ºC) are required to promote crustal melting and granitic magma production (Vielzeuf and Holloway, 1988; Le Breton and Thompson, 1988; Johannes and Holtz, 1996). During anatexis, the magmas peraluminousity is dependent on the source rock composition, pressure, and H_2O concentration (Patiño Douce, 1999; Barbarin, 1996; Villaseca et al., 1998). Meanwhile, pressure, temperature and the H_2O concentration control the volume of peraluminous magmas produced (Clemens and Wall, 1981; Holtz and Johannes, 1991).

The temperature required to melt the crust can be achieved through radiogenic heating in a thickened crust (Nabelek and Liu, 2004; Bea, 2012); mechanical heating associated with shear zones (Nabelek and Liu, 2004; Nabelek et al., 2010); increased mantle heat flow (Currie and Hyndman, 2006; Clark et al., 2011); decompression; delamination of the lithospheric mantle (Nabelek and Liu, 2004; Holm et al., 1997).

According to Nabelek and Liu (2004), radiogenic heating promotes partial melting only in the lower crust, being incapable of providing enough heat to promote partial melting of the upper crust. Furthermore, decompression in collisional orogens can promote partial melting in metasedimentary rocks at depth > 45 km (Nabelek and Liu, 1999, 2004; Nabelek et al., 2001). Neves et al. (2012) reported pressures ranging from 6 to 8 kbar (22–30 km of depth) associated with the metamorphic peak, which is a little higher than those (4.2 to 5.0 kbar) defined to the stability of the muscovite in the Quipapá granitoids. It does not exclude the possibility of the studied granitoids melts be generated by decompression, because the magma could be generated at deeper level and ascent to the muscovite stability level and, the pressure is calculated to the actual erosion level. Conversely, lithospheric mantle delamination could explain the Quipapá granites generation (Holm et al., 1997). However, delamination is associated with basalt injections, not recorded in the Quipapá granites.

Shear heating or strain heating thermic models have also been proposed to explain peraluminous granite genesis in continental orogens (Nabelek and Liu, 1999, 2004; Nabelek et al., 2001; Leloup et al., 1999). This model is based on the thermal response of rocks to ductile deformation or friction in discrete shear zones (Nabelek et al., 2010). Neves et al. (2020) proposed this mechanism to explain the generation of the peraluminous granites with crystallization ages ranging from 573 to 562 Ma, associated with the East Pernambuco shear zone. Basalt underplating of the lower crust, associated to pre-collisional extension, could also increase the crustal temperatures, promoting melt. We favor the shear heating as the main heat source but, other sources, as radioactive heat, and basalt underplating, could be also involved in the generation of the Quipapá granites magma.

Many crustal rock types begin to melt when the metamorphic temperature is higher than 650 ºC under water-present conditions. However, the quantity of melt produced depends on the H_2O available (Sawyer et al., 2011). If H_2O is in excess throughout the rock pores and grain boundaries, partial melting occurs under lower temperatures (600–700 °C; Sawyer et al., 2011). Incongruent melting takes place at a higher temperature with H_2O fluid-absent and lower temperatures with H_2O fluid-present. Crystalline rocks have low porosity and contain little H_2O, producing low amounts of melt. Hence, large volumes of granitic melt in the continental

crust are generated by fluid-absent incongruent melting, except when large volumes of aqueous fluid are introduced into rocks at high temperature (Sawyer et al., 2011). On the other hand, the magmatic fluids increase the aluminum-alkalis balance in the residual melt, favoring Al-rich biotite composition, and muscovite may crystallize initially in metaluminous magmas (Harrison, 1990).

The temperatures (677–788 °C) calculated in the studied granitoids correspond to the temperature intervals in partial melting of crustal lithologies in the presence of H_2O or by muscovite breakdown. Muscovite dehydration melting takes place under temperatures of 650–750 °C (Petö, 1976), as biotite dehydration melting happens at temperatures > 750 °C (Gardien et al., 1995). The temperature of the initial stage of the biotite breakdown is strongly dependent on aH_2O and #Mg (René et al., 2008). The studied rocks show mineralogical and geochemical characteristics of granitic magmas generated by muscovite dehydration melting (Patiño Douce and Harris, 1998) as discussed below.

The Rb/Ba and Rb/Sr ratios and $CaO/Na_2O < 0,3$ (Fig.13a and 13b) suggest that the studied granitoids magmas were generated by melting of metapelites (Sylvester, 1998; Hanson, 1978). REE patterns with Eu negative anomalies and trace elements profiles with troughs at Ba and Sr, can be interpreted as: K-feldspar and plagioclase ± apatite fractionation, or their retention in the source, or a signature inherited from the source rocks. The increasing of Rb/Sr ratios with decreasing in Ba and Sr contents (Fig. 13c and 13d) suggest that the magmas of the granites were generated by muscovite dehydration partial melting (Gardien et al., 1995). Muscovite dehydration partial melting can generate a large volume of peraluminous magmas (Gardien et al., 1995) as recorded in the studied area.

Figura 15 – Figure 13 – Source's discriminant diagrams (Sylvester, 1998) for the Quipapá granites. (a) Rb/Ba vs Rb/Sr ratios with mean compositions of magmas generated by partial melting of metapelites and metapsamites sources, the curve represents progressive mixing of basalt and metapelites; (b) CaO/Na_2O vs Al_2O_3/TiO_2 diagram of Sylvester (1998) for strong peraluminous granites; (c) Covariant diagrams for Rb/Sr versus Ba (c) and Sr (d), the vectors represent partial muscovite dehydration melting **(VA),** Biotite dehydration melting **(VA)** and fluid present melting reactions **(VP).**

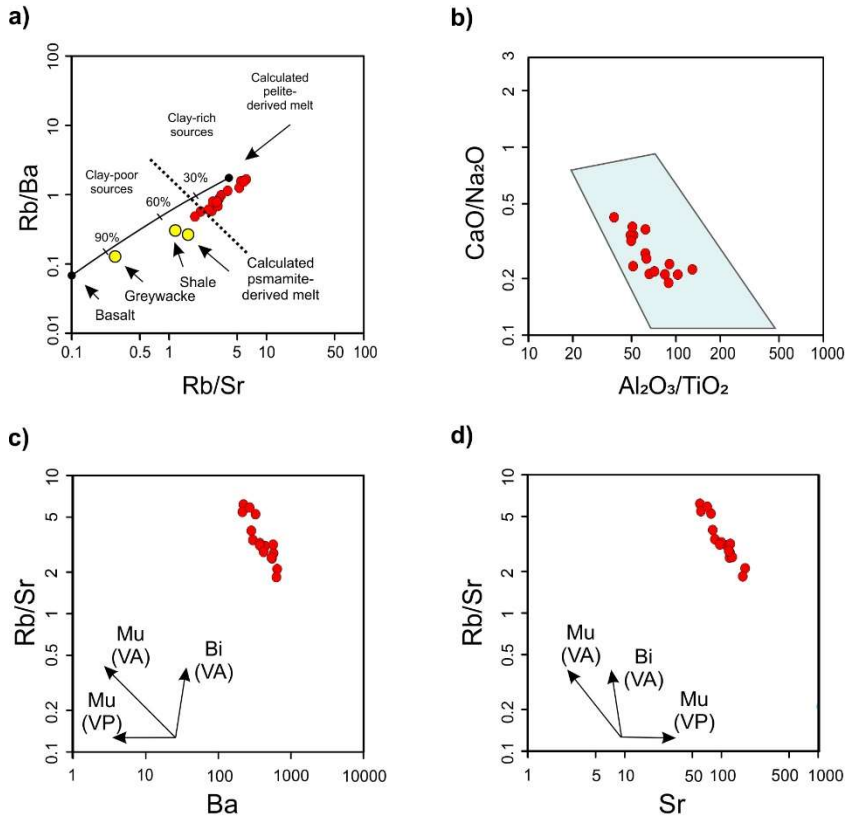

According to Bau (1996), igneous rocks from pure silicate melt systems have Zr/Hf ratios ranging from 26 to 46, while Zr/Hf ratios < 26 are characteristic of aqueous systems. The Zr/Hf ratios (30 – 38) recorded in the studied granites (Fig. 14a) suggest crystallization from pure silicate melts.

Nb and Ta are HFSE with similar geochemical properties due to similar ionic radius and same charge. Nb and Ta are highly incompatible in magmatic systems and Nb/Ta ratios show a wide range of values (2–25; Green, 1995) in granitic rocks. The crustal values of Nb/Ta ratios are lower (11–12) in comparison with mantle values (ca. 17.5), due to fractionation of these two elements during crustal evolution (Green, 1995). Partial melting can produce peraluminous magmas with low or high Nb/Ta ratios, depending on the temperature. If the anatexis occurs under high temperatures, biotite is fully consumed, and Ti-bearing oxide stays in the residue. Because Ta is incorporated preferentially in Ti-bearing oxide (rutile), it results in magmas with

high Nb/Ta ratios. However, if partial melting occurs at low temperatures, biotite is a residual phase and incorporates Nb over Ta, resulting in low Nb/Ta ratios.

According to many authors (e.g., Green, 1995; Reimbault et al., 1995, Dostal and Chatterjee, 1995; Halter et al., 1998; Linnen and Keppler, 1997; Stepanov et al., 2014), low Nb/Ta ratios in leucocratic granitic rocks are the result of fractional crystallization during the magma evolution. In contrast (Dostal and Chatterjee, 2000; Tartesé and Boulvais, 2010; Ballourd et al., 2015; Dostal et al., 2015), low Nb/Ta (<5) ratios in fractionated peraluminous granites resulted from late interactions with magmatic fluids. According to Ballouard et al., (2016), the decrease of Nb/Ta ratio during the magmatic evolution is a consequence of coincident fractional crystallization and sub-solidus hydrothermal alteration. Thus, Nb/Ta ratios ca. 5 mark the magmatic-hydrothermal transition in peraluminous granites.

The analyzed granitoids samples have Nb/Ta > 8, excluding possible interaction with late fluids during the magma evolution. The Nb/Ta ratios show negative correlations with K/Rb, Zr/Hf and Ta and positive correlation with Rb (Figs. 14b, c, d, e). The negative correlation between Nb/Ta and Ta suggest that the phase incorporating Ta over Nb (e.g., rutile) was not fractionated. However, the negative correlation between Nb/Ta and K/Rb ratios and between TiO_2 and Fe_2O_3 with SiO_2 could suggest a small amount of biotite and ilmenite fractionation during the magma evolution.

Figura 16 – Figure 14. The Quipapa granitic analyzed samples projected in the diagrams: (a) K/Rb ratios against Rb (ppm); (b) Zr/Hf vs Zr (ppm); (c) Nb/Ta vs K/Rb; (d) Zr/Hf versus Ta (ppm); (e) Zr/Hf versus Rb (ppm).

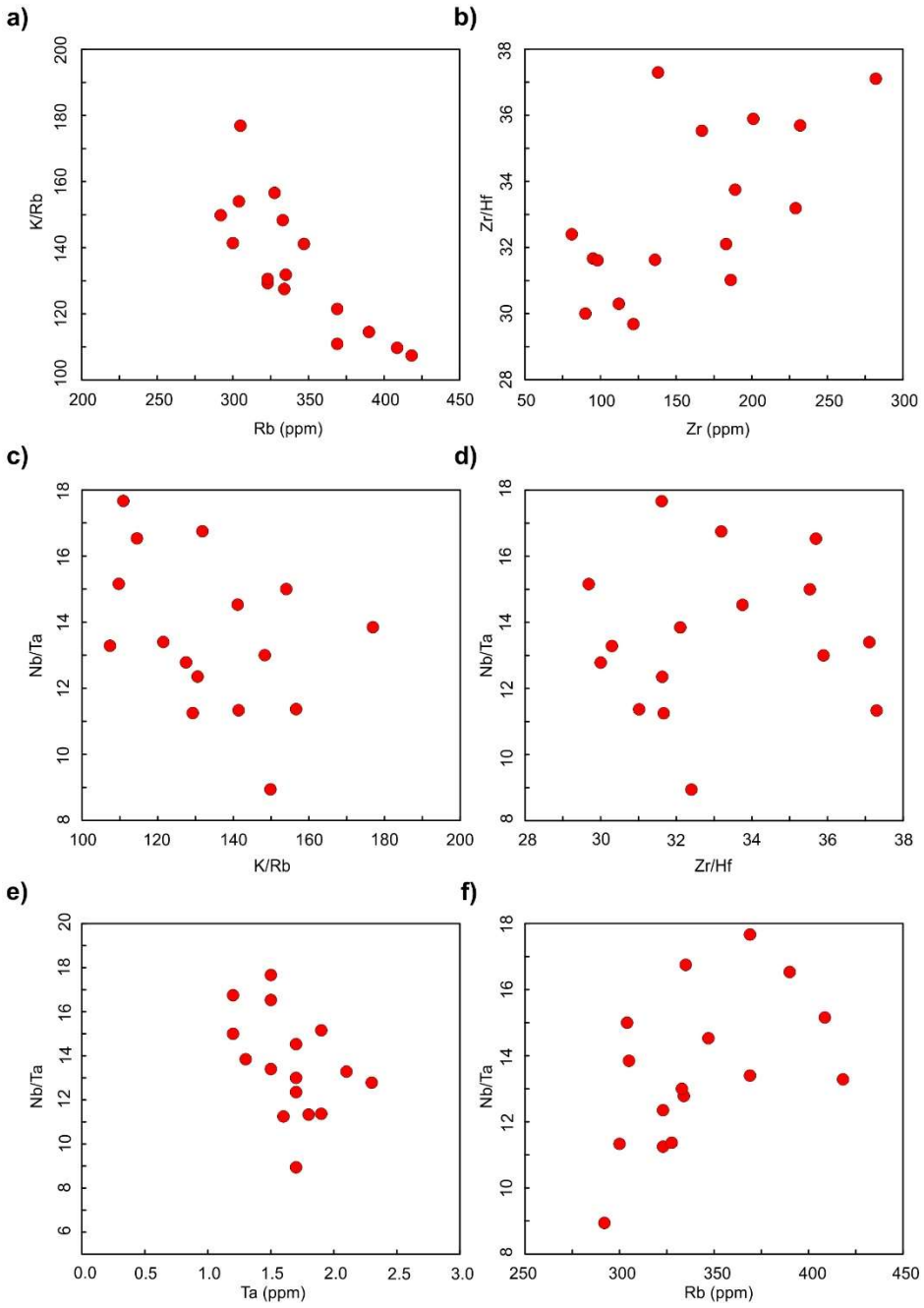

Nd isotopic data presented by Silva Filho et al. (2002), show negative ƐNd 0.6 Ma values (-14.5) and Paleoproterozoic T_{DM} model age of 2.22 Ga, as well as the presence of Paleoproterozoic inherited zircon grains suggest a strong participation of a Paleoproterozoic component in the source of the granitoid magma. The isotopic data associated with geochemical data point to the Palmares metasedimentary country rocks, as the best candidate to the source

of the granitoid magma. However, we cannot exclude some contribution of the Paleoproterozoic basement of the Palmares metasedimentary rocks.

4.8.3. TECTONIC SETTING AND TIMING OF EMPLACEMENT

According to Pearce et al. (1984) and Pearce (1996), the studied granites have a syn-collision to post-orogenic granite geochemical signature (Fig. 15a, b). As previously discussed, the composition of peraluminous magma depends on partial melting temperature and H_2O-content in the source. Biotite is fully consumed, when melting of Nb- and Ta-poor source, occurs at high temperatures, and the resulting magma has high Rb and low Nb and Ta content, which are signatures of syn-collision and post-orogenic granites. Thus, the tectonic discriminants alone cannot infer the tectonic setting in which the studied granitoids was emplaced.

Figura 17 – Figure 15. The Quipapa granites tectonic discriminant diagrams of Pearce et al. (1984) and Pearce (1986). Syn-COLG – Syn-Collision granites; VAG- Volcanic Arc Granites; WPG = Within Plate granites; ORG – Ocean Ridge granites

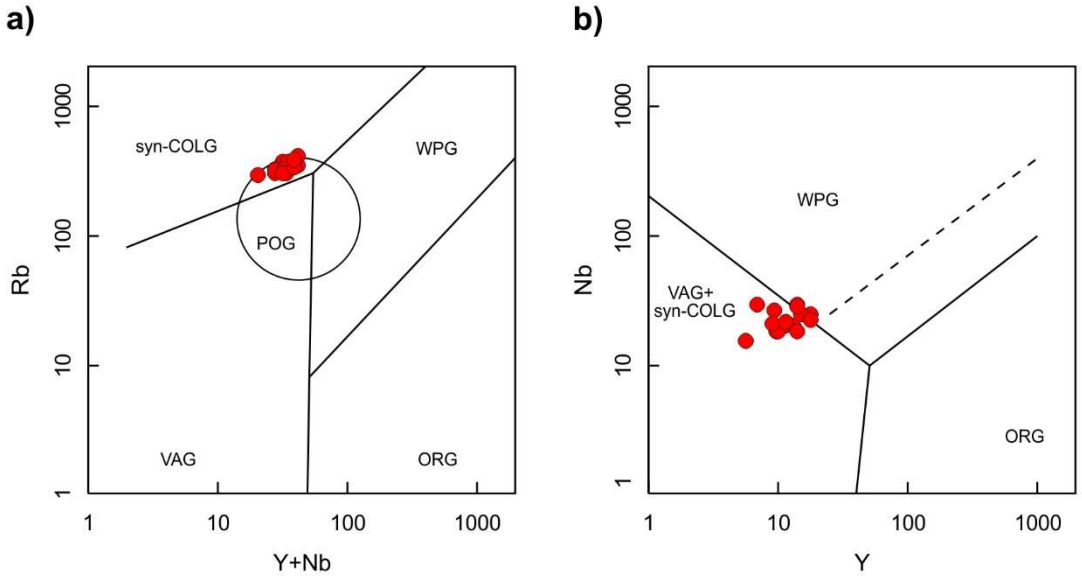

Neves et al. (2015) defined the 623–632 Ma interval as the peak of amphibolite facies (high-T, medium-P) metamorphism associated to the flat-lying foliation in the Quipapá region, and the 640–630 Ma interval as time of the change from extensional to contractional setting. The metamorphic temperatures (640–750 ºC) calculated by Neves et al. (2012) are high enough to promote partial melting of metasedimentary rocks by muscovite dehydration. They are like the temperatures obtained in the studied granites using the zircon saturation geothermometer.

U-Pb zircon crystallization age of ca. 630 Ma for the granites, suggest that they are coeval with the peak of high-temperature amphibolite facies metamorphic event (Neves et al., 2015) associated with the flat-lying foliation related to the contractional stage of the Brasiliano Orogeny (Fig. 16).

Figura 18 – Figure 16. Schematic evolution of the studied area during the later Neoproterozoic. a) 640-590 Ma - Thrusting produces partial melting of metasedimentary rocks, generating the magmas of the two-mica granites of the Quipapa intrusion and other intrusions in the Atalaia – Ipojuca Domain. During the contractional deformation partial melting of lower crust and melting of the lithospheric mantle, generated calc-alkaline magmas as reported by Neves et al. (2020). b) Melting of a variety of sources including lower crust, lithospheric mantle may include basaltic underplated, and metasedimentary rocks, during transpression, generated syn-transcurrent high-K granitoids, most involving magma mixing processes (Panelas Pluton, among others), and two micas granites as reported by Neves et al. (2020) and Osako (2005).

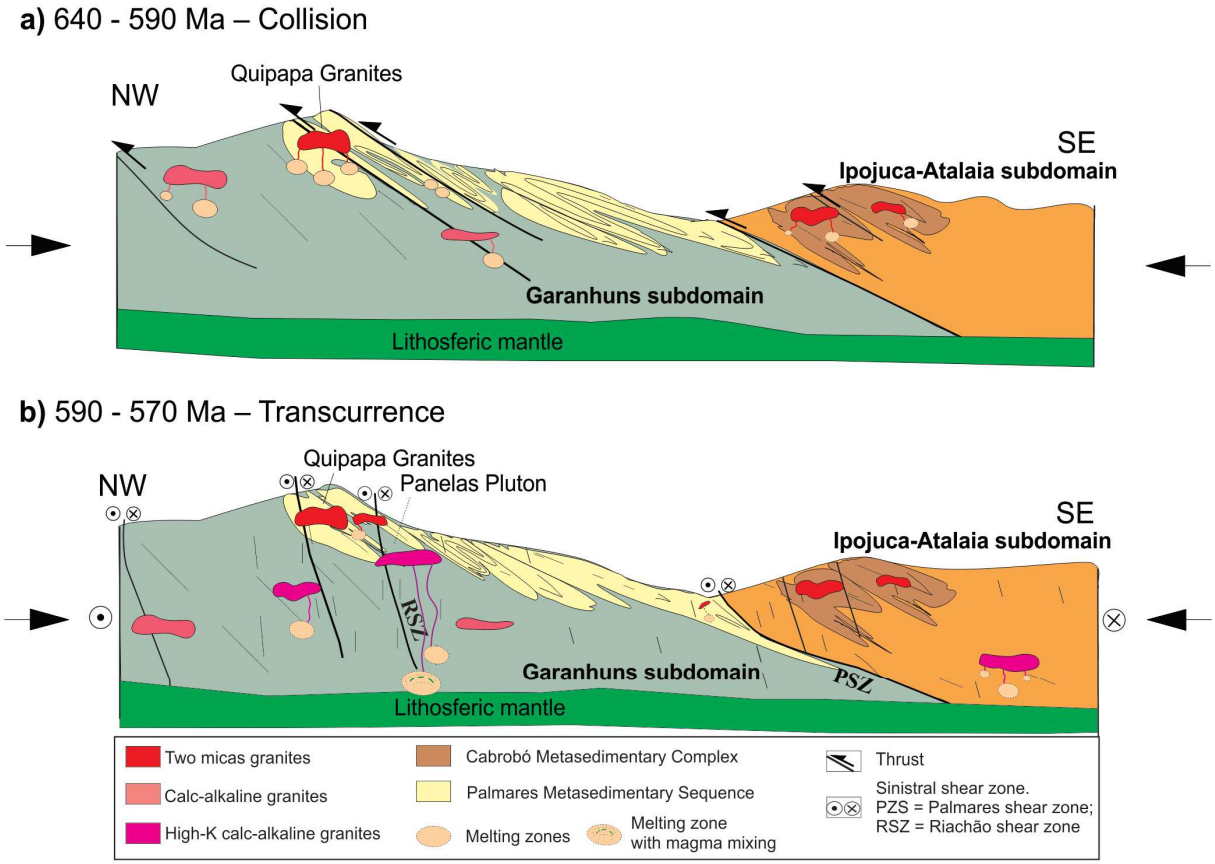

Syn-transcurrent two-mica granitoids (Cabanas Pluton) intruded to the northeast of the Quipapá Pluton, is an elongated, E-W trending, strike-slip shearing deformed body, parallel to the Pernambuco shear zone. It shows U-Pb zircon crystallization age of 573 ± 4 Ma (Neves et al., 2008). Distinct crystallization ages, suggest generation of two-mica granitic magmas, in

distinct stages of the Brasiliano Orogeny, within the Pernambuco Alagoas Domain, i.e., i) during the early stage, in the transition between extension and contraction, the Quipapá granites, and ii) syn - transcurrent, the Cabanas Pluton, (Fig. 16). The generation of the Quipapá granites in a changing tectonic setting, may explain the projection of the studied granitoids in distinct fields of tectonic discriminant diagrams, and their classification as ilmenite series granites. Two-mica granitic intrusions coeval with the studied granitoids are rare within the Garanhuns subdomain of the Pernambuco - Alagoas Domain, being more abundant within the Ipojuca-Atalaia subdomain (Silva Filho et al., 2010; Osako, 2005). However, many occurrences of syn-transcurrent two-mica granites, with ages 580–560 Ma are reported in the PEAL domain (Neves et al., 2020). Kamguia Kamani et al. (2021) reported two-mica orthogneisses with age 624 ± 3 Ma in the Pan-African Belt in Cameroon, which has been considered the continuation of the Pernambuco-Alagoas Domain in Africa, in pre-drift reconstruction. The isotopic signature of the two mica orthogneiss in Cameroon (zircon $\varepsilon Hf_{(t)}$ values varying from +2.9 to +5.2 – Kamguia Kamani et al., 2021) are distinct from the observed for the Quipapá granites, which has Paleoproterozoic Nd TDM model ages. The isotopic signature of the two-mica orthogneiss from Cameroon is like those recorded in granites from the Ipojuca-Atalaia subdomain of the Pernambuco-Alagoas Domain (Silva Filho et al., 2016), suggesting that this area in Cameroon was part of the Ipojuca-Atalaia subdomain in pre-drift reconstruction.

4.9. CONCLUSIONS

The mainly conclusions from this study are as follow:

1. The studied granites comprise biotite-muscovite leuco-syenogranites with modal biotite <8% and modal muscovite >10%. The most evolved facies have modal biotite <3%. They are weakly to strongly peraluminous, ferroan, alkalic-calcic and of the ilmenite-series. Similar crystallization ages, associated to similar petrographic composition and field relationship showing continuity between the two-mica granites in the area, strongly support our interpretation that the studied granites do not comprise two distinct intrusions (Quipapá and Jurema plutons), as proposed in the literature.
2. The Quipapá granites were generated by partial melting of metasedimentary rocks, with muscovite dehydration in the middle crust, at temperatures ranging from 677 to 788 ºC. The heating source was related to shear heating, radioactive heat, and basalt underplating. The best source candidate are metasedimentary rocks like those of the

Palmares Sequence. The biotite compositions and the presence of ilmenite suggest that the Quipapá granite magmas evolved under low to medium fO_2 conditions, near the FMQ buffer, with K-feldspar, ilmenite, and a small amount of biotite fractionation.

3. The Quipapá granites were intruded ca. 630 Ma, coevally with the peak of high-temperature regional metamorphism associated to the beginning of the compressive stage of the Brasiliano Orogeny.

ACKNOWLEDGEMENTS

This research is part of CCGB master's dissertation. CCGB thanks CAPES for supporting his studies with a scholarship, to Dr. Elson Paiva Oliveira- UNICAMP for the zircon CL-images. The project was financially supported by the Brazilian National Research Council - CNPq (Proc. 421353/2018-0).

REFERENCES

Archanjo, C.J., Hollanda, M.H.B.M., Viegas, L.G.F., 2021. Late Ediacaran lateral-escape tectonics as recorded by the Patos shear zone (Borborema Province, NE Brazil). Brazilian Journal of Geology. 51 (2).

Anderson, J.L., 1996. Status of thermobarometry in granitic batholiths. Trans R Soc Edinburgh 87: 125–138.

Abdel-Rahman, A.F.M., 1994. Nature of Biotites from Alkaline, Calc-alkaline, and Peraluminous Magmas. **Journal of Petrology**, 35:2:525–541.

Bau, M., 1996. Controls on the fractionation of isovalent trace elements in magmatic and aqueous systems: Evidence from Y/Ho, Zr/Hf, and lanthanide tetrad effect: Contributions to Mineralogy and Petrology, 123: 323–333.

Ballouard, C., Boulvais, P., Poujol, M., Gapais, D., Yamato, P., Tartèse, R., Cuney, M., 2015. Tectonic record, magmatic history and hydrothermal alteration in the Hercynian Guérande leucogranite, Armorican Massif, France: Lithos, 220–223:1–22

Ballouard, C., Poujol M., Boulvais P., Branquet Y., Tartèse R., Vigneresse J.-L., 2016. Nb-Ta fractionation in peraluminous granites: a marker of the magmatic-hydrothermal transition. **Geology**, 44(3): 231–234

Barbarin, B., 1996. Genesis of the two main types of peraluminous granitoids. Geology, 24 (4): 295–298.

Bea, F., 2012. The sources of energy for crustal melting and the geochemistry of heat-producing elements. Lithos, 153: 278–291.

Boehnke, P., Watson, E. B., Trail D., Harrison, T.M., Schmitt A.K., 2013. Zircon saturation re-revisited. Chemical Geology, 351: 324–334.

Brito Neves, B.B., 1995. Crátons e faixas móveis. Boletim de Geociências da USP, 1: 1–187

Brito Neves, B.B. and Cordani, U.G., 1991. Tectonic evolution of South América during Late Proterozoic. Precambrian Research, 53: 23–40.

Brito Neves, B.B., Van Schmus, W.R., Fetter, A., 2002. Northwestern Africa-North-eastern Brazil. Major tectonic links and correlation problems. J. Afr. Earth Sci., 34: 275–278.

Brito Neves, B. B., Passarelli, C.R., Basei, M.A.S., Santos, E.J., 2003. Idades U–Pb em zircão de alguns granitos clássicos da Província Borborema. Revista do Instituto de Geociências — USP 3: 25–38.

Buddington, A.F. and Lindsley, H.D., 1964. Iron-Titanium oxides minerals and synthetic equivalents. Journal of Petrology, 5(2): 310–357.

Bühn, B., Pimentel, M.M., Matteini, M., Dantas E.L., 2009. High spatial resolution analysis of Pb and U iso- topes for geochronology by laser ablation multi-collector inductively coupled plasma mass spectrometry (LA-MC- ICPMS). Anais da Academia Brasileira de Ciências, 81: 99–114.

Caby, R. 1989. Precambrian terranes of Benin Nigeria and Northeast Brazil and the Late Proterozoic South Atlantic fit. Geological Society of America Special Paper, 230: 145–158.

Castaing, C., Triboulet, C., Feybesse, J.L., Chèvremont, P., 1993. Tectonometamorphic evolution of Ghana, Togo, and Benin in the light of the Pan African/Brasiliano Orogeny. Tectonophysics, 218: 323–342.

Caxito, F.A., Uhlein, A., Stevenson, R., Uhlein, G.J., 2014. Neoproterozoic oceanic crust remnants in northeast Brazil. Geology, 42(5): 387–390.

Caxito, F.A., Uhlein, A., Dantas, E.L., Stevenson, R., Salgado, S.S., Dussin, I.A., Sial, A.N., 2016. A complete Wilson Cycle recorded within the Riacho do Pontal Orogen, NE Brazil: implications for the Neoproterozoic evolution of the Borborema Province at the heart of west Gondwana. Precambrian Research, 282:97–120.

Caxito, F.A., Santos, L.C.M.L., Ganade, C.E.; Bendaoud A., Fettous, El-Hocine; Bouyo M.H. 2020. Toward an integrated model of geological evolution for NE Brazil-NW Africa: the Borborema Province and its connections to the trans-Saharan (Benin-Nigerian and Tuareg shields) and Central African orogens. Brazilian Journal of Geology, 50(2).

Chappell, B.W., White, A.J.R., 1974. Two contrasting granite types. Pacific Geology 8:173–174

Chappell, B.W., White A.J.R., 2001. Two contrasting granite types: 25 years later. Australian Journal Earth Sciences 48: 489–499.

Clarke, D.B., 1981. The Mineralogy of Peraluminous Granites: A Review. Canadian Mineralogist, 19(1): 3–17.

Clark, C., Fitzsimons, I.C.W., Healy, D., Harley, S.L., 2011. How Does the Continental Crust Get Really Hot? Elements, 7(4): 235–240.

Clemens, J.D., Wall, V.J., 1981. Wall; Origin and crystallization of some peraluminous (S-type) granitic magmas. Canadian Mineralogist, 19 (1): 111–131.

Currie, C.A., Hyndman, R.D., 2006. The thermal structure of subduction zone back arcs. Journal of Geophysical Research, 111.

Dantas, E.L. Hackspacher, P.C., Van Schmus, W.R., Brito Neves, B.B., 1998. Archean accretion in the Sao Jose do Campestre Massif, Borborema Province, Northeast Brazil. Revista Brasileira de Geociências, 2(28):221 - 228.

Dantas, E.L., Van Schmus, W.R., Hackspacher, P.C., Fetter, A., Brito Neves, B.B., Cordani, U.G., Nutman, A.P., Williams, I.S., 2004. The 3.4–3.5 Ga Sao Jose do Campestre massif, NE Brazil: Remnants of the oldest crust in South America: Precambrian Research, 130: 113–137.

Dantas, E.L., Souza, Z.S., Wernicke, E., Hackspacher, Martin, H., Xiaodong, L., 2013. Crustal growth in the 3.4 to 2.7 Ga Sao Jose de Campestre Massif, Borborema Province, NE Brazil: Precambrian Research, 227: 120–156.

Deer, W.A., Howie, R.A., Zussman, J., 1992. An introduction to the rock-forming minerals. 2. ed., Harlow, Longman, 696p.

Dostal, J., Chatterjee, A.K., 1995. Origin of topaz-bearing and related peraluminous granites of the Late Devonian Davis Lake pluton, Nova Scotia, Canada: crystal versus fluid fractionation. **Chemical Geology**, 123(1-4): 67–88.

Dostal, J., Chatterjee, A.K., 2000. Contrasting behaviour of Nb/Ta and Zr/Hf ratios in a peraluminous granitic pluton (Nova Scotia, Canada): Chemical Geology, 163: 207– 218.

Dostal, J., Kontak, D.J., Gerel, O., Shellnutt, J.G., Fayek, M., 2015. Cretaceous ongonites (topaz-bearing albite-rich microleucogranites) from Ongon Khairkhan, Central Mongolia: Products of extreme magmatic fractionation and pervasive metasomatic fluid rock interaction, Lithos, (236–237): 173–189.

Ebadi, A., Johannes, W., 1991. Beginning of melting and composition of first melts in the system Qz-Ab-Or-H_2O-CO_2. Contributions to Mineralogy and Petrology, 106:286–295.

Ferreira, V.P., Sial, A.N., Jardim de Sá, E.F., 1998. Geochemical and Isotopic Signatures of Proterozoic Granites in Terranes of the Borborema Structural Province, Northeast Brazil. Journal of South American Earth Sciences, 11(5): 439–455.

Frost, B.R., Arculus, R.J., Barnes, C.G., Collins, W.J., Ellis, D.J., Frost, C.D., 2001. A geochemical classification of granitic rocks. Journal of Petrology 42(11): 2033–2048.

Ganade de Araujo, C.E., Weinberg, R.F.; Cordani, U.G., 2014. Extruding the Borborema Province (NE-Brazil): a two-stage Neoproterozoic collision process. Terra Nova, 26(2):157–168.

Ganade de Araújo, C.E., Cordani, U.G., Agbossoumounde, Y., Caby, R.; Basei, M.A.S., Weinberg, R.F., Sato, K., 2016. Tightening-up NE Brazil and NW Africa connections: New U-Pb/Lu-Hf zircon data of a complete plate tectonic cycle in the Dahomey belt of the West Gondwana Orogen in Togo and Benin. Precambrian Research, 276: 24–42.

Gardien, V., Thompson, A.B., Grujic, D., Ulmer, P., 1995. Experimental melting of biotite + plagioclase + quartz ± muscovite assemblages and implications for crustal melting. Journal of Geophysical Research: Solid Earth, 100(8): 15581–15591.

Guimarães, I.P., Silva Filho, A.F., Almeida, C.N., Van Schmus, W.R., Araujo, J.M.M., Melo, S.C., Melo, E.B., 2004. Brasiliano (Pan-African) granite magmatism in the Pajeu-Paraiba belt, Northeast Brazil: an isotopic and geochronological approach. Prec. Res. 135: 23–53.

Guimarães, I.P., Silva Filho, A.F., Almeida, C.N., Macambira, M.B., Armstrong, R., 2011. U-Pb SHRIMP data constraints on calc-alkaline granitoids with 1.3e1.6 Ga Nd TDM model ages from the Transversal domain of the Borborema province, NE Brazil. Journal of South American Earth Sciences. 31: 383–396.

Guimarães, I.P., Van Schmus, W.R., Brito Neves, B.B., Bittar, S.M.B., Silva Filho A.F., Armstrong R., 2012. U–Pb zircon ages of orthogneisses and supracrustal rocks of the Cariris Velhos belt: onset of Neoproterozoic rifting in the Borborema Province, NE Brazil. Precambrian Research, 192-195: 52–77

Guimarães, I.P.; Brito, M.F.L., Lages, G.A., Silva Filho, A.F., Santos, L., Brasilino, R.G. 2016. Tonian granitic magmatism of the Borborema Province, NE Brazil: a review. Journal of South American Earth Sciences, 68: 97–112.

Green, T.H., 1995. Significance of Nb/Ta as an indicator of geochemical processes in the crust-mantle system: Chemical Geology, 120:347–359.

Hanson G.N., 1978. The application of trace elements to the petrogenesis of igneous rocks of granitic composition. **Earth and Planetary Science Letters**, 38: 26-43.

Harrison, T.N., 1990. Chemical variation in micas from the Cairngorm pluton, Scotland. Mineralogical Magazine, 54(376), 355-366.

Hirth, G., Tullis, J., 1992. Jan. Dislocation creep regimes in quartz aggregates. **Journal of Structural Geology**, 14(2): 145-159

Holm, D.K., Dahl, P.S., Lux, D.R., 1997. $^{40}Ar/^{39}Ar$ evidence for Middle Proterozoic (1300-1500 Ma) slow cooling of the southern Black Hills, South Dakota, midcontinent, North

America: implications for early Proterozoic P-T evolution and post tectonic magmatism. **Tectonics**, 16(4): 609–622.

Holtz, F., Johannes, W., 1991. Genesis of peraluminous granites I. Experimental investigation of melt compositions at 3 and 5 kb and various H_2O activities. Journal of Petrology, 32: 935–958.

Inger, S. and Harris, N., 1993. Geochemical Constraints on Leucogranite Magmatism in the Langtang Valley, Nepal Himalaya**. Journal of Petrology,** 34(2): 345–368.

Jackson, S.E., Pearson, N.J., Griffin, W.L., Belouso- Va E.A., 2004. The application of laser ablation induc- tively coupled plasma mass spectrometry to in situ U-Pb zircon geochronology. Chemical Geology, 211: 47–69.

Jardim de Sá, E.F., 1984. A evolução Proterozoica da Província Borborema. In: Proceedings of the XI Geological Symposium of Northeast Brazil. Extended Abstract: p. 297–316.

Johannes W., Holtz F., 1996. Petrogenesis and Experimental Petrology of Granitic Rocks. Springer, Berlin.

Kalsbeek, F., Ekweume, B.N., Penaye, J., Souza Z.S., Thrane, K. 2013. Recognition of Early and Late Neoproterozoic supracrustal units in West Africa and North-East Brazil from detrital zircon geochronology. Precambrian Research, 226: 105 115.

Kamguia Kamani, M.S., Wang, W., Tchouankoue, J.P., Huang, S.F., Yomeun, B., Xue, E.K., Lu, G.M., 2021. Neoproterozoic syn-collision magmatism in the Nkondjock region at the northern border of the Congo craton in Cameroon: Geodynamic implications for the Central African orogenic belt. Precambrian Res. 353: 106015.

Le Breton, N. and Thompson, A.B. 1998. Fuid-absent (dehydration) melting of biotite in metapelites in the early stages of crustal anatexis. Contributions to Mineralogy and Petrology, 99: 226-237.

Leloup, P.H., Ricard, Y., Battaglia J., Lacassin, R. 1999. Shear heating in continental strike-slip shear zones: model and field examples. **Geophysical Journal International,** 136(1): 19-40

Linnen, R.L., Keppler, H., 1997. Columbite solubility in granitic melts: consequences for the enrichment and fractionation of Nb and Ta in the Earth's crust. Contrib. Mineral. Petrol. 128: 213–227.

Mariano, G., Neves, S.P., Silva Filho, A.F., Guimarães, I.P. 2001. Diorites of the high-K calc-alkalic association: Geochemistry and Sm-Nd Data and implications for the evolution of the Borborema Province, Northeast Brazil. International Geology Review, 10:921-929.

Massonne, H-J., Schreyer, W., 1987. Phengite geobarometry based on the limiting assemblage with K-feldspar, phlogopite and quartz, Contributions to Mineralogy and Petrology, 96:212-224.

Matteini, M., Dantas, E.L., Pimentel, M.M., Bühn, B., 2010. Combined U-Pb and Lu-Hf isotope analyses by laser ablation MC-ICP-MS: Methodology and applications. Anais da Academia Brasileira de Ciências. 82: 479–491.

Medeiros, V.C., 1998. Folha Garanhuns (SC.24-Y-B); CPRM, Recife, unpublished internal report. 22p.

Miller, C.F., Stoddard, E.F., Bradfish, L.J., Dollase, W.A., 1981. Composition of plutonic muscovite; genetic implications. *The Canadian Mineralogist*, 19(1): 25–34.

Miller, C.F., Mcdowell, S.M., Mapes, R.W. 2003. Hot and cold granites? Implications of zircon saturation temperatures and preservation of inheritance. **Geology**, 31(6): 529-530.

Monier, G. and Robert, J-L.1986. Muscovite solid solutions in the system K2O-MgO-FeO-Al_2O_3-SiO_2-H_2O: an experimental study at 2 kbar ph2o and comparison with natural li-free white micas. **Mineralogical Magazine**, 50(356): 257

Montel, J.M., Vielzeuf, D., 1997. Partial melting of metagreywackes, Part II. Compositions of minerals and melts. Contributions to Mineralogy and Petrology, 128(2-3): 176-196.

Nabelek, P.I., 2020. Petrogenesis of leucogranites in collisional orogens. Geological Society of London, Special Publications, 491: 179–207.

Nabelek, P.I., Liu, M., 1999. Leucogranites in the Black Hills of South Dakota: the consequence of shear heating during continental collision. **Geology**, 27(6): 523-526.

Nabelek, P.I. and Liu, M. 2004. Petrologic and thermal constraints on the origin of leucogranites in collisional orogens. **Earth and Environmental Science Transactions of The Royal Society of Edinburgh**, 95(1-2): 73–85.

Nabelek, P.I., Liu, M., Sirbescu, M.L., 2001. Thermo-rheological, shear heating model for leucogranite generation, metamorphism, and deformation during the Proterozoic Trans-Hudson orogeny, Black Hills, South Dakota. **Tectonophysics**, 342(3-4): 371–388.

Nabelek, P.I., Whittington, A.G., Hofmeister, A.M. 2010. Strain heating as a mechanism for partial melting and ultrahigh temperature metamorphism in convergent orogens: implications of temperature-dependent thermal diffusivity and rheology. **Journal of Geophysical Research**, 115(12): 1–17.

Nachit, H., Ibhi, A., Abia, E.H., Ohoud, M.B. 2005. Discrimination between primary magmatic biotites, reequilibrated biotites and neoformed biotites. **Comptes Rendus Geoscience**, 337(16): 1415–1420.

Nakamura, N.1974. Determination of REE, Ba, Fe, Mg, Na and K in carbonaceous and ordinary chondrites. **Geochimica et Cosmochimica Acta**, [S.L.], v. 38(5): 757–775.

Neves, S.P., 2003. Proterozoic history of the Borborema province (NE Brazil): correlations with neighboring cratons and Pan-African belts and implications for the evolution of western Gondwana. Tectonics, 22:1031–1044.

Neves, S.P., Bruguier, O., Vauchez, A., Bosch, D.; Silva, J.M.R., Mariano, G., 2006. Timing of crust formation, deposition of supracrustal sequences, and Transamazonian and Brasiliano metamorphism in the East Pernambuco belt (Borborema Province, NE Brazil): implications for western gondwana assembly. Precambrian Research, 149(3-4): 197–216.

Neves, S.P., Monié, P., Bruguier O., Silva, J.M. R. 2012. Geochronological, thermochronological and thermobarometric constraints on deformation, magmatism and thermal regimes in eastern Borborema Province (NE Brazil). Journal of South American Earth Sciences, 38: 129–146.

Neves, S.P., Bruguier, O., Silva, J.M.R., Mariano, G., Silva Filho, A.F., Teixeira, C.M.L., 2014. From extension to shortening dating the onset of the Brasiliano orogeny in eastern Borborema Province (NE Brazil). **Journal of South American Earth Sciences**, 58: 238-256.

Neves, S.P., Teixeira, C.M.L., Bruguier, O., 2020. Long-lived localized magmatism in central-eastern part of the Pernambuco-Alagoas Domain, Borborema Province (NE Brazil): implications for tectonic setting, heat sources, and lithospheric reworking. **Precambrian Research**, 337: 1–31.

Oliveira, E.P., Toteu, S.F., Araújo, M.N.C., Carvalho, M.J., Nascimento, R.S., Bueno, J.F., McNaughton, N., Basilici, G., 2006. Geologic correlation between the Neoproterozoic Sergipano belt (NE Brazil) and the Yaoundé belt (Cameroon, Africa). Journal of African Earth Sciences, 44: 470–478.

Oliveira, P., Windley, B.F., Araújo, M.N.C., 2010. The Neoproterozoic Sergipano orogenic belt, NE Brazil: a complete plate tectonic cycle in western Gondwana. Precambrian Research, 181(1-4): 64–84.

Osako, L., 2005. Caracterização Geológica da região entre as localidades de Paranatama e Curral Novo, PE, porção centro-norte do complexo Pernambuco-Alagoas, Província Borborema. Doutoral thesis (in Portuguese), Universidade Federal de Pernambuco – UFPE, Brazil, 163 pp.

Patiño Douce, A.E., 1999. What do experiments tell us about the relative contributions of crust and mantle to the origin of granitic magmas? Geological Society, London, Special Publications, 168: 55-75.

Patiño Douce, A.E., Beard, J.S., 1995. Dehydration-melting of Biotite Gneiss and Quartz Amphibolite from 3 to 15 kbar. Journal of Petrology, 36(3): 707-738.

Patiño Douce, A.E., Harris, N. 1998. Experimental Constraints on Himalayan Anatexis. Journal of Petrology, 39(4): 689–710.

Pearce J., Harris N.B.W. Tindle A.D., 1984. Trace element discrimination diagrams for the tectonic interpretation of granitic rocks. Journal of Petrology, 25: 956-983.

Pearce J. 1996. Sources and setting of granitic rocks. **Episodes**, 19 (4):120-125.

Pessoa R. J. R., Ferreira V.P., Sial A.N., 1996. Carta plutônica do Nordeste: petrográfica e litogeoquímica do leucogranito de Ouro Branco, Alagoas. 34th Congresso Brasileiro de Geologia, Salvador 6, 439–442.

Pëto, P., 1976. An experimental investigation of melting relations involving muscovite and paragonite in the sílica-saturated portion of the system K_2O-Na_2O-Al_2O_3-SiO_2-H_2O to 15Kbar total pressure. Progress in experimental petrology, 3: 41–45.

Pichavant M., Montel J-M., Richard L.R., 1992. Apatite solubility in peraluminous liquids: Experimental data and an extension of the Harrison-Watson model. Geochimica et Cosmochimica Acta, 56(10): 3855–3861.

Pitcher, A.W., 1993. The nature and Origin of granites. London, Blackie Academic and Professional, 321p.

Pryer, L.L., Robin, P.Y.F., 1996. Differential stress control on the growth and orientation of flame perthite: a palaeostress-direction indicator. Journal of Structural Geology, 18(9): 1151–1166.

Pryer, L.L., Robin, P.Y F., 1995. Retrograde metamorphic reactions in deforming granites and the origin of flame perthite. Journal of Metamorphic Geology, 13(6): 645-658.

Raimbault, L., Cuney, M., Azencott, C., Duthou, J.-L., Joron, J.L., 1995. Geochemical evidence for a multistage magmatic genesis of Ta-Sn-Li mineralization in the granite at Beauvoir, French Massif Central: Economic Geology and the Bulletin of the Society of Economic Geologists, v. 90: 548–576.

René, M., Holtz, F., Luo, C., Baermann O., Stelling, J., 2008. Biotite stability in peraluminous granitic melts: compositional dependence and application to the generation of two-mica granites in the south bohemian batholith (bohemian massif, Czech Republic). Lithos, 102(3-4): 538–553.

Rieder, M., 1997. Nomenclature of the Micas. Clays and Clay Minerals, (5): 586-595.

Santos, E.J., 1995. O complexo granítico Lagoa das Pedras: Acresção e colisão na região de Floresta (Pernambuco) Província da Borborema. Doutoral thesis (in Portuguese), Universidade de São Paulo – USP, Brazil, 249 pp.

Santos E.J., Brito Neves, B.B., Van Schmus W.R., Oliveira R.G., Medeiros V.C., 2000. An overall view on the displaced terrane arrangement of the Borborema Province, NE Brazil. In: International Geological Congress, 31th, Rio de Janeiro, Brazil, General Symposia, Tectonic Evolution of South American Platform, 5–9.

Santos, E.J., Van Schmus, W.R., Kozuch, M., Brito Neves, B.B., 2010. The Cariris Velhos tectonic event in Northeast Brazil. Journal of South American Earth Sciences, 29(1): 61–76.

Santos, L.C.M., Dantas, E.L., Vidotti, R.M., Cawood, P.A., Santos, E.J., Fuck, R.A., Lima, H.M., 2017. Two-stage terrane assembly in Western Gondwana: Insights from structural geology and geophysical data of Central Borborema Province, NE Brazil. J. Struct. Geology, 103: 167–184.

Santos, L.C.M.L., Dantas, E.L., Cawood, P.A., Lages, G.A., Lima, H.M., Santos, E.J., 2018. Accretion tectonics in western Gondwana deduced from Sm-Nd isotope mapping of terranes in the Borborema Province, NE Brazil. Tectonics, 37: 2727–2743.

Sawyer, E.W., Cesare, B., Brown, M., 2011. When the continental melts. Elements, 7: 229–234.

Sial, A.N., 1986. Granite-types of Northeast Brazil: current knowledge. *Revista Brasileira de Geociências*, 16:54–72.

Siégel, C., Bryan, S.E., Allen, C.M., Gust, D.A., 2018. Use and abuse of zircon-based thermometers: A critical review and a recommended approach to identify antecrystic zircons. Earth-Science Reviews 176, 87–116.

Silva Filho, A.F., Guimarães I.P., Van Schmus W.R. 2002. Crustal evolution of the Pernambuco–Alagoas Complex, Borborema Province, NE Brazil; Nd isotopic data from Neoproterozoic granitoids. Gond Res 5: 409–422.

Silva Filho, A. F., Guimarães, I. P., Rangel, J. M., Brasil, E., Lima, D., 2010. Programa Geologia do Brasil - PGB. Palmares. Folha SC.25-V-A-IV. Estado de Pernambuco. Carta Geológica e de Recursos Minerais. Recife/CPRM. 1:100.000. Online. http://www.cprm.gov.br

Silva Filho, A.F., Guimarães I.P., Van Schmus W.R., Armstrong R.A., Silva J.M.R., Osako L.S., Cocentino L.M., 2014. SHRIMP U–Pb zircon geochronology and Nd signatures of supracrustal sequences and orthogneisses constrain the Neoproterozoic evolution of the Pernambuco–Alagoas domain, southern part of Borborema Province, NE Brazil. **International Journal of Earth Sciences**, 103(8): 2155–2190.

Silva Filho, A.F., Guimarães, I.P., Santos, L., Armstrong, R., Van Schmus, W.R., 2016. Geochemistry, U-Pb geochronology, Sm-Nd and O isotopes of ca. 50 Ma long Ediacaran High-K Syn-Collisional Magmatism in the Pernambuco Alagoas Domain, Borborema Province, NE Brazil. Journal of South American Earth Sciences, 68:134–154.

Stepanov, A., Mavrogenes J.A., Meffre S., Davidson P., 2014. The key role of mica during igneous concentration of tantalum. **Contr. to Mineralogy and Petrology,** 167(6): 1009–1016.

Sylvester, P.J., 1998. Post-collisional strongly peraluminous granites. Lithos, 45(1-4): 29–44.

Stussi, J.M. and Cuney, M., 1996. Nature of biotites from alkaline, calc-alkaline and peraluminous magmas by Abdel-Fattah M. Abdel-Rahman: a comment. Journal of Petrology, 37: 1025–1029

Tartèse, R., Boulvais, P., 2010, Differentiation of peraluminous leucogranites “en route” to the surface: Lithos, 114: 353–368.

Tappert M.C., Rivard B., Giles, D., Tappert R., Mauger A., 2013. The mineral chemistry, near infrared, and mid-infrared reflectance spectroscopy of phengite from the Olympic Dam IOCG deposit, South Australia. **Ore Geology Reviews,** 53: 26–38.

Thompson, R.N., 1982. Magmatism of the British Tertiary Volcanic Province. **Scottish Journal of Geology,** 18(1): 49–107.

Toteu, S.F., Penaye, J., Van Schmus, W.R., Michard A., 1994. Preliminary U-BP and Sm–Nd geochronologic data on the North-Central of Cameroon: contribution of an Archean and Paleoproterozoic crust to the edification of an active domain of the Pan African orogeny. C.R. Acad. Sci. Paris, 319: 1519–1524.

Toteu, S.F., Van Schmus, W.R., Penaye, J., Michard, A., 2001. New U–Pb and Sm–Nd data from north-central Cameroon and its bearing on pre-Pan African history of central Africa. Precambrian Res., 108: 45–73.

Trompette, R., 1994. Geology of Western Gondwana. A. Balkema, Amsterdam. p. 350.

Van Schmus, W.R., Brito Neves, B.B., Hackspacher, P., Babinski, M. 1995. U/Pb and Sm/Nd geochronolgic studies of eastern Borborema Province, northeastern Brazil: initial conclusions. Journal of South American Earth Sciences, 8(3-4): 267–288.

Van Schmus, W.R., Oliveira E.P., Silva Filho, A.F., Toteu, F., Penaye, J., Guimarães, I.P., 2008. Proterozoic Links between the Borborema Province, NE Brazil, and the Central African Fold Belt. Geological Society, London, Special Publication, 294: 69–99.

Van Schmus, W.R., Kozuch, M., Brito Neves, B.B., 2011. Precambrian history of the Zona Transversal of the Borborema Province, NE Brazil: Insights from Sm-Nd and U-Pb geochronology. Journal of South American Earth Sciences, 31(2-3): 227–252.

Viegas, L.G.F., Archanjo, C.J., Hollanda, M.H.B.M., Vauchea, A., 2014. Microfabrics and zircon U-Pb (SHRIMP) chronology of mylonites fromthe Patos shear zone (Borborema Province, NE Brazil). Precambrian Research. 243: 1–17.

Vielzeuf, D., Holloway, J.R., 1988. Experimental determinations of fluid-absent melting relations in the politic system. Contr. to Mineralogy and Petrology, 90: 257–76.

Vielzeuf, D., Montel, J.M., 1994. Partial melting of metagreywackes. Part I. Fluid-absent experiments and phase relationships. Contr. to Mineralogy and Petrology, 117: 375–393.

Villaseca, C., Barbero, L., Herreros, V., 1998. A re-examination of the typology of peraluminous granite types in intracontinental orogenic belts. Earth and environmental science and transactions of the Royal Society of Edinburg, 89: 113–119.

Watson, E.B., Harrison, T.M., 1983. Zircon saturation revisited: temperature and composition effects in a variety of crustal magma types. Earth and Planetary Science Letters, 64: 295–304.

Weinberg, R.F., Hasalová, P., 2015. Water-fluxed melting of the continental crust: A Review. **Lithos**, (212-215): 158-188

ARTIGO 2 – PETROGENESIS OF EDIACARAN LEUCOGRANITES IN THE BORBOREMA PROVINCE, NE BRAZIL: U-Pb ZIRCON GEOCHRONOLOGICAL, GEOCHEMICAL AND Lu-Hf ISOTOPIC DATA CONSTRAINTS

Brainer C.C.G.[1], Guimarães I.P.[1], Silva Filho A.F.[1], Lima J.V.[1], Lana C.[2]

[1]Geosciences Post Graduation Programme - Pernambuco Federal University, Brazil

[2] Geosciences Post Graduation Programme - Ouro Preto Federal University, Brazil

ABSTRACT

Two-mica and biotite leucogranites occur through all Borborema Province with ages within 640-600 Ma and 590-560 Ma intervals. The only occurrence of two-mica granites within the Transversal subprovince, the Mamanguape pluton, were studied in detail in this work. It comprises muscovite, biotite sieno- to monzogranite intruded in metasedimentary rocks. The Mamanguape pluton like others peraluminous leucogranites from the Borborema Province are ferroan and alkali-calcic. The spidergrams of the Mamanguape granites are characterized by troughs at Ba, Nb, Sr, P and Ti. The REE patterns are fractionated, with (Ce/Yb)N ratios ranging from 12 to 15, and characterized by deep negative Eu anomalies, with Eu/Eu* ratios varying between 0.18 and 0.25. The geochemical signature of the two-micas granites of the Mamanguape pluton is like others peraluminous leucogranites from the Borborema Province with crystallization ages related to the contractional (640 - 600 Ma) and transcurrent (580 - 560 Ma) stages of the Brasiliano/Pan-African Orogeny. Their generation is interpreted as the result of partial melting of metasedimentary rocks, involving muscovite dehydration melting process. The crystallization ages of the two- mica Mamanguape granites suggest intrusion related to the transcurrent stage of the Brasiliano Orogeny. Zircon xenocrysts with Cryogenian to Ediacaran ages, ƐHf(t) values ranging between +1.4 and -13.7, and Hf TDM model age between 1.4 and 2.2 Ga, suggest that the magma was generated by partial melting of metasedimentary rocks that received a large contribution of Cryogenian/Ediacaran igneous sources and small contribution of mantle melts. Mantle melt contributing to the source of the two-mica granites is support by the presence of mafic enclaves.

Keywords: Leucogranites. Two-mica granites. Biotite granites. Geochemistry. Geochronology. Borborema Province.

5.1. INTRODUCTION

Granite is the most abundant rock in the continental crust, displaying great diversity of chemical and isotopic composition. The relative contributions of mantle and crust-derived components is of crucial importance to specific granites genesis, and to understanding the origin and evolution of the continental crust. Chappell and White (1974) based on the granites of the Lachlan fold belt of eastern Australia, proposed the S–I classification (Alphabetic classification), in which S-type granites, comprise strongly peraluminous mafic minerals such as cordierite, derived from partial melting of supracrustal metasedimentary rocks, while the I-type granites comprise metaluminous to weakly peraluminous amphibole granites, derived from partial melting of igneous infracrustal rocks. Subsequent papers (Chappell 1984, 1999; Chappell and White 1992, 2001; Chappell et al. 1987, 2004, 2012) emphasized that granitic composition is only dependent of its source, and to explain the compositional variability of the S- and I-type granites, Chappell et al. (1987) proposed the restite-unmixing hypothesis. However, the hypothesis that the chemical composition of granites is the image of their source is not well accepted. Instead, many papers emphasized the importance of mantle derived melts, reworking metasedimentary rocks (Keay et al. 1997; Kemp et al. 2007; Brown 2013), or mixing with melts generated by fusion of supracrustal metamorphic rocks (Patiño Douce 1999). According to Clemens et al. (2011) and Clemens and Stevens (2012) the I-type granites magma are generate in the crust, but from source involving mantle and crustal components. Patiño Douce (1999) based on experimental studies, concluded that only peraluminous granites, such as muscovite-bearing granites, represent pure crustal sources melts derived by dehydration melting of muscovite-rich metasedimentary rocks.

Bonin et al. (2020) argue against the alphabetic classification, due to rocks crystallized from magmas generated by partial melting of immature greywackes, would acquire geochemistry signature like I-type granites with low ASI values. The ASI values of felsic I-type granites also tend to overlap those of S-type (Chappel, 1999). According to Zen (1986), only pockets of peraluminous melts can be formed through extreme fractional crystallization of amphiboles and pyroxenes or, by extensive fractionation of feldspars from a mafic metaluminous melt. Because S-type granites were defined as cordierite-bearing granites, the S-type cannot be used to define all peraluminous granites.

In collisional orogens, peraluminous granites constitute the dominant magmatic feature, and their generation are related to crustal thickening and the active deformation and metamorphism of metapelites (Nabelek 2020). In thick collisional orogens, the mantle heat is

unable to promote crustal melting, and the thermal models for the generation of peraluminous granites can involve flux melting, radiogenic heat, decompression, or shear heating (Nabelek 2020). The principal process that generates peraluminous melts are muscovite and/or biotite-dehydration melting and muscovite vapor present reactions (Nabelek 2020).

In all subprovinces of the Borborema Province (Fig. 1), peraluminous granites with ages ranging from 630 to 560 Ma are reported syn-collision (Brainer et al., 2021, Silva Filho et al. 2021) and syn- to late-transcurrence (Neves et al., 2020; Amorim et al., 2019; Santos et al. 2015). They comprise two-mica granites, which is a typical mineralogy of peraluminous granites (Clarke 1981) and slightly peraluminous to metaluminous biotite granites.

This work presents and discuss the petrography, geochemistry, Lu-Hf isotopic signature and U-Pb zircon geochronology of the Mamanguape pluton, a two-mica leucogranite, intruded in metasedimentary rocks of the Transversal subprovince, which constitute up to now, the only occurrence of two-mica granites in this area, and compare their geochemical and isotopic signature with peraluminous leucogranites from others subprovinces of the Borborema Province. We also show the geochemical and source differences between the biotite and the two-mica leucogranites and discuss the heat source promoting melting. Our data provide further constraints on the petrogenesis of the two-mica granites and aim to contribute with the evolution of the Borborema Province during the Brasiliano/Pan-African Orogeny.

Figura 19 – Figure 1 – Geologic Map of Borborema Province modified from Medeiros et al. (2021) with peraluminous leucogranites numbered. 1 = Banabuiu pluton (Lima et al., 2014); 2 = Dona Inês pluton (Guimarães et al., 2016); 3 = Mamanguape pluton (This work); 4 = Serra Branca pluton (Santos, 2013); 5 = Garanhuns pluton (Neves et al., 2020); 6 = Chã Grande and Cabanas plutons (Neves et al., 2020), Quipapá and Jurema plutons (Brainer et al., 2021); 7 = Xingó Complex (Guimarães e Silva Filho 1995), Poço Redondo, Angico, Areias, Santa Helena and Glória plutons (Oliveira et al., 2015), Glória Sul pluton (Conceição et al., 2016)

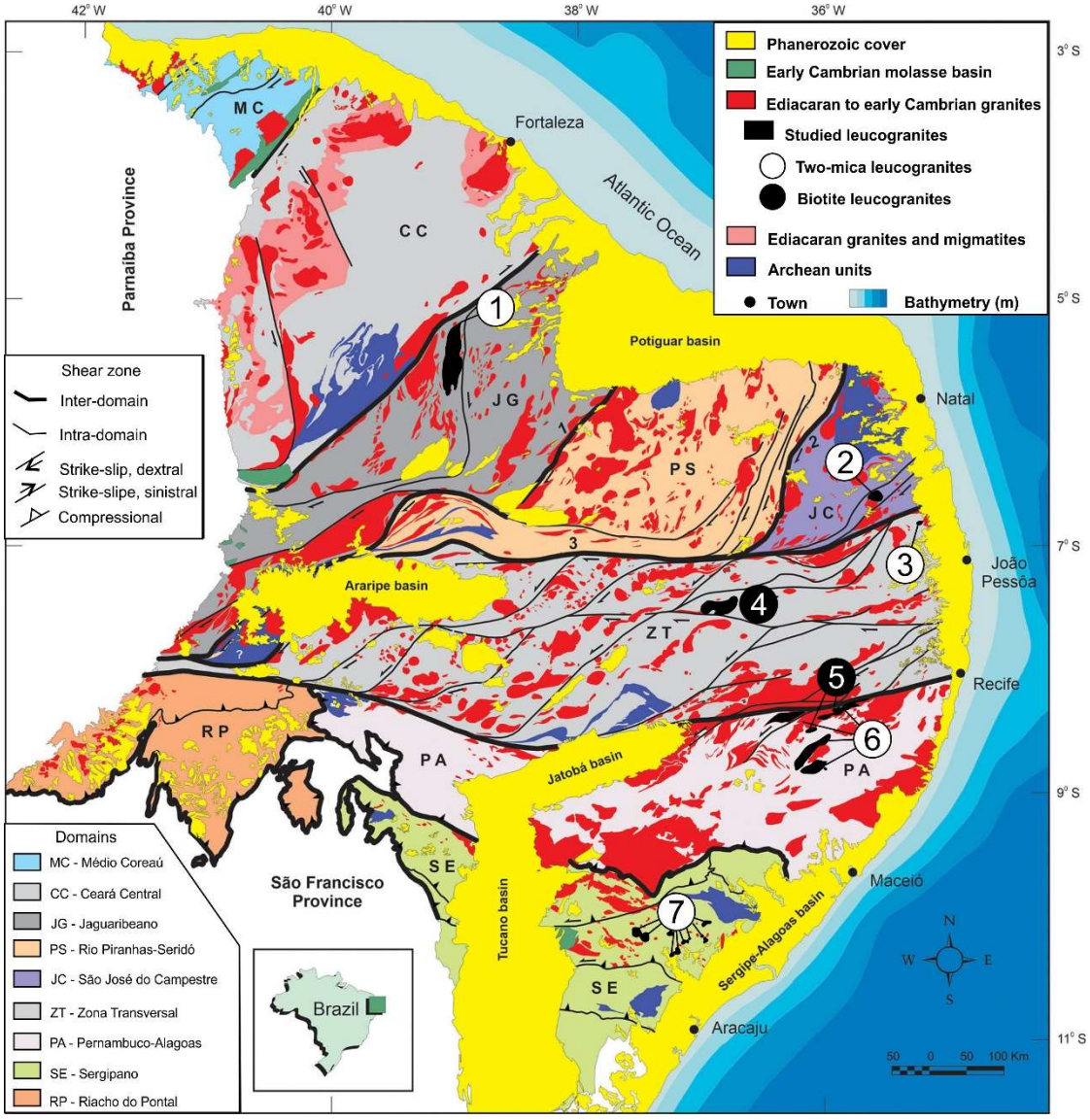

5.2. GEOLOGICAL SETTING

The Borborema Province (Almeida et al. 1981) comprises most of the northeastern Brazil. It is limited to the north and east by the coastal basins, to the south by the São Francisco Craton and to the west by the Parnaíba Basin. According to Van Schmus et al. (2008), the Borborema Province comprehends an orogenic belt localized in the northwestern part of Gondwana, in pre-drift reconstructions.

The Borborema Province comprises a basement composed of gneisses and migmatites complexes of Paleoproterozoic ages (Van Schmus et al., 1995, 2008, 2011) with small Archean nuclei (Dantas et al., 1998, 2004), Neoproterozoic supracrustal sequences of Tonian and Criogenian/ Ediacaran ages (Santos 1995, Brito Neves et al. 2001, dos Santos et al. 2010, Guimarães et al., 2012), magmatism with Paleoproterozoic to Neoproterozoic ages (Sial, 1986; Ferreira et al. 1998, 2011; Guimarães et al., 2004, 2009, 2011; Neves et al., 2008, 2020; Silva Filho et al., 2016) and transcurrent E-W to NE-SW trending shear zones of continental scale, with counterparts on the African continent (Caby et al., 1981; Bertrand and Jardim de Sá, 1990; Castaing et al., 1994; Toteu et al., 2001; Oliveira et al., 2006; Van Schmus et al., 2008).

Van Schmus et al. (1995) used the Neoproterozoic dextral ductile kinematics E – W trending Patos and Pernambuco shear zones, to divide the Borborema Province in three subprovinces (Van Schmus et al., 2011): 1) Northern subprovince, localized on the north of Patos shear zone; 2) Central or Transversal, between Patos and Pernambuco shear zones and the Southern, south of Pernambuco shear zone. Each subprovince was subdivided in many domains (Fig. 1), following previous divisions (Brito Neves, 1982; Santos, 1995, 2010; Brito Neves et al. 2000, 2001; Van Schmus et al, 1995; 2008 among others): The Northern subprovince comprises the Medio Coreaú, Ceara Central, Orós - Jaguaribeano, Seridó and Rio Grande do Norte domains. In this subprovince, a mega structure, Transbrasiliano - Kandi - 4º50′ transcontinental Lineament, separates the Medio Coreau and Ceará Central domains. This lineament was interpreted as the main collisional suture zone of West Gondwana (Caby, 1989; Arthaud et al., 2008, Cordani et al., 2013; Ganade de Araujo et al., 2014, among others).

The Southern subprovince comprises the Pernambuco – Alagoas, Sergipano, Rio Preto and Riacho do Pontal domains. To the south, this subprovince contacts the São Francisco cratonic block. Detailed U-Pb zircon data from metasedimentary sequences of the Pernambuco - Alagoas domain and Transversal subprovince suggest that the East part of the Pernambuco Lineament (East Pernambuco Lineament of Neves et al., 2004) is not the north limit of the Southern subprovince (Neves et al., 2020; Silva Filho et al., 2021).

The Transversal subprovince was subdivided in: Piancó - Alto Brígida (PAB), Alto Pajeú (AP), Alto Moxotó (AM) and Rio Capibaribe (RC). The Mamanguape Pluton is localized in the Alto Pajeú Domain, one of the most studied areas from the Transversal subprovince. Brito Neves et al. (1995) recognized a belt, designated of Cariris Velhos, in the Alto Pajeú domain, composed of metasedimentary rocks, bimodal metavolcanic rocks intruded by Tonian metaplutonic rocks. This belt was interpreted as formed through a complete orogenic circle by many authors (Brito Neves et al., 1995; Santos, 1995; Brito Neves et al., 2001; Kozuch, 2003; Santos et al., 2010; Caxito et al, 2020, 2021). However, some others consider that the belt represents a continental rift, intruded by intraplate granites, deformed, and metamorphosed during the Brasiliano Orogeny (Neves, 2003, Guimarães and Brito Neves, 2004, Guimarães et al., 2012, 2016; Neves et al., 2004). and abundant Ediacaran/Cryogenian granitic magmatism (Sial, 1986; Ferreira et al., 2004, 2011; Sial and Ferreira, 2016; Guimarães et al., 2004, 2011).

In the Borborema Province, Northeastern Brazil, the Brasiliano Orogeny (630-540 Ma) was characterized by intense granitic magmatism (Sial 1986, Ferreira et al. 1998,2011, Brito Neves et al. 2003, Guimarães et al. 2004, Guimarães et al. 2011, Silva Filho et al. 2016, Neves et al. 2020) and large-scale shear zones (Vauchez et al. 1995). Peraluminous granites are reported in all subprovinces (Van Schmus et al., 2011) of the Borborema Province (Fig. 1), with ages ranging from 630 to 560 Ma. They are classified as two-mica granites, which is a typical mineralogy of peraluminous granites (Clarke 1981) and slightly peraluminous to metaluminous biotite granites.

During the Brasialino Orogeny an extensive shear zones system, was developed and interpreted either as an accretionary orogens forming at intraoceanic and continental margin convergent plate boundaries (Brito Neves et al., 2000; Cavalcante et al., 2003; Fuck et al., 2008) or an intracontinental orogeny that reworked a Paleoproterozoic accretionary orogen during the Neoproterozoic (Neves, 2015).

Several geodynamics models have been proposed to describe the late Neoproterozoic evolution of the Borborema Province. Some authors defended accretion of distinct tectonostratigraphic terranes (Santos 1995; Brito Neves et al., 2000), others (Ganade de Araujo et al., 2014; Oliveira et al., 2010; Caxito et al., 2016, 2020) argue in favor of a complete Wilson Cycle model involving rifting, ocean closures, subduction, and collision, while intracontinental models based on extension and convergence of blocks were proposed by Neves (2003, 2011, 2015).

5.3. GEOLOGY AND PETROGRAPHY OF TWO – MICA GRANITES

The Mamanguape pluton occur as a small pluton (Fig. 2a) intruded in the garnet-muscovite-biotite paragneisses of the the Sertânia Complex, being partially covered by Cenozoic sediments. It comprises fine to medium-grained equigranular and slightly porphyritic leucocratic sienogranites with mineral assemblage composed by quartz, K-feldspar, plagioclase, muscovite, and biotite. Two distinct facies were observed based on the modal proportion of biotite and presence of K-feldspar phenocrysts about 1 cm long. Xenoliths of metasedimentary rocks, partially digested, are commonly observed in the Mamanguape pluton (Fig. 2b). Although rare, mafic enclaves with elongated shape were recorded.

Quartz occurs as anhedral crystals exhibiting undulatory extinction and sub grains formation (Fig. 2c). Microcline occurs as large subhedral phenocrystals exhibiting tartan twinning and flame perthites (Fig. 2c). Myrmekite replacing the margins of K-feldspar grains are recorded locally, which according to Vernon (1991, 2000) is evidence of fluid percolation during deformation (“solid-state flow”). Plagioclase occurs as small subhedral crystals showing common alteration to sericite. Muscovite appears as large euhedral to subhedral crystals (Fig. 2d), while biotite occurs as small euhedral and subhedral crystals associated with muscovite and showing locally alteration to chlorite (Fig. 2d). Ilmenite, apatite, zircon, and monazite are the accessory phases.

Figura 20 – Figure 2 – (a) Overview of a Mamanguape pluton outcrop, (b) Angular metasedimentary xenolith, enclosed by the Mamanguape granites (c) Fractured K-feldspar phenocryst with flame perthite, (d) Large muscovite crystals (Ms) associated with small biotite flakes.

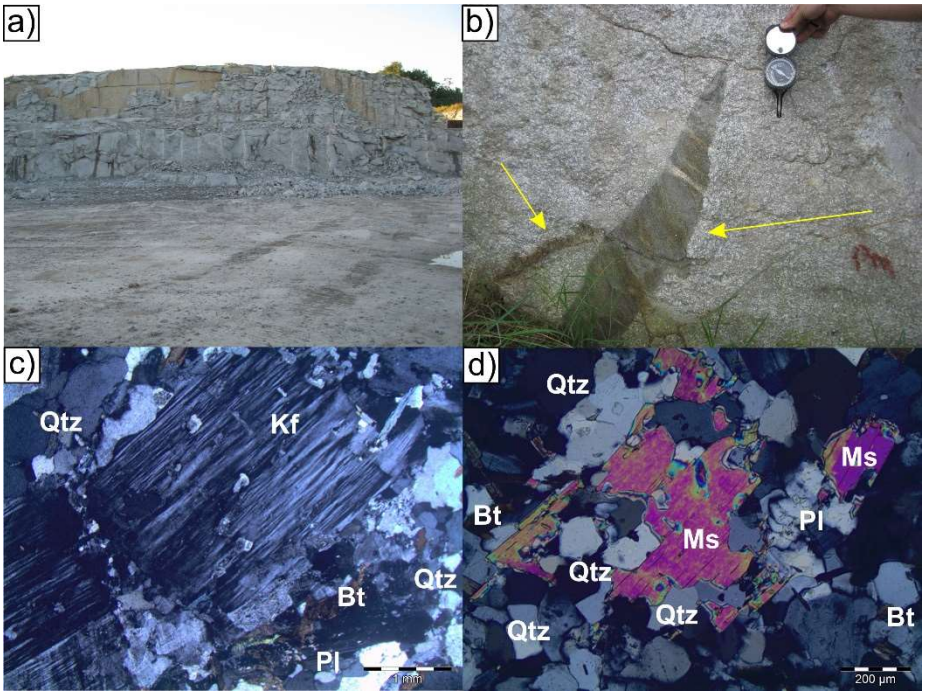

5.4. GEOCHEMISTRY

Whole rock geochemical analyses for major and trace elements were realized at the ALS laboratory - Canada by inductively coupled plasma-mass spectrometry (ICP-MS). The results are shown in Table A8.

The Mamanguape pluton show high SiO_2 (72.7-74.4%) and Al_2O_3 (13.6-14.15%) values, total alkalis ($K_2O + Na_2O$) contents (ranging between 8.28 and 9.19 wt. %), K2O/Na2O ratios varying between 1.37 and 2.53 and low CaO contents (0.6–1.01). They are peraluminous with alumina saturation index (ASI) ranging from 1.08 to 1.13 (Fig 3a), show high FeOt/(FeOt+MgO) ratios (0.84-0.85), and are classified as ferroan. (Fig. 3b) and alkali-calcic (Fig. 3c).

Figura 21 – Figure 3 – (a) ASI index diagram after Shand (1943) for the Mamanguape pluton and others leucogranites from the Borborema Province. (b) $FeO_t/(FeO_t+MgO)$ versus SiO_2 diagram proposed by Frost et al., (2001) and (c) Modified Alkalis – Lime index (MALI) versus SiO_2 diagram (Frost et al., 2001).

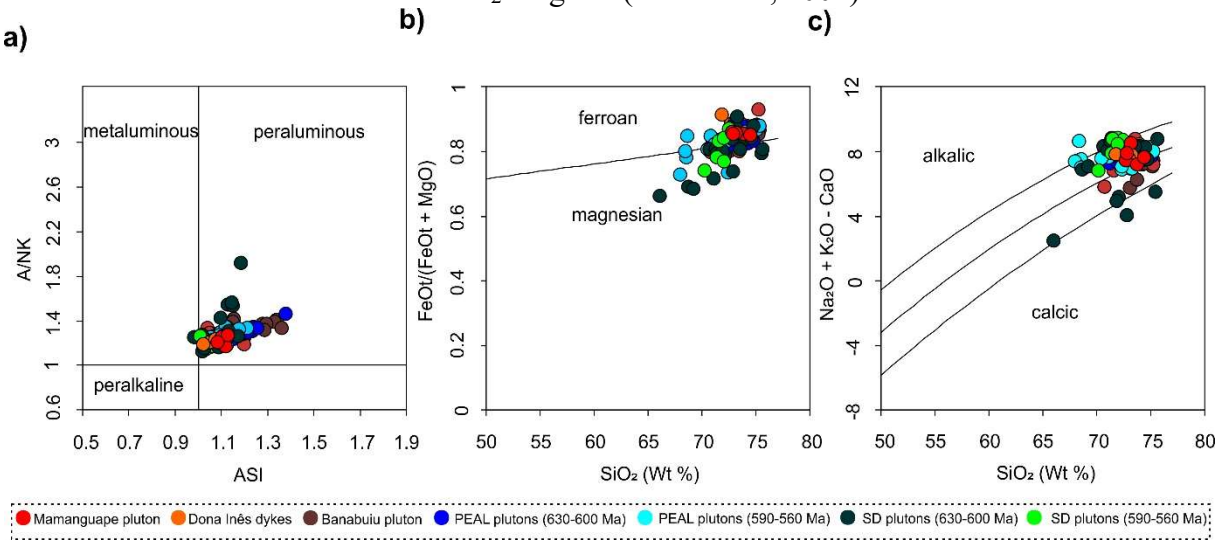

Leucogranites from other subprovinces display similar geochemical aspects, with SiO_2 ranging from 70 to 75%, total alkalis content also has a similar trait (7.3-10.2%), K_2O/Na_2O ratios with slightly different values (0.78-2.53) and CaO values varying between 0.35 and 2%. They show a ASI >1 and FeOt/(FeOt+MgO) ratios (0.73-0.94), being classified in its majority as ferroan (Fig. 3b). The majority of samples are classified as alkali-calcic (Fig. 3c).

The samples from leucogranites of Sergipano beld display a slightly different geochemical aspect, with SiO_2 ranging from 66 to 76% and samples with total alkalis ranging from 5.67 to 9.96 % (mean: 8.76%). They have ASI ranging from 0.98 to 1.3, FeOt/(FeOt+MgO) values between 0.66 and 0.91 (Fig. 3b) and have samples classification in MALI diagram varying from calcic to slightly alkali (Fig. 3c).

The REE patterns of the Mamanguape granites, normalized to the chondrite values of Nakamura (1974), show low fractionation (Fig. 4a), with $(Ce/Yb)_N$ ratios ranging from 11.99 to 15.12, and are characterized by pronounced negative Eu anomalies, with Eu/Eu* ratios varying between 0.18 and 0.25. Granites from other subprovinces of the Borborema Province also show enrichment in LREE over HREE in variable degrees (Fig. 4b, 4c and 4d) and negative Eu anomalies, except the granitoids from the Sergipano belt, that have REE patterns characterized by lack of Eu anomalies. The REE patterns of the biotite leucogranites are less fractionated and characterized by deeper negative Eu anomalies (Fig 4b).

Figura 22– Figure 4 – Chondrite normalized REE patterns (Nakamura, 1974) for Mamanguape pluton (a), Northern subprovince (b), Southern subprovince subdivided in PEAL Domain (c) and Sergipano Belt (d).

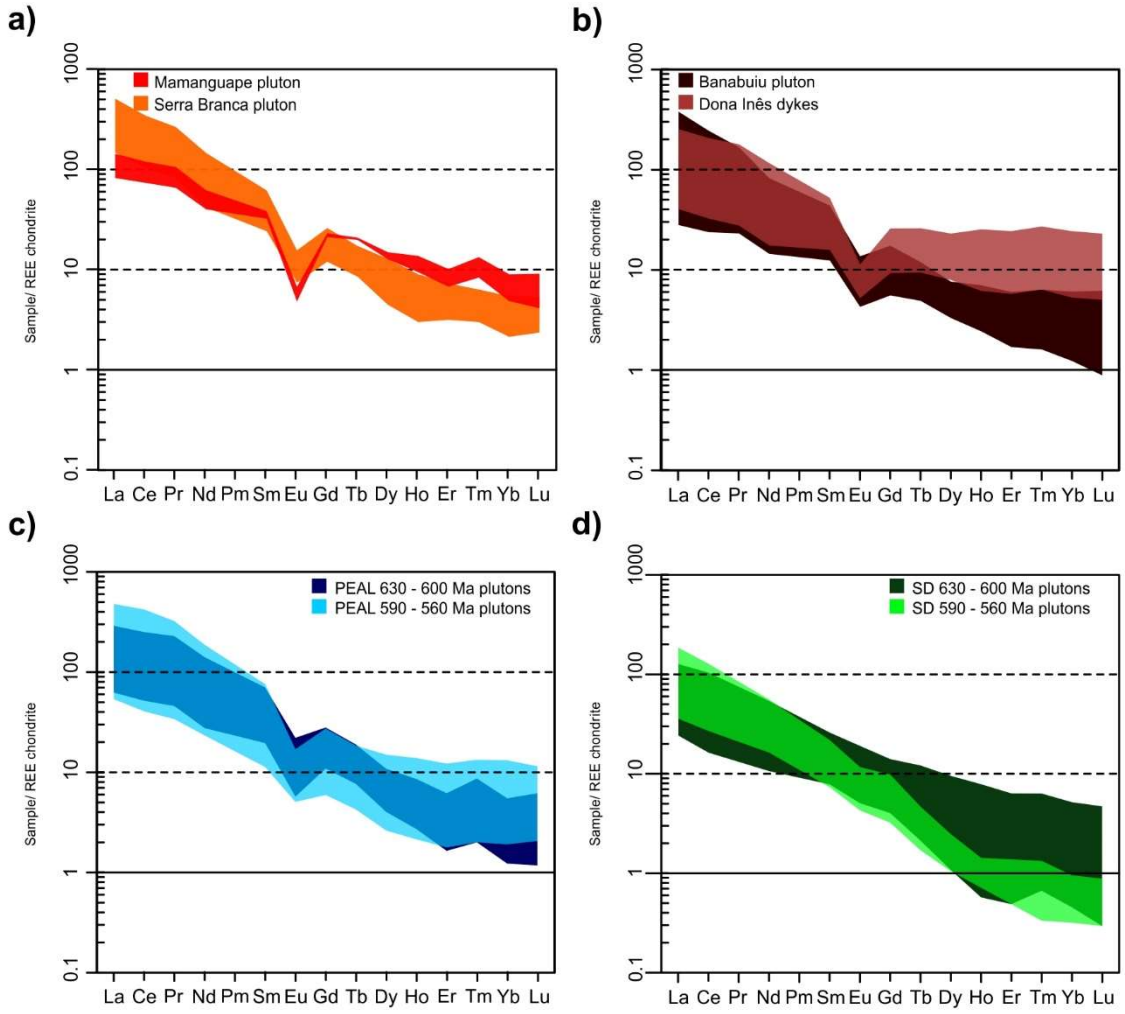

The multielement variation diagrams, normalized to the values suggested by Thompson (1982), all analyzed samples from the Mamanguape pluton show identical patterns, except for little variation, concerning slightly lower contents of Sr, La, Ce, and ETRP recorded in one sample. In general, the patterns are characterized by enrichment in large ion lithophile elements (Rb, Th and K) and deep troughs at Ba, Nb, Sr, P and Ti (Fig. 5a).

Figura 23 – Figure 5 – Spidergrams normalized to the values suggested by Thompson (1982) for the granites of Mamanguape pluton (a), Northern subprovince (b), Southern subprovince subdivided in PEAL domain (c) and Sergipano belt (d).

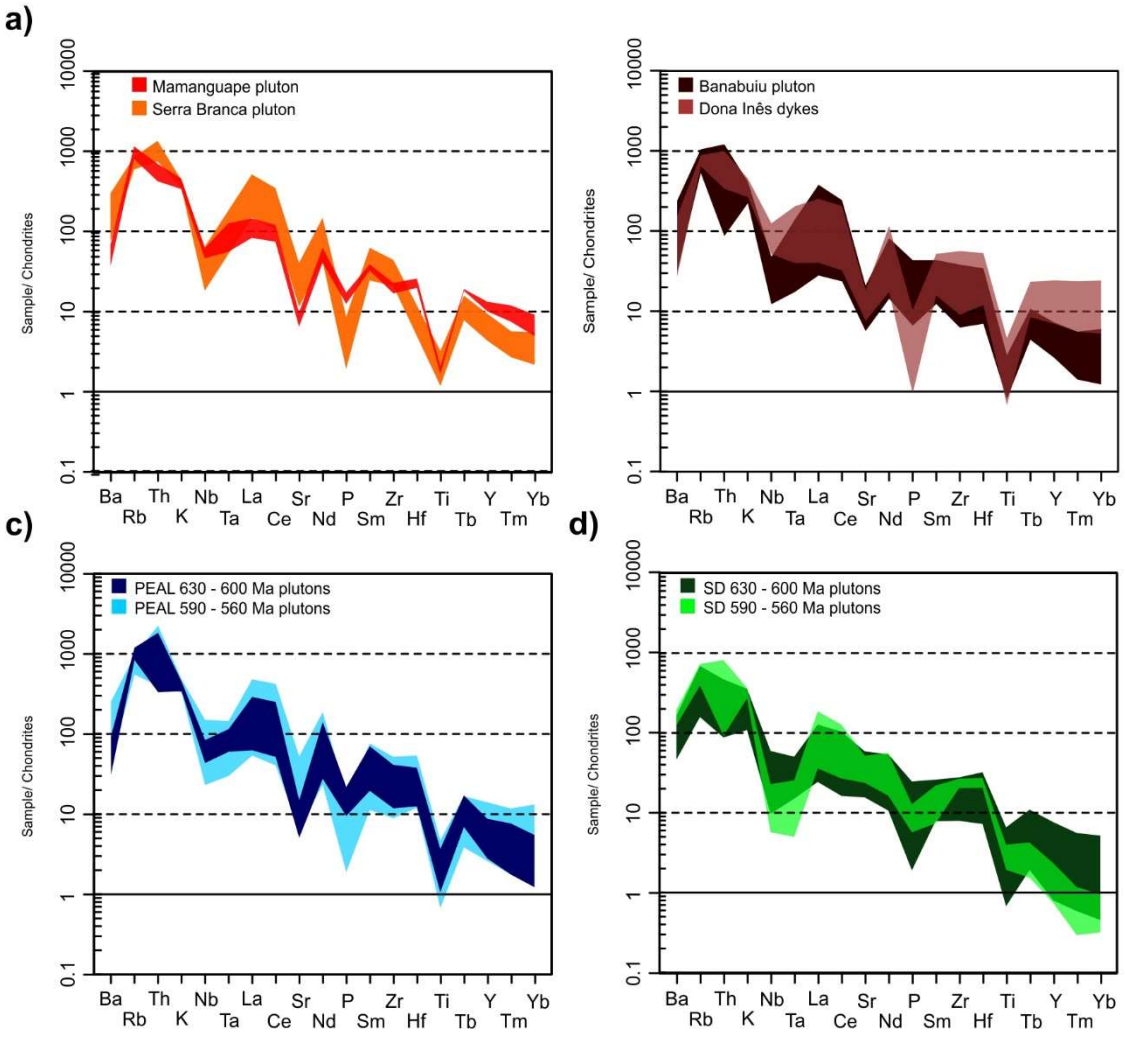

The multielement variation diagrams for other granites of the Borborema Province show relatively similar patterns, characterized by enrichment of LILE (Rb, Th and K) and troughs at Ba, Nb, Sr, P (on variable degrees) and Ti (Fig. 5b, 5c and 5d). The Sergipano belt granites show patterns slightly distinct from the other granites, due to lack of troughs at Sr.

The multi-element patterns of the two-mica granites age groups of the PEAL and Sergipano domains show some distinctions. In the PEAL domain, the younger group are Ba- and total REE-richer and have spidergrams characterized by deeper troughs at P and variable troughs at Nb and Ta, while the younger group of the Sergipano domain have lower HREE, Nb and Ta contents and higher P and Ti contents, compared to the older granites (630-600 Ma).

The absence of troughs at Sr, recorded in the granites of the Sergipano belt, suggest that was not a residual phase. It is explained by the presence of water in the source, as proposed by

Oliveira et al. (2015), promoting decreasing in the liquidus temperature and melting of plagioclase.

5.5. THERMOMETRY

Temperatures were calculated using the geothermometers of zircon saturation, with calibration proposed by Boehnke et al. (2013) and apatite saturation with calibration proposed by Pichavant et al. (1992) for granites of the Mamanguape pluton and others peraluminous leucogranites from the Borborema Province. The obtained temperatures, using the zircon saturation, varied from 713 to 742 °C for the Mamanguape pluton with an average of ~727 °C, like the average temperature of the others peraluminous leucogranites from the other sectors of Borborema Province (~732 °C).

Harrison and Watson (1984) studied the saturation behavior of apatite in metaluminous and peralkaline crustal melts containing 0-10% water in the temperature range 850°-1500°C and concluded that apatite saturation is dependent only on temperature and melt SiO_2 content. However, according to Bea et al. (1992), the P_2O_5 contents in granitic rocks are related to changes in the Aluminum Saturation Index [ASI = mol. $A1_2O_3$ / (K_2O + Na_2O + CaO)] and depend on the bulk-chemistry of rocks. Temperatures obtained using the saturation apatite model of Bea et al. (1992) show variation within the 892 and 941°C for the granites of the Mamanguape Pluton, and from 659 to 969 °C intervals to others peraluminous granites from the Borborema Province. Most of the obtained temperatures are higher than those expected for granitic melts derived by crustal melting.

The apatite saturation geothermometer proposed by Pichavant et al. (1992) for the Mamanguape granites, yielded temperatures ranging from 615 to 719°C (average of 658 °C) and from 335 to 828 °C (average of 595 °C) for others leucogranites. Most zircon saturation temperatures fall in the range between 650 and 800 °C (Fig. 6a), while half of the apatite saturation temperatures are below 600 °C (Fig. 6b). According to Pichavant et al. (1992), the apatite solubility is fO_2 dependent, i.e., under low fO2, the apatite solubility is low, and in consequence, the melt generated has low P_2O_5 contents. On the other hand, P_2O_5 contents in peraluminous crustally derived melts are affected by fractionation processes controlled by melt structure during the magmatic evolution, rather than source dependent as proposed by Watson and Capobianco (1981) and Chappell et al. (1987) in their concept of apatite restitic nature in peraluminous granitic melts. Thus, the temperature of the peraluminous melts of the

Mamanguape Pluton granites and the others peraluminous leucogranites taken under consideration in this work is better constraint using zircon saturation geothermometer.

Figura 24 – Figure 6 – (a) Zircon saturation temperatures according to the calibration of Boenke *et al.* (2013) and (b) Apatite saturation temperatures with calibration of Pichavant *et al.* (1992).

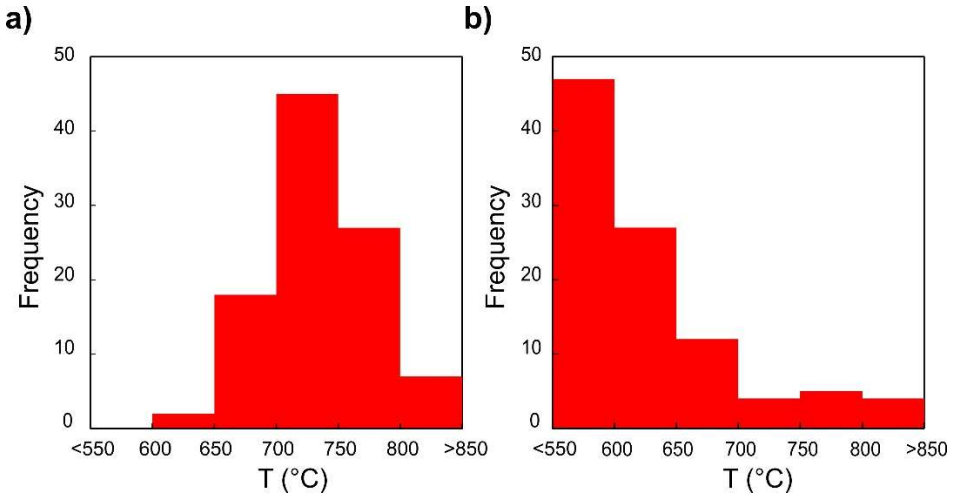

5.6. U – Pb ZIRCON GEOCHRONOLOGY

The zircon concentration was carried out at the NEG/LABISE (Granite Studied Group/Stable Isotope Laboratory) laboratory of the Pernambuco Federal University. Samples were crushed and undergo through a disk mill. The obtained material was then concentrated using a pan, dried between 50 and 70 degrees Celsius and the magnetic fraction was separated using a neodymium magnet. The nonmagnetic fraction of the concentrated material was separated in a portion with density higher than 3.31 and other with density lower than 3.31, using a decantation funnel and diiodomethane. The denser material undergoes Frantz magnetic separator machine for the segregation in diamagnetic and paramagnetic portions. Diamagnetic material was mounted in acrylic resin and polished using alumina powder. The cathodoluminescence images (CL) were obtained in a Scanning Electron Microscope (SEM) JEOL 6510 in the Isotopic Geochemistry Laboratory in the Federal University of Ouro Preto (UFOP), Brazil. U-Pb analysis were obtained using an Element 2 Thermo Finnigan coupled with a Photon-Machines 193 nm laser system at the Isotopic Geochemistry Laboratory of the Federal University of Ouro Preto, Brazil. Data were acquired using peak jumping mode with background measurement for 20 seconds, zircon ablation for 20 seconds and 30 micrometers spot size. Data reduction was done in GLITTER Software. Common lead correction was

applied using an Ms Excel spreadsheet program (Gerdes and Zeh, 2006) based on Stacey and Kramers (1975) Pb composition model. Isoplot (Ludwig, 2001) was used, and the errors were presented in 2δ. The results were built according to Horstwood et al. (2016) and are shown in Table A9.

Zircon grains were extracted from sample GB-105, a coarse- to medium - grained two -mica granite. The analyzed zircon grains show elongated prismatic shape, with length ranging from 100 to >200 μm and length/width ratio of 2:1 to 4:1, and magmatic oscillatory zoning (Fig. 7a). Fourteen analyses of magmatic rims yielded a Concordia age of 574 ± 2 Ma (Fig. 7b), interpreted as the Mamanguape pluton crystallization age. Six analyzed xenocrystic nucleus, without Pb loss, have $^{206}Pb/^{238}U$ ages ranging from 658 to 610 Ma, suggesting that the source of the Mamanguape granites were Neoproterozoic rocks.

Figura 25 – Figure 7 – (a) Representative cathodoluminescence images of zircon grains from sample GB-105 of the Mamanguape pluton, (b) Concordia age of magmatic zircon rims, defining the crystallization age of the Mamanguape granites.

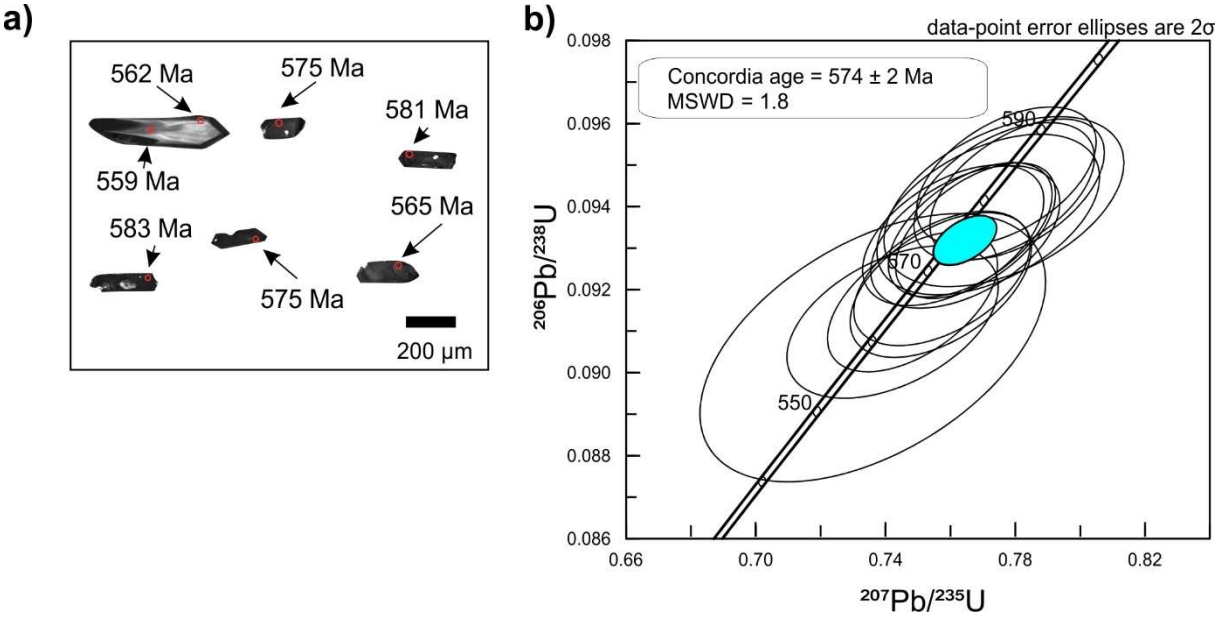

There is no geochronological data for the metasedimentary rocks hosting the Mamanguape Pluton. However, zircon grains with ages in this time spam (Fig. 8a and 8b), are reported by Guimaraes et al. (2012) in metasedimentary rocks located 72 km to southwest, which is interpreted as the same metasedimentary sequence hosting the Mamanguape granites, and the best candidate to its source.

Figura 26 – Figure 8 – Histograms comparing zircon ages obtained on the sample GB-105 of Mamanguape Pluton (a) and a sample from a Neoproterozoic metasedimentary sequence cropped out to the west of the studied area (b), obtained by Guimarães *et al.* (2012).

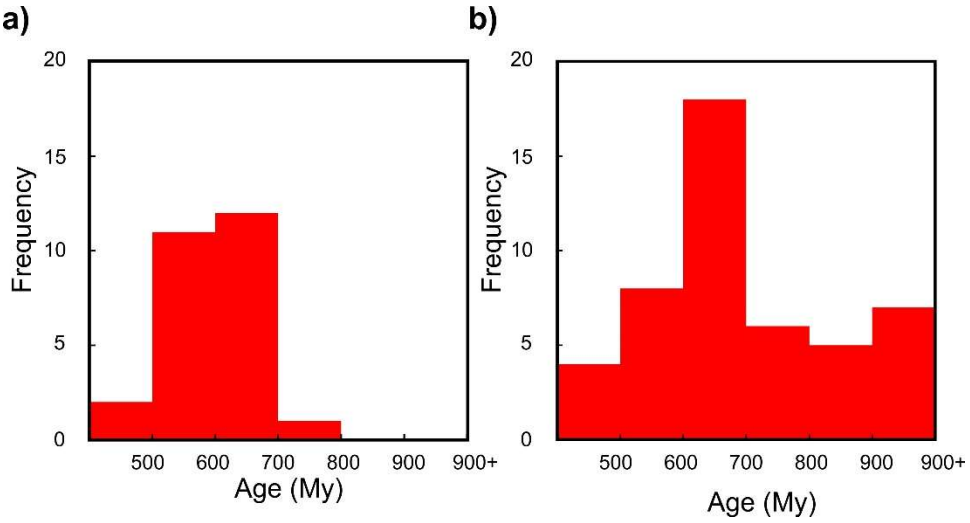

The analyzed zircon grain rims, used to define the crystallization age of the Mamanguape granites, show Th/U ratios ranging from 0.11 to 0.77. However, two concordant spots with $^{206}Pb/^{238}U$ ages like the crystallization age of the studied granites (569 Ma and 575 Ma) have low Th/U ratios (0.04 and 0.08, respectively).

Th/U ratios less than 0.1 are used to discriminate metamorphic zircons according to some authors (Williams and Claesson, 1987; Hoskin and Black, 2000; Rubatto, 2002). However, according to Lopez-Sanchez et al. (2018), zircons with U contents >1000 ppm and Th/U < 0.1 are common on peraluminous granites. In low-Ca peraluminous granites, such as the Mamanguape pluton, the Th and U contents are concentrated in the accessory phases, such as monazite and zircon (Bea, 1996). The distinct partition behavior of Th and U between zircon and the magma, play an important role in the Th/U ratios (Lopez-Sanchez et al. 2016). In monazite, the Th partition coefficient is 16-24 times greater than the U partition coefficient. Thus, the relative timing of zircon and monazite growth during cooling and melt crystallization has an important role in the Th/U ratio of zircon and, monazite fractionation increases LREE/HREE and Th/U ratios in the melt (Stepanov et al., 2012).

During metamorphism, the main control of zircon Th/U ratio is the concentration of Th and U in the system and timing of monazite growth. Early zircon growth, near the peak of metamorphism, is expected to have elevated Th/U ratios while those that grew near the solidus is predicted to have relatively low Th/U ratios, reflecting the coeval growth with monazite (Lopez-Sanchez et al., 2016). These arguments can explain the low Th/U ratios recorded in the magmatic zircon grains rims with ages like the crystallization age of studied granites.

5.7. Lu-Hf ISOTOPES

The isotopic Hf analyses were realized at Ouro Preto Federal University - Brazil, using a Thermo-Fisher Neptune MC-ICP-MS coupled with a Photon Machines 193 nm laser ablation system. Calculation of εHf(t) and Hf model ages were realized utilizing the ^{176}Lu decay constant $\lambda = 1.867 \times 10^{-11}$ year^{-1} from Söderlund et al. (2004), a mean average crustal $^{176}Lu/^{177}Hf$ ratio value of 0.0113 (Rudnick and Gao, 2013), Chondritic Uniform Reservoir (CHUR) values of $^{176}Lu/^{177}Hf = 0.0336$ and $^{176}Hf/^{177}Hf = 0.282785$ from Bouvier et al. (2008), and Depleted Mantle (DM) values of $^{176}Lu/^{177}Hf = 0.03933$ and $^{176}Hf/^{177}Hf = 0.283294$ from Blichert-Toft and Puchtel (2010). Isotopic data and ratios are shown in Table A10.

Zircon grains of the sample GB-105 from the Mamanguape Pluton, show a wide range of εHf(t) values, within the +1.4 to -13.7 interval, and TDM model ages (Blichert-Toft, 2008) between 1.4 to 2.2 Ga (Fig. 9a). Eight Lu-Hf isotope analyses were carried out in the same spots previously analyzed for U-Pb isotope. The plot of ƐHf(t) versus Th/U ratios (Fig. 9b), suggest two groups/trends of samples, and in each group, despite the low number of analyses, ƐHf(t) values correlate positively with Th/U ratios.

Figura 27 – Figure 9 – (a) εHf(t) vs age plot, and (b) ƐHf(t) versus Th/U ratios of zircon grains from the Mamanguape pluton.

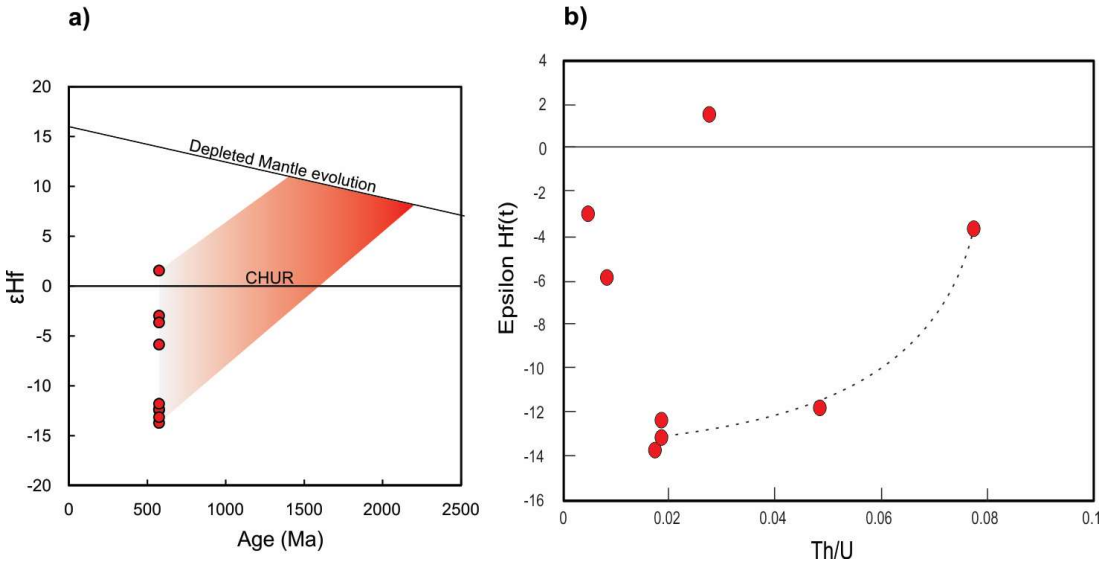

5.8. Sm-Nd ISOTOPES

Sm-Nd data analyses (Table A11) were realized at the Isotope Laboratory of the Brasilia University. Sm-Nd isotopic data from leucogranites of the PEAL domain were obtained for four samples, two of Jurema pluton, one for Quipapá pluton and another from the Mamanguape Pluton. Sm-Nd data from other leucogranites from Northern subprovince and Sergipano domain were compiled from Lima et al. (2010) and Oliveira et al. (2015), respectively.

The Jurema and Quipapá plutons show εNd values ranging between -10.83 and -14.34 and Paleoproterozoic TDM model ages ranging from 1.96 to 2.22 Ga (Fig. 10a). The ƐNd (t) values are slightly higher in the Jurema granites than the Quipapá granites, been like the Mamanguape granites.

Sm-Nd isotope data, compiled from the Sergipano domain, show εNd values between -9.9 and -12.2 and TDM model ages ranging from 1.2 to 1.86 Ga (Fig. 10b). Sm-Nd isotopic data from the Northern subprovince show higher εNd(t) values (-19.6 to -23.2), and older TDM model ages varying from 2.43 to 2.59 Ga (Fig. 10c).

Figura 28 – Figure 10 – εNd(t) vs age plot for leucogranites from (a) PEAL domain (This work), (b) Sergipano domain (Oliveira et al., 2015) and (c) Northern subprovince (Lima et al., 2014).

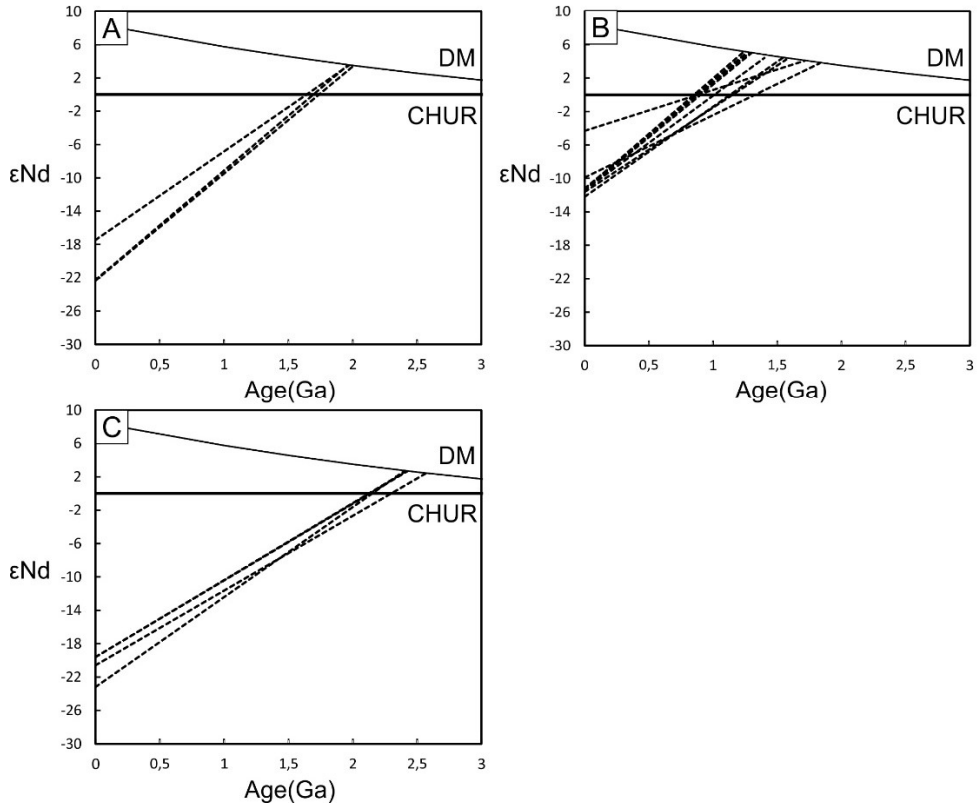

5.9. DISCUSSION

5.9.1 PETROGENESIS AND MAGMA SOURCE

According to Barbarin (1999), peraluminous granites comprise: a) cordierite-bearing peraluminous granitoids (CPG) and b) muscovite-bearing peraluminous granitoids (MPG). The CPG are the typical S-type granites of Chappell and White (1974), described in the Lachan Fold Belt, Australia. Muscovite can be an accessory phase in many types of granitoids, but large flakes of primary muscovite is abundant only in two-mica granites. The MPG frequently contain tourmaline, garnet, and monazite as accessory mineral phase. Enclaves are rare and when present, are generally xenoliths of the country rocks, fragments of chilled margins, and/or restite.

Patiño Douce (1999) based on experimental studies concluded that MPGs represent pure crustal melts derived by dehydration-melting of muscovite-rich metasedimentary rocks, that agrees with the classification proposed by Barbarin (1999).

Biotite granites from the Northern subprovince from the Borborema Province are intruded in orthogneisses and are interpreted as generated by melting of lower crustal source (Guimarães et al. 2017), with some of them, (Guimarães et al. 2017) showing geochemical similarities with A-type aluminous granites (King et al. 1997). Jiang and Zhou (2017) studied biotite granites and muscovite- bearing granites from South China and concluded that biotite granites are S-type, whereas the muscovite-bearing granites are the result of highly fractionated biotite granites and proposed to extend their finding to granites worldwide. This assumption can be true to the South China granites but cannot be applied to the granites of the Borborema Province.

Peraluminous granites are common rocks in collisional orogens, frequently associated with metasediments. The mineralogical assemblage constituted by primary muscovite, aluminous biotite, garnet, or other aluminous rich minerals are characteristics of rocks derived by partial melting of metasedimentary rocks (Chappell and White, 2001). The geochemical composition of the Mamanguape pluton and other peraluminous granitoids with the same age all along the Borborema Province share similar characteristics, with differences being results from variable degrees of process of partial melting and fractional crystallization. The main differences are observed in the isotope data.

In the Rb/Ba versus Rb/Sr diagrams proposed by Sylvester (1998) (Fig. 11a) the samples from peraluminous granites of Borborema Province shows a heterogeneity of sources ranging

from pelites to greywackes. According to Sylvester (1998) the predominance of pelite of psammite derived melts in collisional orogens may reflect the maturity of crustal blocks, as mature plates are constituted by pelites and immature by psammites. The dominantly psammite derived melts possibly reflects anatexis of immature sediments. Dominantly pelite derived melts are suggested for collision and anatexis of mature platforms. The CaO/Na_2O versus Al_2O_3/TiO_2 diagram (Fig. 11b) indicates that the Mamanguape granites have a dominant metapelitic source, with $CaO/Na_2O < 0.3$ (Sylvester, 1998), while most of the Borborema peraluminous granites show heterogeneous sources, with rocks associated with metapelites and metagreywakes.

Figura 29 – Figure 11 – (a) Rb/Ba vs Rb/Sr ratios with mean compositions of magmas generated by partial melting of metapelites and metapsamites sources. The curve represents progressive mixing of basalt and metapelites (Sylvester 1998). (b) CaO/Na2O vs Al2O3/TiO2 diagram with field for strong peraluminous granites proposed by Sylvester et al., (1989). Covariant diagrams for Rb/Sr versus Ba (c) and Sr (d), the vectors represent partial muscovite dehydration melting (VA), Biotite dehydration melting (VA) and fluid present melting reactions (VP) (Inger and Harris, 1983).

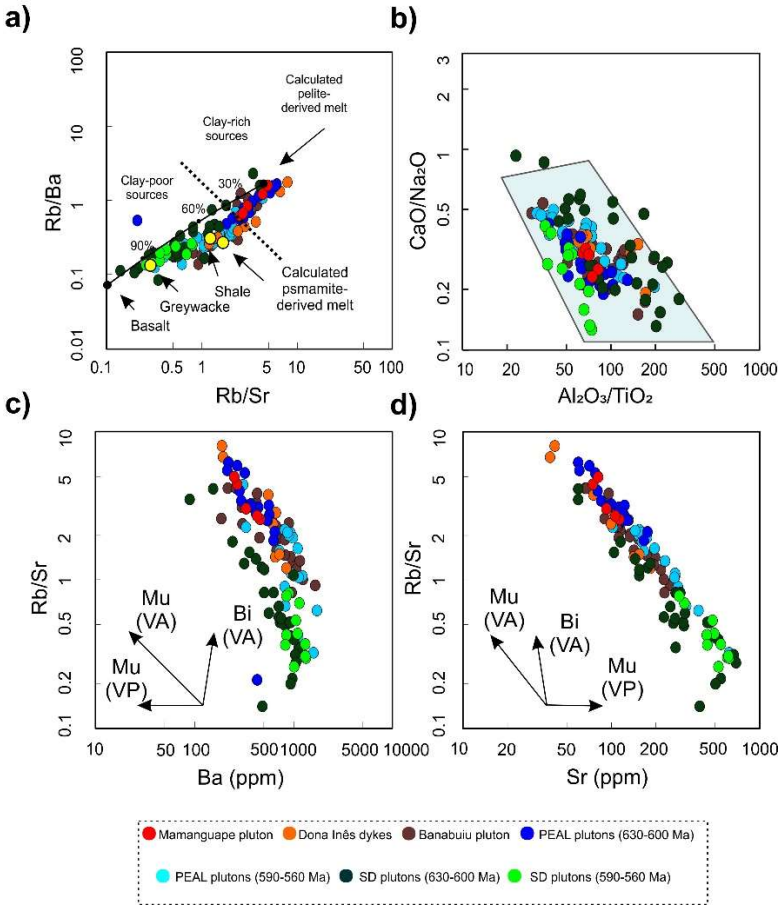

Rb/Sr versus Ba and Sr plots (Fig. 11c, d) shows negative correlation for most peraluminous granites of the Borborema Province, parallel to the trend of melts generated by dehydration melting of muscovite (Inger and Harris, 1993). However, the absence of Eu and Sr anomalies on the Sergipano domain granites may indicate partial melting in the presence of water, which induced consumption of plagioclase in the melting reaction (Patiño Douce and Harris 1998).

Zirconium is an abundant element in the continental crust, with a mean of 193 ppm in the upper crust and 68 ppm in the lower crust (Rudnick and Gao, 2003). Zirconium variation in the continental crust was interpreted by M. Tang et al. (2014) as the result of slow disequilibrium melting of zircon, during crustal melting. This premises is important to interpret the Lu-Hf isotope data. According to M. Tang et al. (2014), Hf isotope composition in zircon grains, may significantly deviate to the source, because zircon grains crystallizing in a recharged magma chamber, have a variable Hf isotope composition, while those crystallized in the early melts are highly radiogenic due to the retention of 177Hf. M. Tang et al. (2014) also stated that zircon Hf isotope compositions may resulted from varying melting conditions (rate, degree and so on) and not necessarily indicate multi-source magma mixing, unless there is evidence for magma mixing. However, the two groups of zircon grains showing positive correlation between ƐHf(t) and Th/U ratios (Fig. 9b), the zircon grains with positive ƐHf(t) values, associated to the presence of small number of mafic enclaves, suggest small participation of mantle melts in the source of the Mamanguape granites. Hf isotope data are not available for the Jurema and Quipapá granites. However, the presence of mafic enclaves in the Jurema granites, even in small number, and similarity of Nd isotope composition between the Mamanguape and Jurema granites, are evidence of small volume of mantle melts participation in the source of the Jurema granites. Biotite granites from the Northern subprovince have Nd isotope composition like the migmatized orthogneisses country rocks (Lima et al., 2010). Two-mica granites and biotite granites from Sergipano domain show Sm-Nd isotope composition similar to the metasediments they intrude (Oliveira et al., 2015).

The average crystallization temperature of 727 °C, for the Mamanguape pluton, is like the average of crystallization temperature (~732 °C) of others two-mica granites reported in the Borborema Province (Guimarães and Silva Filho, 1995; Lima et al., 2010, Oliveira et al., 2015; Conceição et al., 2016; Guimarães et al., 2017; Neves et al., 2020, Brainer et al., 2021). According to Miller (2003), temperatures below 800 °C, are characteristics of granites with high zircon heritage, being a great estimative of the magma temperature in the source, which is coherent with muscovite dehydration temperatures between 650 and 750 °C (Petö, 1976).

5.9.2 TECTONIC SETTING AND HEAT SOURCES

Despite its geochemical similarities, the leucogranites from the Borborema Province represent two distinct magmatic episodes with ages of 590-562 Ma and 630-600 Ma (Table A12). They were intruded under distinct tectonic settings during the Brasiliano Orogeny. On tectonic discriminant diagrams of Pearce et al. (1984) and Pearce (1996), the studied granitoids and most of the granites of the Borborema Province, fall in the post-orogenic granites (POG) field, overlapping the syn- collisional granites (syn-COLG) field, with a few samples projected on volcanic arc granites (VAG) and within plate granites (WPG) field (Fig. 12a, b). Although the leucogranites samples on projected diagram have distinct ages, related to collision and transcurrent stages of Brasiliano orogeny, they fall in the same tectonic field. It suggests that the Pearce diagrams are not suitable to discriminate the tectonic setting of the studied granitoids.

Figura 30 – Figure 12 – Tectonic discriminant diagrams of Pearce et al. (1984) and Pearce (1996) projections of Mamanguape and other leucogranites. Syn-COLG = Syn-Collision granites; VAG = Volcanic Arc Granites; WPG = Within Plate granites; ORG = Ocean Ridge granites.

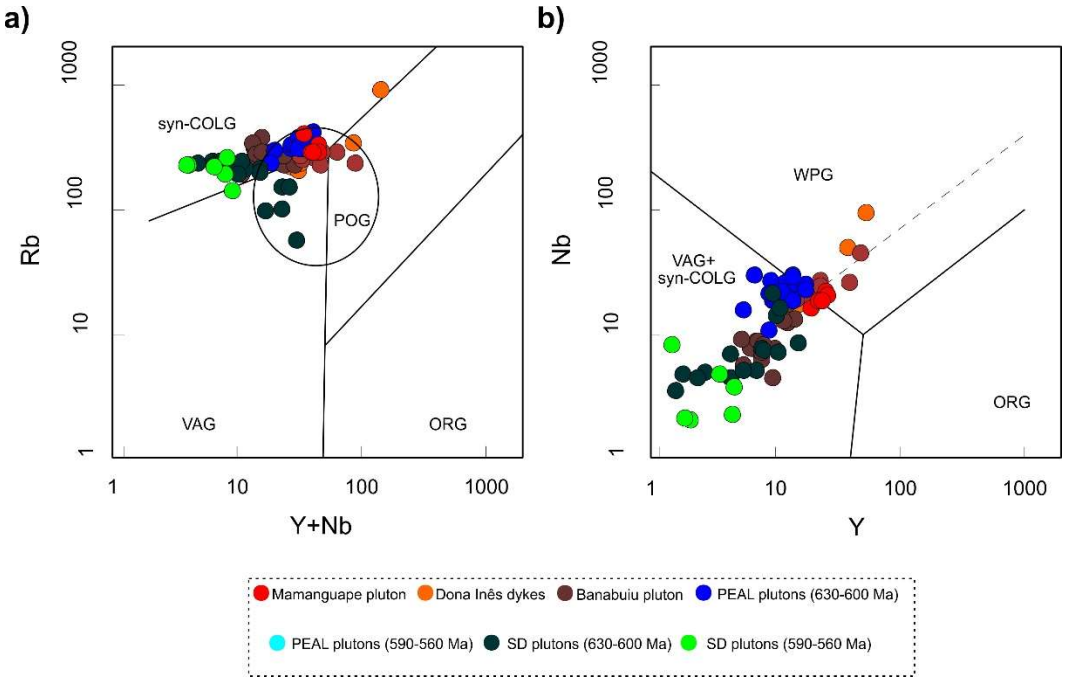

The crystallization age (574 ± 2 Ma) of the Mamanguape pluton, like many others two-mica leucogranites from the Borborema Province (Table A12), are contemporaneous with gabbroic intrusion from the Transversal (Almeida et al., 2002) and Northern Province

(Guimarães et al., 2017). They are also related with extensive high-K granites (Guimarães et al., 2004, 2009, Neves et al., 2008, 2020, Silva Filho et al. 2016) and the main transcurrent tectonic period of the Brasiliano Orogeny. Guimarães et al. (2004) suggested that granites with such crystallization age, represents magmatism associated to the final stages of the lateral escape of the Brasiliano contractional event and, initial stages of orogenic collapse in the Transversal subprovince. However, in the Northern subprovince, granites with similar ages (578 ± 6 Ma, Lima et al., 2010), as the Banabuiu Batholith granitoids, are interpreted as syn-collision granites. In the Northern subprovince, peraluminous granites usually have topaz as the accessory phase, result from partial melting of metasedimentary sequences coeval with the crustal thickening (Arthaud et al. 2008). In general, they form small intrusions, directly associated with the anatectic sources, and only two intrusions between the Senador Pompeu and Orós shear zones, display batholith dimensions, showing evidence of solid-state deformation, along the shear zones. Ages within the interval 623-614 Ma were reported to two-mica granites in the region (Fetter 1999). Souza et al. (2006) estimated the peak of high temperature metamorphic event of ca. 574 Ma, like the ca. 575 Ma age obtained by Archanjo et al. (2013) for a transpressional event to the west. This event promoted a generalized migmatization on the supracrustal metapelites and orthogneisses from the basement of Rio Grande do Norte Domain.

In the Southern subprovince, two-mica granites occur according to ages groups: 640-600 Ma and 590-562 Ma. The granites with crystallization ages between 640 and 600 Ma mark the first stages of the Brasiliano – Pan-African collision, (Oliveira et al. 2015; Conceição 2019; Silva Filho et al. 2021, Brainer et al., 2021).

Most of the two-mica leucogranite intrusions in the Borborema Province, are in the Pernambuco-Alagoas Domain, with the Quipapá pluton, constitutes one of the largest intrusions. It is characterized as syn-collisional granites, showing crystallization ages of 630 ± 5 Ma (Silva Filho et al. 2021) and 641 ± 5 Ma (Brainer et al. 2021), and interpreted as formed at the early stages of collision associated to crustal thickening coupled with shear heating. Two-mica granites with ages between 590-570 Ma were reported in the PEAL and Sergipano Domain. In the PEAL Domain, Neves et al. (2020) associated this two-mica leucogranites with ages between 573 and 562 Ma to the transcurrent regime, in which shear heating may played a major role as the heat source.

In the Sergipano domain, the Poço Redondo two-mica granites resulted from melting of the metasedimentary rocks, have U-Pb zircon crystallization age of 623 ± 7 Ma, (Bueno et al., 2009, Oliveira et al., 2015). The necessary heat generating crustal melting in the region resulted

from uplift of the asthenosphere associated to slab break-off. Similar Nd isotope signature between the Poço Redondo migmatites and granites (Oliveira et al. 2015) suggest that they have the same source, and this melting event charactering the beginning of collision between the São Francisco Craton and the PEAl Domain. Corrêa-Gomes et al. (2022) based on surface geology, gravimetric and magnetotelluric data suggested that the Sergipano domain or Orogen, resulted from the collision between the PEAL domain and the São Francisco Craton.

The geochemical signature of the Sergipano domain granites suggests participation of water in the melting reactions. Oliveira et al. (2010) suggest that the evolution of the Sergipano domain underwent a small ocean closure at ca. 630 Ma, and the subduction of an oceanic basin beneath the Poço Redondo - Marancó domain, which may have provided the necessary water to start fluid present melting on crustal lithologies. However, according to Bueno et al. (2009), the Brasiliano collision in the Sergipano domain, last for 75 Ma, which suggest that the granites with crystallization ages between 590 and 570 Ma in the Sergipano domain, and in the south part of the PEAL Domain are also related to the collision between the São Francisco Craton and the Pernambuco-Alagoas Domain. However, in the north part of the PEAL Domain and in the Transversal and Northern subprovinces, the contractional period of the Brasiliano/Pan-African Orogeny ended by 590 Ma (Guimarães et al. 2004, Neves et al. 2004, 2008, 2012, 2020). Ganade de Araújo et al. (2014) and Caxito (2020) suggested that the period 590 – 560Ma of extrusion tectonics of the Borborema Province.

In continental collision, several thermal models are proposed to generation of peraluminous leucogranites. According to Nabelek et al. (2020) the principal thermal models for generation of leucogranites in collisional orogens where lack evidence for mantle-derived magmas heat sources (Thompson and Connolly 1995, Nabelek and Liu 2004, Nabelek et al. 2010, Nabelek 2020) are: 1) flux melting; 2) decompression melting; 3) radiogenic heating production and 4) shear heating.

According to the shear heating model proposed by Leloup et al. (1999), syn-tectonic (syn-transcurrent) magmatism can be explained by lower crust partial melting inducted by shear heating in the lithospheric mantle and the rising of melts through the shear zones, which further increases the temperatures in the crust. Reactivation of the Patos Shear zone ca. 566 Ma (Viegas et al. 2014) may have induced new pulses of magmatism in the adjacent shear zones through shear heating. Many shears related high-K calc alkaline metaluminous to slightly peraluminous granitoids intruded in the Transversal subprovince, in the PEAL and Rio Grande do Norte domains, are related to a lower crustal source. They have crystallization ages ranging from 582 to 560 Ma (Almeida et al, 2002; Guimarães et al. 2004, Archanjo et al. 2008, Ferreira et al.,

2010, Santos et al., 2014, Lima et al. 2017, Neves et al., 2008, 2020). According to Nabelek et al. (2010), magmas produced through strain-related melting, may be episodic because as the partially molted increases, strain heating cease and, only after melts extraction from the molten zone occurs, strain heating can recommence, leading to production of a new generation of partial melts. Episodic strain-related magmatism is suggested by Harrison et al. (1999) to explain the time spam of the granitic intrusion in the Central Himalaya. It could explain more than 20 Ma of syn-transcurrent magmatism in the studied region. However, many transcurrent related granitoids in the studied region, coeval with two-mica granites i.e., pure crustal magmas, show evidence of evolution through magma mixing processes, involving magmas of crustal and small volume of mantle (basalt underplating?) sources. We suggest that at least two heating source promoted melting during the 590-560 Ma interval in the Borborema Province, i.e., strain-related heating and heating promoted by the accretion of lithospheric mantle magmas to the crust.

5.10. CONCLUSIONS

- The Mamanguape pluton comprises two-mica peraluminous, ferroan, alkali-calcic granites. The presence of Cryogenian/ Ediacaran zircon xenocrists, small number of mafic enclaves, associated with εHf (575Ma) values ranging from +1.4 and -13.7 and TDM model ages varying from 1.4 to 2.2 Ga, suggest that the source rocks received contribution of metasedimentary rocks, described in the literature as the Sertania Complex. However, interaction with mantle derived melt, may had occurred in small proportion, during the magmatic evolution explaining the presence of mafic enclaves and positive ƐHf (t) values. The studied granites have geochemical signature like many other two-mica granites of the Southern subprovince, with variable ages, except for differences in their isotopic signatures, interpreted as resulted from distinct contribution to the metasedimentary rock sources.
- Peraluminous two-mica granites in the Borborema Province with ages intervals between 640-600 Ma and 590-562 Ma seems to be generated by muscovite dehydration melting from various sources, with the only exception being the Sergipano domain granites, where melting may occur in presence of water.
- We suggest that shear heating coupled with input of small volume of mantle melts, during the transcurrent event of the Brasiliano Orogeny, were the heating sources promoting crustal melting and generating the 590-560 Ma two-mica leucogranites magmas. On the other hand, the heat source generating the two-mica granites with ages 640-600 Ma in the

Pernambuco-Alagoas domain and Sergipano domain, was also shear heating, associated to the contractional stage of the Brasiliano Orogeny.

• Two-mica granites associated to the contractional stage of the Brasiliano/Pan-African Orogeny (640-600 Ma) are not yet reported in the Transversal and Northern (Rio Grande do Norte domain) subprovinces. On the other hand, the transcurrent event (590-560 Ma), was marked by localized melting of metasedimentary rocks, generating small volume of magmas, intruded as dyke swarm and the Mamanguape two-mica granites, extensive migmatization and partial melting of lower crust and lithospheric mantle, generating the biotite granites and large volume of high-K granites.

ACKNOWLEDGEMENTS

This research is part of CCGB master's dissertation. CCGB thanks CAPES for supporting his studies with a scholarship. The project was financially supported by the Brazilian National Research Council - CNPq (Proc. 421353/2018-0).

REFERENCES

Almeida C.N., Guimarães I.P., Silva Filho A.F. 2002. A-Type Post-Collisional Granites in the Borborema Province - NE Brazil: The Queimadas Pluton. Gondwana Research, 5:667–681. https://doi.org/10.1016/s1342-937x(05)70637-7

Almeida F.F.M., Hasui Y., de Brito Neves B.B., Fuck R.A. 1981 Brazilian structural provinces: An introduction. Earth Science Reviews, 17:1–29. https://doi.org/10.1016/0012-8252(81)90003-9

Archanjo, C.J., Hollanda, M.H.B.M., Rodrigues, S.W.O., Neves, B.B.B., Armstrong, R., 2008. Fabrics of pre- and syntectonic granite plutons and chronology of shear zones in the Eastern Borborema Province, NE Brazil. J. Struct. Geol. 30, 310–326. https://doi.org/10.1016/J.JSG.2007.11.011

Archanjo C.J., Viegas L.G.F., Hollanda M.H.B.M., Souza L.C., Liu D. 2013. Timing of the HT/LP transpression in the Neoproterozoic Seridó Belt (Borborema Province, Brazil): Constraints from UPb (SHRIMP) geochronology and implications for the connections

between NE Brazil and West Africa. Gondwana Researchearch. 23:701–714. https://doi.org/10.1016/j.gr.2012.05.005

Arthaud M.H., Caby R., Fuck R.A., Dantas E.L., Parente C.V. 2008. Geology of the northern Borborema Province, NE Brazil and its correlation with Nigeria, NW Africa. Geol. Soc. Spec. Publ, 294:49–67. https://doi.org/10.1144/SP294.4

Barbarin B. 1999. A review of the relationships between granitoid types, their origins and their geodynamic environments. Lithos, 46:605–626. https://doi.org/10.1016/S0024-4937(98)00085-1

Bea F., Fershtater G., Corretgé L.G. 1992. The geochemistry of phosphorus in granite rocks and the effect of aluminium. Lithos, 29:43–56. https://doi.org/10.1016/0024-4937(92)90033-U

Bea F. 1996. Residence of REE, Y, Th and U in granites and crustal protoliths; implications for the chemistry of crustal melts. J Petrol, 37:521–552. https://doi.org/10.1093/petrology/37.3.521

Bertrand J.M., Sá E.E.J. 1990. Where are the Eburnian-Transamazonian collisional belts ?'. Can J Earth Sci, 27(10):1382–1393. https://doi.org/10.1139/e90-148

Blichert-Toft J. 2008. The Hf isotopic composition of zircon reference material 91500. Chemical Geology, 253:252– 257. https://doi.org/10.1016/j.chemgeo.2008.05.014

Blichert-Toft J., Puchtel I.S. 2010. Depleted mantle sources through time: evidence from Lu-Hf and Sm-Nd isotope systematics of Archean komatiites. Earth and Planetary Science Letters 297:598-606. https://doi.org/10.1016/j.epsl.2010.07.012

Boehnke P., Watson E.B., Trail D., Harrison T.M., Schmitt A.K. 2013. Zircon saturation re-revisited. Chem. Geol., 351:324–334. https://doi.org/10.1016/j.chemgeo.2013.05.028

Bonin, B., Janoušek, V., Moyen, J.F., 2020. Chemical variation, modal composition and classification of granitoids, Geological Society Special Publication, 491:9–51. https://doi.org/10.1144/SP491-2019-138

Bouvier A., Vervoort J.D., Patchett P.J. 2008. The Lu-Hf and Sm-Nd isotopiccomposition of CHUR: constraints from unequilibrated chondrites and implications for the bulk composition of terrestrial planets. Earth and Planetary Science Letters, 273:48-57. https://doi.org/10.1016/j.epsl.2008.06.010

Brainer, C.C.G., Guimarães, I.P., Silva Filho, A.F., Lima, J. V., Amorim, J.V.A., 2021. Early Ediacaran two-mica granites marking the contractional stage of the Brasiliano Orogeny in the Pernambuco-Alagoas Domain, NE Brazil. J. South Am. Earth Sci. 111, 103506. https://doi.org/10.1016/J.JSAMES.2021.103506

Brito Neves B.B., Santos E.J., Van Schmus W.R. 2000. Tectonic History of the Borborema Province. In: Cordani U.G., Milani E.J., Thomaz Filho A., Campos D.A. (eds.), Tectonic Evolution of South America. Rio de Janeiro, 31st. International Geological Congress, p. 151-182.

Brito Neves B.B., Campos Neto M.D.C., Van Schmus W.R., Fernandes T.M.G., Souza S.L. 2001. O terreno Alto Moxotó no Leste da Paraíba ("Maçico Caldas Brandão"). Rev. Bras. Geociências 32: 185–194.

Brito Neves B.B., Passarelli C.R., Basei M.A.S., Santos E.J. 2003. U-Pb ages in zircon of some granites in the Borborema Province. Geol USP - Ser Cient 3:25–38. https://doi.org/10.5327/s1519-874x2003000100003

Brown M., 2013. Granite: from genesis to emplacement. GSA Bulletin 125, 1079–1113.

Bueno J.F., Oliveira E.P., McNaughton N.J., Laux J.H. 2009. U-Pb dating of granites in the Neoproterozoic Sergipano domain, NE-Brazil: Implications for the timing and duration of continental collision and extrusion tectonics in the Borborema Province. Gondwana Research, 15:86–97. https://doi.org/10.1016/j.gr.2008.06.003

Caby R., Bertrand J.M.L., Black R. 1981. Pan-African Ocean Closure and Continental Collision in the Hoggar-Iforas Segment, Central Sahara. Dev Precambrian Geol, 4:407–434. https://doi.org/10.1016/S0166-2635(08)70021-5

Castaing C., Feybesse J.L., Thiéblemont D., Triboulet C., Chèvremont P. 1994. Palaeogeographical reconstructions of the Pan-African/Brasiliano orogen: closure of an oceanic domain or intracontinental convergence between major blocks? Precambrian Research 69:327–344. https://doi.org/10.1016/0301-9268(94)90095-7

Caxito F.A., Uhlein A., Dantas E.L., Stevenson R., Salgado S.S., Dussin I.A., Sial A.N. 2016. A complete Wilson Cycle recorded within the Riacho do Pontal Orogen, NE Brazil: Implications for the Neoproterozoic evolution of the Borborema Province at the heart of West Gondwana. Precambrian Res, 282:97-120. https://doi.org/10.1016/j.precamres.2016.07.001

Caxito F.A, Santos L.C.M.L., Ganade C.E., Bendaoud A., Fettous E.H., Bouyo M.H. 2020. Toward an integrated model of geological evolution for NE Brazil-NW Africa: The Borborema Province and its connections to the Trans-Saharan (Benino-Nigerian and Tuareg shields) and Central African orogens. Brazilian J. Geol. 50(2):. https://doi.org/10.1590/2317-4889202020190122

Chappell B.W., 1984. Source rocks of I- and S-type granites in the Lachlan fold belt, southeastern Australia. Philos. Trans. R. Soc. London 310, 693–707. https://doi.org/10.1098/rsta.1984.0015

Chappell B.W. 1999 Aluminium saturation in I- and S-type granites and the characterization of fractionated haplogranites. Lithos 46:535–551. https://doi.org/10.1016/S0024-4937(98)00086-3

Chappell B.W., White A.J.R. 1974. Two contrasting granite types. Pacific Geol 173–174

Chappell B.W., White A.J.R., Wyborn D. 1987. The importance of residual source material (restite) in granite petrogenesis. J Petrol 28:1111–1138. https://doi.org/10.1093/petrology/28.6.1111

Chappell, B.W., Bryant, C.J., Wyborn, D., 2012. Peraluminous I-type granites. Lithos 153, 142–153. https://doi.org/10.1016/J.LITHOS.2012.07.008

Chappell B.W., White A.J.R. 2001. Two contrasting granite types: 25 years later. Aust J Earth Sci 48:489–499. https://doi.org/10.1046/j.1440-0952.2001.00882.x

Clarke D.B. 1981. The mineralogy of peraluminous granites: A review. 7:3–17

Chappell, B.W., White, A.J.R., 1992. I- and S-type granites in the Lachlan Fold Belt. Transactions of the Royal Society of Edinburgh: Earth Sciences 83, 1–26.

Chappell, B.W., White, A.J.R., Williams, I.S., Wyborn, D., 2004. Low- and high-temperature granites. Transactions of the Royal Society ofEdinburgh: Earth Sciences 95, 125–140.

Clemens, J.D., Stevens, G., 2012. What controls chemical variation in granitic magmas? Lithos 134–135, 317–329.

Clemens, J.D., Stevens, G., Farina, F., 2011. The enigmatic sources of I-type granites: the peritectic connexion. Lithos 126, 174–181.

Conceição J.A., Rosa M.D.L.D.S., Conceição H. 2016. Sienogranitos leucocráticos do Domínio Macururé, Sistema Orogênico Sergipano, Nordeste do Brasil: Stock Glória Sul. Brazilian J Geol, 46:63–77. https://doi.org/10.1590/2317-4889201620150044

Conceição J.A. 2019. Magmatismo leucogranítico do domínio macururé, sistema orogênico sergipano, província borborema, NE do brasil. Ph.D. Thesis, Universidade Federal da Bahia (UFBA), Salvador, 62 p.

Corrêa-Gomes, L.C., Batista, J.C., Sampaio, E.E.S., Oliveira, E.P., Barbosa, J.S.F., Vitorello, Í., 2022. Geophysical data reveal a tectonic indentation and constrain the transition zone between the São Francisco Craton and the Borborema Paleoplates across the Neoproterozoic Sergipano Orogen, beneath the Cretaceous Tucano Basin, NE Brazil. Tectonophysics 833, 229296. https://doi.org/10.1016/J.TECTO.2022.229296

Dantas E.L., Hackspacher P.C., Van Schmus W.R., Brito Neves B.B. 1998. Archean Accretion in the São José Do Campestre Massif, Borborema Province, Northeast Brazil. Rev Bras Geociências 28:221–228. https://doi.org/10.25249/0375-7536.1998221228

Dantas E.L., Van Schmus W.R., Hackspacher P.C., Fetter A.H., Brito Neves B.B., Cordani U., Nutman A.P., Williams I.S. 2004. The 3.4-3.5 Ga São José do Campestre massif, NE Brazil: Remnants of the oldest crust in South America. Precambrian Research 130:113–137. https://doi.org/10.1016/j.precamres.2003.11.002

Ebert H. 1970. The precambrian geology of Borborema Belt (states of Paraíba and Rio Grande do Norte, northearsten Brazil), and origin of its mineral resources. Geologische Rundschau 5:1299-1326.

Ferreira M.A.F., Ferreira V.P., Sial A.N., Pimentel M.M., Armstrong R., Silva Filho A.F., Guimarães, I.P. 2010. 564 Ma S-Type Peraluminous Leucogranite in the Alto Pajeú Terrane, Borborema Province, NE Brazil. In: South American Symposium on Isotope Geology (VII SSAGI). Brasília, p. 49-52

Ferreira V.P., Sial A.N., Jardim de Sá E.F. 1998. Geochemical and isotopic signatures of Proterozoic granitoids in terranes of the Borborema structural province, northeastern Brazil. J South Am Earth Sci, 11:439–455. https://doi.org/10.1016/S0895-9811(98)00027-3

Ferreira V.P., Sial A.N., Pimentel M.M., Armstrong R., Spicuzza M.J., Guimarães I.P., Silva Filho A.F. 2011. Contrasting sources and P-T crystallization conditions of epidote-bearing granitic rocks, northeastern Brazil: O, Sr, and Nd isotopes. Lithos, 121:189–201. https://doi.org/10.1016/j.lithos.2010.11.002

Fetter A.A. 1999. U/Pb and Sm/Nd geochronological constraints on the crustal framework and geologic history of Ceará State, NW Borborema Province, NE Brazil; implications for the assembly of Gondwana. Ph.D. thesis, University of Kansas, Kansas, 164 p.

Frost B.R., Barnes C.G., Collins W.J., Arculus R.J., Ellis D.J., Frost, C.D. 2001. A geochemical classification for granitic rocks. J. Petrol., 42:2033–2048. https://doi.org/10.1093/petrology/42.11.2033

Ganade de Araujo C.E., Weinberg R.F., Cordani U.G. 2014. Extruding the Borborema Province (NE-Brazil): a two-stage Neoproterozoic collision process. Terra Nova, 26(2):157-168.

Gerdes A., Zeh A. 2006. Combined U-Pb and Hf isotope LA-(MC-)ICP-MS analyses of detrital zircons: Comparison with SHRIMP and new constraints for the provenance and age of an Armorican metasediment in Central Germany. Earth Planet Sci Lett, 249:47–61. https://doi.org/10.1016/j.epsl.2006.06.039

Guimarães I.P., Silva Filho A.F. 1995. An example of in situ granite formation in the northern boundary of the Proterozoic Sergipano fold belt, NE Brazil: the Xingó Complex. J South Am Earth Sci, 8:341–354. https://doi.org/10.1016/0895-9811(95)00018-B

Guimarães I.P., Silva Filho A.F., Almeid, C.N., Van Schmus W.R., Araújo J.M.M., Melo S.C., Melo E.B. 2004. Brasiliano (Pan-African) granitic magmatism in the Pajeú- Paraíba belt, Northeast Brazil: An isotopic and geochronological approach. Precambrian Research 135:23–53. https://doi.org/10.1016/j.precamres.2004.07.004

Guimarães I.P., Silva Filho A.F., Araújo D.B., Almeida C.N., Dantas L. 2009. Trans-alkaline magmatism in the Serrinha-Pedro Velho Complex, Borborema Province, NE Brazil and its correlations with the magmatism in eastern Nigeria. Gondwana Research 15:98–110. https://doi.org/10.1016/j.gr.2008.06.011

Guimarães I.P., Silva Filho A.F., Almeida,C.N., Macambira M.B., Armstrong R.,2011. U-Pb SHRIMP data constraints on calc-alkaline granitoids with 1.3-1.6 Ga Nd TDM model ages from the central domain of the Borborema province, NE Brazil. J. South Am. Earth Sci. 31: 383–396. https://doi.org/10.1016/j.jsames.2011.03.001

Guimarães I.P., Silva Filho A.F., Armstrong R. 2017. Origin and age of coeval gabbros and leucogranites in the northern subprovince of the borborema province, NE Brazil. J South Am Earth Sci, 76:71–93. https://doi.org/10.1016/j.jsames.2017.02.014

Guimarães I.P., Van Schmus W.R., Brito Neves B.B., Bretas Bittar, S.M., Silva Filho A.F., Armstrong R. 2012. U-Pb zircon ages of orthogneisses and supracrustal rocks of the Cariris Velhos belt: Onset of Neoproterozoic rifting in the Borborema Province, NE Brazil. Precambrian Research 192–195:52–77. https://doi.org/10.1016/j.precamres.2011.10.008

Harrison T.M., Grove M., Lovera O.M., Catlos E.J., D'Andrea J. 1999. The origin of Himalayan anatexis and inverted metamorphism: Models and constraints. J. Asian Earth Sci., 17:755–772. https://doi.org/10.1016/S1367-9120(99)00018-8

Harrison T.M., Watson E.B. 1984. The behavior of apatite during crustal anatexis: Equilibrium and kinetic considerations. Geochim Cosmochim Acta, 48:1467–1477. https://doi.org/10.1016/0016-7037(84)90403-4

Hoskin P.W.O., Black L.P. 2000. Metamorphic zircon formation by solid-state recrystallization of protolith igneous zircon. J Metamorph Geol 18:423–439. https://doi.org/10.1046/j.1525-1314.2000.00266.x

Horstwood M.S.A., Košler J., Gehrels G., Jackson S.E., McLean N.M., Paton C., Pearson N.J., Sircombe K., Sylvester P., Vermeesch P., Bowring J.F., Condon D.J., Schoene B. 2016. Community-Derived Standards for LA-ICP-MS U-(Th-)Pb Geochronology – Uncertainty

Propagation, Age Interpretation and Data Reporting. Geostandards and Geoanalytical Research, 40:311-332. https://doi.org/10.1111/j.1751-908X.2016.00379.x

Inger S., Harris N. 1993. Geochemical constraints on leucogranite magmatism in the Langtang Valley, Nepal Himalaya. J Petrol., 34(2):345–368. https://doi.org/10.1093/petrology/34.2.345

Jiang Y.H., Zhu S.Q. 2017. Petrogenesis of the Late Jurassic peraluminous biotite granites and muscovite-bearing granites in SE China: geochronological, elemental and Sr–Nd–O–Hf isotopic constraints. Contrib to Mineral Petrol, 172:1–27. https://doi.org/10.1007/s00410-017-1422-5

Keay S., Collins W.J., McCulloch M.T. 1997. A three-component Sr-Nd isotopic mixing model for granitoid genesis, Lachlan fold belt, eastern Australia. Geology 25, 307–310.

Kemp A.I., Hawkesworth C.J., Foster, G.L., Paterson B.A., Woodhead, J.D., Hergt, J.M., Gray, C.M., Whitehouse, M.J., 2007. Magmatic and crustal differentiation history of granitic rocks from Hf–O isotopes in zircon. Science 315, 980–983.

King P.L., White A.J.R., Chappell B.W., Allen C.M. 1997. Characterization and origin of aluminous A-type granites from the Lachlan Fold Belt, Southeastern Australia. J Petrol 38:371–391. https://doi.org/10.1093/petroj/38.3.371

Kozuch M. 2003. Isotopic and trace element geochemistry of early Neoproterozoic gneissic and metavolcanic rocks in the Cariris Velhos orogen of the Borborema Province, Brazil, and their bearing on tectonic setting. Ph.D. Thesis, University of Kansas, Lawrence, 199 p.

Leloup P.H., Ricard Y., Battaglia J., Lacassin R. 1999. Shear heating in continental strike-slip shear zones: Model and field examples. Geophys J Int., 136:19–40. https://doi.org/10.1046/j.1365-246X.1999.00683.x

Lima M., Nogueira Neto, J.A., Azevedo M.R., Valle Aguado, B. 2010. Geología y geocronología U-Pb del granito de Banabuiú, Noroeste Ceará, Brasil. Estudios Geológicos, 66(1):35-44. https://doi.org/10.3989/egeol.40196.113

Lima J.V., Guimarães I.P., Santos L., Amorim J.V.A., Douglas J.S.F. 2017. Geochemical and isotopic characterization of the granitic magmatism along the Remígio - Pocinhos shear zone, Borborema Province, NE Brazil. Journal of South American Earth Sciences, 75:116-133.

Lopez-Sanchez M.A., Aleinikoff J.N., Marcos A., Martínez F.J., Llana-Fúnez S. 2016. An example of low-Th/U zircon overgrowths of magmatic origin in a late orogenic variscan intrusion: The San Ciprián massif (NW Spain). J. Geol. Soc. London., 173:282–291. https://doi.org/10.1144/jgs2015-071

Lopez-Sanchez M.A., García-Sansegundo J., Martínez F.J. 2018. The significance of early Permian and early Carboniferous U–Pb zircon ages in the Bossòst and Lys-Caillaouas granitoids (Pyrenean Axial Zone). Geol J, 54:2048–2063. https://doi.org/10.1002/gj.3283

Ludwig KR (2001) Isoplot/Ex 2.49. Berkley Geocronology Center.

Medeiros V., Cavalcante R., Santos F., Rodrigues J., Santana, J. Costa A., Cabral Neto I. 2021. The Rio Piranhas-Seridó Domain, Borborema Province, Northeastern Brazil: Review of geological-geochronological data and implications for stratigraphy and crustal evolution. J. Geol. Surv. Brazil 4, 179–207. https://doi.org/10.29396/jgsb.2021.v4.n3.1

Miller C.F., McDowell S.M., Mapes R.W. 2003. Hot and cold granites: Implications of zircon saturation temperatures and preservation of inheritance. Geology, 31:529–532. https://doi.org/10.1130/0091-7613(2003)031<0529:HACGIO>2.0.CO;2

Nabelek P.I. (2020) Petrogenesis of leucogranites in collisional orogens. In: Janoušek, V., Bonin, B., Collins, W.J., Farina, F. & Bowden, P. (eds) 2020. Post-Archean Granitic Rocks: Petrogenetic Processes and Tectonic Environments. Geol Soc Spec Publ 491:179–207. https://doi.org/10.1144/SP491-2018-181

Nabelek P.I., Liu M. 2004. Petrologic and thermal constraints on the origin of leucogranites in collisional orogens. Trans R Soc Edinburgh, Earth Sci., 95:73–85. https://doi.org/10.1017/s0263593300000936

Nabelek P.I., Whittington A.G., Hofmeister A.M. 2010. Strain heating as a mechanism for partial melting and ultrahigh temperature metamorphism in convergent orogens: Implications of temperature-dependent thermal diffusivity and rheology. J Geophys Res Solid Earth, 115:. https://doi.org/10.1029/2010JB007727

Nakamura N. 1974. Determination of REE, Ba, Fe, Mg, Na and K in carbonaceous and ordinary chondrites. Geochim Cosmochim Acta., 38(5)757-775. https://doi.org/10.1016/0016-7037(74)90149-5

Neves S.P. 2003. Proterozoic history of the Borborema province (NE Brazil): Correlations with neighboring cratons and Pan-African belts and implications for the evolution of western Gondwana. Tectonics 22:. https://doi.org/10.1029/2001TC001352

Neves S.P. 2011. Atlantica revisited: New data and thoughts on the formation and evolution of a long-lived continent. Int Geol Rev, 53:1377–1391. https://doi.org/10.1080/00206814.2010.527676

Neves S.P. 2015. Constraints from zircon geochronology on the tectonic evolution of the Borborema Province (NE Brazil): Widespread intracontinental Neoproterozoic reworking of

a Paleoproterozoic accretionary orogen. J South Am Earth Sci, 58:150–164. https://doi.org/10.1016/j.jsames.2014.08.004

Neves S.P., Melo S.C., Moura C.A.V., Mariano G., Silva, J.M.R. 2004. Zircon Pb-Pb geochronology of the Caruaru area, northeastern Brazil: Temporal constraints on the Proterozoic evolution of borborema province. Int. Geol. Rev., 46:52–63. https://doi.org/10.2747/0020-6814.46.1.52

Neves S.P., Bruguier O., Bosch D., Silva J.M.R., Mariano G. 2008. U-Pb ages of plutonic and metaplutonic rocks in southern Borborema Province (NE Brazil): Timing of Brasiliano deformation and magmatism. J. South Am. Earth Sci. 25:285–297. https://doi.org/10.1016/j.jsames.2007.06.003

Neves S.P., Monié P., Bruguier O., Silva J.M.R. 2012. Geochronological, thermochronological and thermobarometric constraints on deformation, magmatism and thermal regimes in eastern Borborema Province (NE Brazil). J South Am Earth Sci, 38:129–146. https://doi.org/10.1016/j.jsames.2012.06.003

Neves S.P., Teixeira C.M.L., Bruguier O. 2020. Long-lived localized magmatism in central-eastern part of the Pernambuco-Alagoas Domain, Borborema Province (NE Brazil): Implications for tectonic setting, heat sources, and lithospheric reworking. Precambrian Res 337: https://doi.org/10.1016/j.precamres.2019.105559

Oliveira E.P., Toteu S.F., Araújo M.N.C., Carvalho M.J., Nascimento R.S., Bueno J.F., McNaughton N., Basilici G. 2006. Geologic correlation between the Neoproterozoic Sergipano domain (NE Brazil) and the Yaoundé belt (Cameroon, Africa). Journal of African Earth Sciences, 44:470–478. https://doi.org/10.1016/j.jafrearsci.2005.11.014

Oliveira E.P., Windley B.F., Araújo M.N.C. 2010. The Neoproterozoic Sergipano orogenic belt, NE Brazil: A complete plate tectonic cycle in western Gondwana. Precambrian Res 181:64–84. https://doi.org/10.1016/j.precamres.2010.05.014

Oliveira E.P., Bueno J.F., McNaughton N.J., Silva Filho A.F., Nascimento R.S., Donatti-Filho J.P. 2015. Age, composition, and source of continental arc- and syn-collision granites of the Neoproterozoic Sergipano domain, Southern Borborema Province, Brazil. Journal of South American Earth Sciences58:257–280. https://doi.org/10.1016/j.jsames.2014.08.003

Patiño Douce A.E., Beard J.S. 1995 Dehydration-melting of biotite gneiss and quartz amphibolite from 3 to 15 kbar. J Petrol. https://doi.org/10.1093/petrology/36.3.707

Patiño Douce A.E., Harris N. 1998. Experimental constraints on Himalayan anatexis. Journal of Petrology, 39:689–710. https://doi.org/10.1093/petroj/39.4.689

Patiño Douce A.E. 1999. What do experiments tell us about the relative contributions of crust and mantle to the origin of granitic magmas? Geological Society Special Publications, 168:55–75. https://doi.org/10.1144/GSL.SP.1999.168.01.05

Pearce J., Harris N.B.W., Tindle A.D. 1984. Trace element discrimination diagrams for the tectonic interpretation of granitic rocks. J Petrol 25:659–983.

Pearce J., Leng M.J. 1996. Sources and settings of granitic rocks. Episodes 19:120–125

Petö P. 1976. An experimental investigation of melting reactions involving muscovite and paragonite in the silica-satured portion of the system K2O-Na2O-Al2O3-SiO2-H2O to 15kbar total pressure. Progress on Experimental Petrology, 3:41-45.

Pichavant M., Montel J.M., Richard L.R. 1992 Apatite solubility in peraluminous liquids: Experimental data and an extension of the Harrison-Watson model. Geochimica et Cosmochimica Acta, 56:3855–3861. https://doi.org/10.1016/0016-7037(92)90178-L

Rubatto D. 2002 Zircon trace element geochemistry: Partitioning with garnet and the link between U-Pb ages and metamorphism. Chemical Geology, 184:123–138. https://doi.org/10.1016/S0009-2541(01)00355-2

Rudnick R.L., Gao, S. 2003. Composition of the continental crust. In: Rudnick, R.L. (Ed.), Treatise on Geochemistry. Elsevier-Pergamon, Oxford, p. 1-64.

Santos E.J. 1995. O complexo granítico Lagoa das Pedras: Acresção e colisão na região de Floresta (Pernambuco) Província da Borborema. Ph.D. thesis, Universidade de São Paulo, São Paulo, 228 p.

Santos E.J., Medeiros V.C. 1999. Constraints From Granitic Plutonism on Proterozoic Crustal Growth of the Transverse Zone, Borborema Province, Ne Brazil. Revista Brasileira de Geociências, 29:73–84. https://doi.org/10.25249/0375-7536.1999297384

Santos E.J., Van Schmus W.R., Kozuch M., Brito Neves B.B. 2010. The Cariris Velhos tectonic event in Northeast Brazil. Journal of South American Earth Sciences29:61–76. https://doi.org/10.1016/j.jsames.2009.07.003

Santos L., Guimarães I.P., Silva Filho A.F, Farias DJS *et al*. (2014) Ediacaran extensional magmatism in the Borborema Province, NE Brazil: Serra Branca Pluton. Comunicações Geológicas 101:199-203

Sial A.N. 1986. Granite-types in northeast Brazil: current knowledge. Revista Brasileira de Geociencias, 16:54-72. https://doi.org/10.25249/0375-7536.19865472

Sial A.N., Ferreira V.P. 2016. Magma associations in Ediacaran granitoids of the Cachoeirinha–Salgueiro and Alto Pajeú terranes, northeastern Brazil: Forty years of studies. Journal of South American Earth Sciences, 68:113-133. https://doi.org/10.1016/j.jsames.2015.10.005

Silva Filho A.F., Guimarães I.P., Brito M.E.L., Pimentel M.M. 1997. Geochemical signatures of main neoproterozoic late-tectonic granitoids from the proterozoic sergipano fold belt, brazil: Significance for the brasiliano orogeny. Internation Geology Review, 39:639–659. https://doi.org/10.1080/00206819709465293

Silva Filho A.F., Guimarães I.P., Van Schmus W.R., Armstrong R.A., Silva, J.M.R., Osako L.S., Cocentino L.M.. 2014. SHRIMP U–Pb zircon geochronology and Nd signatures of supracrustal sequences and orthogneisses constrain the Neoproterozoic evolution of the Pernambuco–Alagoas domain, southern part of Borborema Province, NE Brazil. International Journal of Earth Sciences. 103:2155–2190. https://doi.org/10.1007/s00531-014-1035-4

Silva Filho A.F., Guimarães I.P., Santos L., Armstrong R., Van Schmus W.R. 2016. Geochemistry, U–Pb geochronology, Sm–Nd and O isotopes of ca. 50 Ma long Ediacaran High-K Syn-Collisional Magmatism in the Pernambuco Alagoas Domain, Borborema Province, NE Brazil. Journal of South American Earth Sciences, 68:134–154. https://doi.org/10.1016/j.jsames.2015.12.013

Silva Filho A.F., Guimarães I.P., Armstrong R.A., Silva J.M.R, Schmus W.R., Farias D.S., Ferreira V.P., Amorim J.V.A., Souza K. & Cocentino L.M. 2021. A major neoproterozoic crustal boundary in the Borborema province of ne Brazil, International Geology Review, https://doi.org/10.1080/00206814.2021.1966681

Souza Z.S., Montel J.M., Gioia S.M.L.C., Hollanda M.H.B.M., Nascimento M.A.L., Jardim de Sá E.F., Amaro V.E., Pimental M., Lardeaux J.M., Veschambre M. 2006. Eletron micropobe dating of monazite from high-T shear zones in the São José do Campreste Massif, NE Brazil. Gondwana Research. 9:441-455. https://doi.org/10.1016/j.gr.2005.11.008

Söderlund U., Patchett J.P., Vervoort J.D., Isachsen C.E. 2004. The ^{176}Lu decay constant determined by Lu-Hf and U-Pb isotope systematics of Precambrian mafic intrusions. Earth and Planetary Science Letters, 219:311-324. https://doi.org/10.1016/S0012-821X(04)00012-3

Stacey J.S., Kramers J.D. 1975. Approximation of terrestrial lead isotope evolution by a two-stage model. Earth and Planetary Science Letters, 26:207–221. https://doi.org/10.1016/0012-821X(75)90088-6

Stepanov, A.S., Hermann, J., Rubatto, D., Rapp, R.P., 2012. Experimental study of monazite/melt partitioning with implications for the REE, Th and U geochemistry of crustal rocks. Chem. Geol. 300–301, 200–220. https://doi.org/10.1016/J.CHEMGEO.2012.01.007

Sylvester P.J. 1998. Post-collisional strongly peraluminous granites. Lithos, 45:29–44. https://doi.org/10.1016/S0024-4937(98)00024-3

Tang, M., Wang, X.L., Shu, X.J., Wang, D., Yang, T., Gopon, P., 2014. Hafnium isotopic heterogeneity in zircons from granitic rocks: Geochemical evaluation and modeling of "zircon effect" in crustal anatexis. Earth Planet. Sci. Lett. 389, 188–199. https://doi.org/10.1016/J.EPSL.2013.12.036

Thompson R.N. 1982 Magmatism of the British Tertiary Volcanic Province. Scottish Journal of Geology, 18(1):49–107. https://doi.org/10.1144/sjg18010049

Thompson A.B., Connolly J.A.D. 1995. Melting of the continental crust: some thermal and petrological constraints on anatexis in continental collision zones and other tectonic settings. Journal of Geophysical Research, 100:565–579. https://doi.org/10.1029/95jb00191

Toteu S.F., Van Schmus W.R., Penaye J., Michard A. 2001. New U-Pb and Sm-Nd data from north-central Cameroon and its bearing on the pre-Pan African history of Central Africa. Precambrian Research, 108:45–73. https://doi.org/10.1016/S0301-9268(00)00149-2

Vauchez A., Neves S.P., Caby R., Corsini M., Egydio-Silva M., Arthaud M., Amaro V. 1995. The Borborema shear zone system, NE Brazil. Journal of South American Earth Sciences, 8:247–266. https://doi.org/10.1016/0895-9811(95)00012-5

Van Schmus W.R., Brito Neves B.B., Hackspacher P., Babinski M. 1995. U Pb and Sm Nd geochronologic studies of the eastern Borborema Province, Northeastern Brazil: initial conclusions. Journal of South American Earth Sciences, 8:267–288. https://doi.org/10.1016/0895-9811(95)00013-6

Van Schmus W.R., Kozuch M., Brito Neves B.B. 2011. Precambrian history of the Zona Transversal of the Borborema Province, NE Brazil: Insights from Sm-Nd and U-Pb geochronology. Journal of South American Earth Sciences, 31:227–252. https://doi.org/10.1016/j.jsames.2011.02.010

Van Schmus WR, Oliveira EP, Da Silva Filho AF, *et al* (2008) Proterozoic links between the Borborema Province, NE Brazil, and the Central African fold belt. Geol Soc Spec Publ 294:69–99. https://doi.org/10.1144/SP294.5

Vernon, R.H. 1991. Interpretation of microstructures of microgranitoid enclaves. In: Didier, J. & Barbarin, B. (eds): Enclaves and Granite Petrology. Elsevier, Amsterdam, 277-291.

Vernon, R.H. 2000. Review of microstructural evidence of magmatic and solid-state flow. Electronic Geosciences 5:1-23. https://doi.org/10.1007/s10069-000-0002-3

Viegas L.G.F., Archanjo C.J., Hollanda M.H.B.M., Vauchez A. 2014. Microfabrics and zircon U-Pb (SHRIMP) chronology of mylonites from the Patos shear zone (Borborema Province,

NE Brazil). Precambrian Research 243:1–17. https://doi.org/10.1016/j.precamres.2013.12.020

Watson E.B., Capobianco C.J. 1981. Phosphorus and the rare earth elements in felsic magmas: an assessment of the role of apatite. Geochim Cosmochim Acta 45:2349–2358. https://doi.org/10.1016/0016-7037(81)90088-0

Williams I.S., Claesson S. 1987. Isotopic evidence for the Precambrian provenance and Caledonian metamorphism of high grade paragneisses from the Seve Nappes, Scandinavian Caledonides - II. Ion microprobe zircon U-Th-Pb. Contributions to Mineralogy and Petrology, 97:205–217. https://doi.org/10.1007/BF00371240

Zen E.A. 1986. Aluminum enrichment in silicate melts by fractional crystallization: Some mineralogic and petrographic constraints. Journal of Petrology, 27:1095–1117. https://doi.org/10.1093/petrology/27.5.1095

6 CONCLUSÕES

Os aspectos petrográficos, geoquímicos e geocronológicos dos plutons a duas micas Quipapá e Mamanguape são bastante similares aos leucogranitos peraluminosos a duas micas e biotita granitos presentes em toda as porções da província Borborema. Em suma, os dados adquiridos e a comparação entre estas rochas nos permite as presentes conclusões:

1. Mineralogicamente são constituídos por quartzo, K-feldspato, plagioclásio, muscovita e biotita em diferentes proporções modais. Correspondem em sua maioria a sienogranitos e monzogranitos.

2. Os leucogranitos são todos peraluminosos com A/CNK > 1. Assim como a definição clássica dos granitos tipo-S possuem elevados teores de SiO_2 (em sua grande maioria >70%), sendo relativamente ricos em K_2O (3,23-6,93%) e pobres em Na_2O (<2,59-4,16%).

3. Baseado nos dados geocronológicos os leucogranitos a duas micas e biotita granitos da Província Borborema apresentam se em dois intervalos de idades de cristalização distintos: 1) 640-600 Ma, associados ao estágio compressional da orogênese Brasiliana e 2) 590-560 Ma, associados a fase transcorrente.

Os leucogranitos a duas micas com cristalização entre 640–600 Ma são descritos unicamente na subprovíncia Sul, nos domínios PEAL e Sergipano, não sendo até o momento descritos em outras subprovíncias. As rochas pertencentes a este grupo, (eg. pluton Quipapá) marcam os estágios iniciais do estágio compressivo da orogênese Brasiliana no domínio PEAL da Província Borborema. A provável fonte de calor responsável pela gênese destas rochas foi o *shear heating* ou s*train heating* produzido com o empilhamento crustal durante a colisão entre o domínio PEAL e o Cráton São Francisco.

Por outro lado, os leucogranitos que apresentam cristalização compreendida entre o intervalo de 590-560 Ma (eg. pluton Mamanguape) estão presentes em todas as porções de Província Borborema estando em sua maioria associados ao estágio transcorrente da orogênese Brasiliana, cuja fonte de calor foi o *shear heating*.

As características geoquímicas observadas nos leucogranitos a duas micas e biotita granitos apontam para gênese oriunda de fusão parcial de litologias majoritariamente crustais

através da desidratação de muscovita, tendo pouca ou nenhuma participação de material mantélico juvenil.

REFERÊNCIAS

ALONSO-PEREZ, R.; MÜNTENER, O.; ULMER, P. Igneous garnet and amphibole fractionation in the roots of island arcs: Experimental constraints on andesitic liquids. **Contributions to Mineralogy and Petrology**, v. 157, n. 4, p. 541–558, 2009.

ANNEN, C.; SPARKS, R. S. J. Effects of repetitive emplacement of basaltic intrusions on thermal evolution and melt generation in the crust. **Earth and Planetary Science Letters**, v. 203, n. 3–4, p. 937–955, 2002.

BARBARIN, B. Genesis of the two main types of peraluminous granitoids. **Geology**, v. 24, n. 4, p. 295-298, 1996.

BARBARIN, B. A review of the relationships between granitoid types, their origins and their geodynamic environments. **Lithos**, v. 46, n. 3, p. 605–626, 1999.

BOWEN, N. L. The granite problem and the method of multiple prejudices. **Memoir of the Geological Society of America**, v. 28, p. 79–90, 1948.

BRITO NEVES, B. B. et al. O Evento Cariris Velhos Na Província Borborema: Integração De Dados, Implicações E Perspectivas. **Revista Brasileira de Geociências**, v. 25, n. 4, p. 279–296, 1995.

BRITO NEVES, B. B. et al. O terreno Alto Moxotó no Leste da Paraíba ("Maçico Caldas Brandão'). Revista Brasileira de Geociências, v. 32, n. 2, p. 185–194, 2001.

BRITO NEVES, B. B.; CORDANI, U. G. Tectonic evolution of South America during the Late Proterozoic. **Precambrian Research**, v. 53, n. 1–2, p. 23–40, 1991.

BRITO NEVES, B. B.; VAN SCHMUS, W. R.; FETTER, A. North-western Africa-North-eastern Brazil. Major tectonic links and correlation problems. **Journal of African Earth Sciences**, v. 34, n. 3–4, p. 275–278, 2002.

CABY, R. Precambrian terranes of Benin-Nigeria and northeast Brazil and the Late Proterozoic south Atlantic fit. **Special Paper of the Geological Society of America**, v. 230, p. 145–158, 1989.

CASTAING, C. et al. Palaeogeographical reconstructions of the Pan-African/Brasiliano orogen: closure of an oceanic domain or intracontinental convergence between major blocks? **Precambrian Research**, v. 69, n. 1–4, p. 327–344, 1994.

CAXITO, F. A. et al. Neoproterozoic oceanic crust remnants in northeast Brazil. Geology, v. 42, n. 5, p. 387–390, 2014.

CAXITO, F. A. et al. A complete Wilson Cycle recorded within the Riacho do Pontal Orogen, NE Brazil: Implications for the Neoproterozoic evolution of the Borborema Province at the heart of West Gondwana. **Precambrian Research**, 2016.

CAXITO, F. A. et al. Toward an integrated model of geological evolution for NE Brazil-NW

Africa: The Borborema Province and its connections to the Trans-Saharan (Benino-Nigerian and Tuareg shields) and Central African orogens. **Brazilian Journal of Geology**, v. 50, n. 2, 2020.

CHAPPELL, B. W.; WHITE, A. J. R. Two contrasting granite types. **Pacific Geology**, p. 173–174, 1974.

CHAPPELL, B.W.; WHITE, A.J.R. Two contrasting granite types: 25 years later. **Australian Journal Earth Sciences** v. 48, p. 489–499, 2001.

CLARK, D. B. The mineralogy of peraluminou granites: A review. **Canadian mineralogist**, v. 19, p. 3-18, 1981

CROSS, W. et al. A Quantitative Chemico-Mineralogical Classification and Nomenclature of Igneous Rocks. **The Journal of Geology**, v. 10, n. 6, p. 555–690, 1902.

DANTAS, E. L. et al. Archean Accretion in the São José Do Campestre Massif, Borborema Province, Northeast Brazil. **Revista Brasileira de Geociências**, v. 28, n. 2, p. 221–228, 1998.

DANTAS, E. L. et al. The 3.4-3.5 Ga São José do Campestre massif, NE Brazil: Remnants of the oldest crust in South America. **Precambrian Research**, v. 130, n. 1–4, p. 113–137, 2004.

DE ALMEIDA, F. F. M. et al. Brazilian structural provinces: An introduction. **Earth Science Reviews**, v. 17, n. 1–2, p. 1–29, 1981.

FERREIRA, V. P.; SIAL, A. N.; JARDIM DE SÁ, E. F. Geochemical and isotopic signatures of Proterozoic granitoids in terranes of the Borborema structural province, northeastern Brazil. **Journal of South American Earth Sciences**, v. 11, n. 5, p. 439–455, 1998.

FERREIRA, V. P. et al. Contrasting sources and P-T crystallization conditions of epidote-bearing granitic rocks, northeastern Brazil: O, Sr, and Nd isotopes. **Lithos**, v. 121, n. 1–4, p. 189–201, 2011.

FROST, B. R. et al. A geochemical classification for granitic rocks. **Journal of Petrology**, v. 42, n. 11, p. 2033–2048, 2001.

GANADE DE ARAUJO, C. E.; WEINBERG, R. F.; CORDANI, U. G. Extruding the Borborema Province (NE-Brazil): A two-stage Neoproterozoic collision process. **Terra Nova**, v. 26, n. 2, p. 157–168, 2014.

GANADE, C. E. et al. Tightening-up NE Brazil and NW Africa connections: New U-Pb/Lu-Hf zircon data of a complete plate tectonic cycle in the Dahomey belt of the West Gondwana Orogen in Togo and Benin. **Precambrian Research**, v. 276, p. 24–42, 2016.

GUIMARÃES, I. P. et al. Brasiliano (Pan-African) granitic magmatism in the Pajeú- Paraíba belt, Northeast Brazil: An isotopic and geochronological approach. **Precambrian Research**, v. 135, p. 23–53, 2004.

GUIMARÃES, I. P. et al. U-Pb SHRIMP data constraints on calc-alkaline granitoids with 1.3-1.6 Ga Nd TDM model ages from the central domain of the Borborema province, NE

Brazil. **Journal of South American Earth Sciences**, v. 11, n. 4, p. 383-396, 2011.

GUIMARÃES, I. P. et al. U-Pb zircon ages of orthogneisses and supracrustal rocks of the Cariris Velhos belt: Onset of Neoproterozoic rifting in the Borborema Province, NE Brazil. **Precambrian Research**, v. 192-193, n. 1, p. 52-77, 2012.

HUERTA, A. D.; ROYDEN, L. H.; HODGES, K. V. The thermal structure of collisional orogens as a response to accretion, erosion, and radiogenic heating. **Journal of Geophysical Research: Solid Earth**, v. 103, n. 7, p. 15287–15302, 1998.

JARDIM DE SÁ, E.F. A evolução proterozóica da Província Borborema. In: Proceedings of the XI Geological Symposium of Northeast Brazil. Extended Abstract. [S.l], 1984, p. 297–316.

JOHANNES, W.; HOLTZ, F. **Petrog. Exp. Petrol. granitic rocks**. Berlin: Springer Berlin Heidelberg, 1996.

KALSBEEK, F. et al. Recognition of Early and Late Neoproterozoic supracrustal units in West Africa and North-East Brazil from detrital zircon geochronology. **Precambrian Research**, v. 226, p. 105–115, 2013.

KILPATRICK, J. A.; ELLIS, D. J. C-type magmas: Igneous charnockites and their extrusive equivalents. **Transactions of the Royal Society of Edinburgh: Earth Sciences**, v. 83, n. 1–2, p. 155–164, 1992.

LE BRETON, N.; THOMPSON, A. B. Fluid-absent (dehydration) melting of biotite in metapelites in the early stages of crustal anatexis. **Contributions to Mineralogy and Petrology**, v. 99, p. 226-237, 1988.

LE FORT, P. et al. Crustal generation of the Himalayan leucogranites. **Tectonophysics**, v. 134, n. 1–3, p. 39–57, 1987.

LEITE, P. R. B. et al. Timing of granitic magmatism in the northern Borborema Province, Brazil: A U-Pb study of granitoids from the Alto Pajeu Terrain. **Journal of South American Earth Sciences**, v. 13, n. 6, p. 549–559, 2000.

LELOUP, P. H. et al. Shear heating in continental strike-slip shear zones: Model and field examples. **Geophysical Journal International**, v. 136, n. 1, p. 19–40, 1999.

LOISELLE, M. C.; WONES, D. R. Characteristics and origin of anorogenic granites. In: ANNUAL MEETINGS OF THE GEOLOGICAL SOCIETY OF AMERICA AND ASSOCIATED SOCIETIES, 1979, San Diego. Abstracts. San Diego, 1979. v. 11, p. 468.

MATTEINI, M. et al. Combined U-Pb and Lu-Hf isotope analyses by laser ablation MC-ICP-MS: Methodology and applications. **Anais da Academia Brasileira de Ciencias**, v. 82, n. 2, p. 479–491, 2010.

NABELEK, P. I. Petrogenesis of leucogranites in collisional orogens. In: Janoušek, V., Bonin, B., Collins, W.J., Farina, F. & Bowden, P. (eds) 2020. Post-Archean Granitic Rocks: Petrogenetic Processes and Tectonic Environments. **Geological Society Special Publication**,

v. 491, n. 1, p. 179–207, 2019.

NABELEK, P. I.; LIU, M. Leucogranites in the Black Hills of South Dakota: The consequence of shear heating during continental collision. **Geology**, v. 27, n. 6, p. 523–526, 1999.

NABELEK, P. I.; LIU, M. Petrologic and thermal constraints on the origin of leucogranites in collisional orogens. **Transactions of the Royal Society of Edinburgh, Earth Sciences**, v. 95, n. 1–2, p. 73–85, 2004.

NABELEK, P. I.; LIU, M.; SIRBESCU, M. L. Thermo-rheological, shear heating model for leucogranite generation, metamorphism, and deformation during the ProterozoiTrans-Hudson orogeny, Black Hills, South Dakota. **Tectonophysics**, v. 342, n. 3–4, p. 371–388, 2001.

NABELEK, P. I.; WHITTINGTON, A. G.; HOFMEISTER, A. M. Strain heating as a mechanism for partial melting and ultrahigh temperature metamorphism in convergent orogens: Implications of temperature-dependent thermal diffusivity and rheology. **Journal of Geophysical Research: Solid Earth**, v. 115, n. 12, 2010.

NEVES, S. P. et al. From extension to shortening: Dating the onset of the Brasiliano Orogeny in eastern Borborema Province (NE Brazil). **Journal of South American Earth Sciences**, v. 58, p. 238–256, 2015.

NEVES, S. P. Atlantica revisited: New data and thoughts on the formation and evolution of a long-lived continent. **International Geology Review**, v. 53, n. 11–12, p. 1377–1391, 2011.

NEVES, S. P. Constraints from zircon geochronology on the tectonic evolution of the Borborema Province (NE Brazil): Widespread intracontinental Neoproterozoic reworking of a Paleoproterozoic accretionary orogen. **Journal of South American Earth Sciences**, v. 58, p. 150–164, 2015.

NEVES, S. P. Proterozoic history of the Borborema province (NE Brazil): Correlations with neighboring cratons and Pan-African belts and implications for the evolution of western Gondwana. **Tectonics**, v. 22, n. 4, 2003.

OLIVEIRA, E. P. et al. Geologic correlation between the Neoproterozoic Sergipano belt (NE Brazil) and the Yaoundé belt (Cameroon, Africa). **Journal of African Earth Sciences**, v. 44, n. 4- 5 SPEC. ISS., p. 470–478, 2006.

OLIVEIRA, E. P.; WINDLEY, B. F.; ARAÚJO, M. N. C. The Neoproterozoic Sergipano orogenic belt, NE Brazil: A complete plate tectonic cycle in western Gondwana. **Precambrian Research**, v. 181, n. 1–4, p. 64–84, 2010.

PATIÑO DOUCE, A. E.; HARRIS, N. Experimental constraints on Himalayan anatexis. **Journal of Petrology**, v. 39, p. 689-710, 1998.

PATIÑO DOUCE, A. E. What do experiments tell us about the relative contributions of crust and mantle to the origin of granitic magmas? **Geological Society Special Publications**, v. 168, p. 55-75. 1999.

PETÖ, P. An experimental investigation of melting reactions involving muscovite and paragonite in the silica-satured portion of the system K2O-Na2O-Al2O3-SiO2-H2O to 15kbar total pressure. **Progress on Experimental Petrology**, v. 3, p. 41-45, 1976.

PITCHER, W. S. **The Nature and Origin of Granite**. 1. ed. London - Glasgow: Chapman and Hall, 1993.

SANTOS, E. J. **O complexo granítico Lagoa das Pedras: Acresção e colisão na região de Floresta (Pernambuco) Província da Borborema**. 1995. Universidade de São Paulo, 1995.

SANTOS, E. J. et al. The Cariris Velhos tectonic event in Northeast Brazil. **Journal of South American Earth Sciences**, v. 29, n. 1, p. 61–76, 2010.

SANTOS, L. C. M. L. et al. Accretion Tectonics in Western Gondwana Deduced From Sm-Nd Isotope Mapping of Terranes in the Borborema Province, NE Brazil. **Tectonics**, v. 37, n. 8, p. 2727–2743, 2018.

SIAL, A. N. Granite-types in northeast Brazil: current knowledge. **Revista Brasileira de Geociencias**, 1986.

SILVA FILHO, A. F. et al. SHRIMP U–Pb zircon geochronology and Nd signatures of supracrustal sequences and orthogneisses constrain the Neoproterozoic evolution of the Pernambuco–Alagoas domain, southern part of Borborema Province, NE Brazil. **International Journal of Earth Sciences**, v. 103, n. 8, p. 2155–2190, 2014.

SILVA FILHO, A. F. et al. Geochemistry, U–Pb geochronology, Sm–Nd and O isotopes of ca. 50 Ma long Ediacaran High-K Syn-Collisional Magmatism in the Pernambuco Alagoas Domain, Borborema Province, NE Brazil. **Journal of South American Earth Sciences**, v. 68, p. 134–154, 2016.

STEVENS, G.; CLEMENS, J. D. Fluid-absent melting and the roles of fluids in the lithosphere: a slanted summary? **Chemical Geology**, v. 108, n. 1–4, p. 1–17, 1993.
STRECKEISEN, A. To each plutonic rock its proper name. **Earth Science Reviews**, v. 12, n. 1, p. 1–33, 1976.

SYLVESTER, P.J. Post-collisional strongly peraluminous granites. **Lithos**, v. 45, n. (1-4), p. 29-44, 1998.

THOMPSON, A. B.; CONNOLLY, J. A. D. Melting of the continental crust: some thermal and petrological constraints on anatexis in continental collision zones and other tectonic settings. **Journal of Geophysical Research**, v. 100, n. B8, p. 565–579, 1995.

TOTEU, S. F. et al. New U-Pb and Sm-Nd data from north-central Cameroon and its bearing on the pre-Pan African history of Central Africa. **Precambrian Research**, 2001.

TOTEU, S. F. et al. Preliminary U-Pb and Sm-Nd geochronologic data on the north-central Cameroon: contribution of an Archean and paleo-Proterozoic crust to the edification of an active domain of the Pan-African orogeny. **Comptes Rendus - Academie des Sciences, Serie II: Sciences de la Terre et des Planetes**, v. 319, n. 12, p. 1519–1524, 1994.

VAN SCHMUS, W. R. et al. Proterozoic links between the Borborema Province, NE Brazil, and the Central African fold belt. **Geological Society Special Publication**, v. 294, p. 69–99, 2008.

VAN SCHMUS, W. R. et al. U Pb and Sm Nd geochronologic studies of the eastern Borborema Province, Northeastern Brazil: initial conclusions. **Journal of South American Earth Sciences**, v. 8, n. 3–4, p. 267–288, 1995.

VAN SCHMUS, W. R.; KOZUCH, M.; DE BRITO NEVES, B. B. Precambrian history of the Zona Transversal of the Borborema Province, NE Brazil: Insights from Sm-Nd and U-Pb geochronology. **Journal of South American Earth Sciences**, v. 31, n. 2–3, p. 227–252, 2011.

VAUCHEZ, A. et al. The Borborema shear zone system, NE Brazil. **Journal of South American Earth Sciences**, 1995.

WEDEPOHL, K. H. Chemical composition and fractionation of the continental crust. **Geologische Rundschau**, v. 80, n. 2, p. 207–223, 1991.

WEINBERG, R. F.; HASALOVÁ, P. Water-fluxed melting of the continental crust: A review. **Lithos**, v. 212–215, p. 158–188, 2015.

WHITE, A. J. R. Sources of granite magmas. 1979, [S.l: s.n.], 1979. p. 539.

WHITE, R. W.; STEVENS, G.; JOHNSON, T. E. Is the crucible reproducible? Reconciling melting experiments with thermodynamic calculations. **Elements**, v. 7, n. 4, p. 241–246, 2011.

YOUNG, D. A. **Mind over Magma. The Story of Igneous Petrology**. Princeton and Oxford: Princeton University Press, 2003.

APÊNDICE A – TABELAS SUPLEMENTARES

Table A1 – Representative electron microprobe analyses of muscovite from Quipapá pluton.

SAMPLES	CG05B11	CG05B12	CG05B14	CG1751	CG09C31	CG0932	CG05A4	CG05A4
SiO_2	44.70	46.73	45.28	46.67	46.54	45.04	46.29	45.69
TiO_2	1.04	1.09	0.89	1.04	1.04	1.01	0.22	0.68
Al_2O_3	33.10	34.17	33.24	28.82	32.06	31.95	29.68	27.96
FeO_t	2.45	2.54	2.28	4.27	2.80	2.07	2.59	3.23
MnO	0.05	0.03	0.07	0.07	0.01	0.02	0.00	0.07
MgO	0.75	0.77	0.70	1.22	1.02	0.84	0.98	1.19
CaO	0.00	0.00	0.01	0.00	0.03	0.00	0.05	0.01
Na_2O	0.46	0.54	0.59	0.25	0.24	0.41	0.25	0.25
K_2O	9.85	9.90	9.48	8.13	8.42	9.64	10.33	10.06
F	0.00	0.00	0.00	0.00	0.00	0.00	0.00	0.00
Cl	0.01	0.025	0	0.006	1.04	1.008	0.22	0.68
Cr_2O_3	0.00	0.07	0.00	0.01	2.80	2.07	2.59	3.23
NiO	0.00	0.01	0.05	0.00	0.12	0.00	0.00	0.00
TOTAL	92.41	95.87	92.58	90.49	96.11	94.07	93.18	93.05
Structural formulae based on 11 O								
Si	3.08	3.10	3.11	3.28	3.12	3.09	3.20	3.20
Al_{iv}	0.92	0.90	0.89	0.72	0.88	0.91	0.80	0.80
Al_{vi}	1.78	1.77	1.79	1.66	1.65	1.68	1.62	1.51
Ti	0.05	0.05	0.05	0.05	0.05	0.05	0.01	0.04
Cr	0.00	0.00	0.00	0.00	0.15	0.11	0.14	0.18
Fe	0.14	0.14	0.13	0.25	0.16	0.12	0.15	0.19
Mn	0.00	0.00	0.00	0.00	0.00	0.00	0.00	0.00
Mg	0.08	0.08	0.07	0.13	0.10	0.09	0.10	0.12
Ni	0.00	0.00	0.00	0.00	0.01	0.00	0.00	0.00
Ca	0.00	0.00	0.00	0.00	0.00	0.00	0.00	0.00
Na	0.06	0.07	0.08	0.03	0.03	0.06	0.03	0.03
K	0.87	0.84	0.83	0.73	0.72	0.84	0.91	0.90

Table A2 – Representative electron microprobe analyses of biotite from Quipapá pluton.

SAMPLE	CG05B12	CG05B31	CG1721	CG05A3	CG092	CG095	CG05A3	CG05A4
SiO_2	34.00	34.63	36.41	35.46	36.27	36.76	35.3	34.1
TiO_2	2.22	2.21	2.29	1.81	1.94	2.61	2.0	2.6
Al_2O_3	17.01	17.73	15.34	17.15	16.57	17.26	17.2	16.3
FeO_t	26.82	27.05	23.85	25.67	25.09	24.67	26.2	26.7
MnO	0.45	0.61	0.28	0.56	0.34	0.35	0.8	0.7
MgO	4.13	4.11	5.97	5.23	6.43	5.95	4.5	5.0
CaO	0.01	0.00	0.03	0.03	0.00	0.00	0.0	0.0
Na_2O	0.06	0.07	0.05	0.01	0.02	0.10	0.0	0.0
K_2O	9.39	9.67	9.32	9.06	9.23	9.33	9.4	9.1
F	0.63	0.44	0.00	0.00	0.20	0.00	0.0	0.0
Cl	0.05	0.06	0.04	0.04	0.05	0.09	0.0	0.0
Cr_2O_3	0.02	0.00	0.13	0.00	0.09	0.01	0.0	0.0
NiO	0.00	0.04	0.00	0.00	0.01	0.04	0.0	0.0
TOTAL	94.80	96.62	93.71	95.00	96.24	97.17	95.4	94.5
Structural formulae based on 22 O								
Si	5.48	5.46	5.78	5.59	5.63	5.62	5.6	5.5
Al_{iv}	2.52	2.54	2.22	2.41	2.37	2.38	2.4	2.5
Al_{vi}	0.71	0.76	0.65	0.78	0.67	0.73	0.8	0.6
Ti	0.27	0.26	0.27	0.22	0.23	0.30	0.2	0.3
Cr	0.00	0.00	0.02	0.00	0.01	0.00	0.0	0.0
Fe	3.62	3.57	3.16	3.39	3.26	3.16	3.5	3.6
Mn	0.06	0.08	0.04	0.07	0.05	0.04	0.1	0.1
Mg	0.99	0.97	1.41	1.23	1.49	1.36	1.1	1.2
Ni	0.00	0.01	0.00	0.00	0.00	0.01	0.0	0.0
Ca	0.00	0.00	0.00	0.00	0.00	0.00	0.0	0.0
Na	0.02	0.02	0.01	0.00	0.01	0.03	0.0	0.0
K	1.93	1.95	1.89	1.82	1.83	1.82	1.9	1.9
Al total	3.2	3.3	2.9	3.2	3.0	3.1	3.2	3.1
Fe/Fe+Mg	0.8	0.8	0.7	0.7	0.7	0.7	0.8	0.8

Table A3 – Representative electron microprobe analyses of plagioclase from Quipapá pluton.

SAMPLE	CG05A1(e)	CG05A2	CG094	CG094	CG05B21	CG05B31	CG05B51	CG05A4
SiO_2	68.63	68.20	66.79	65.97	68.10	67.46	66.70	65.59
TiO_2	0.00	0.00	0.00	0.01	0.07	0.05	0.00	0.00
$Al2O_3$	19.93	20.53	20.38	20.74	19.88	20.78	21.21	19.48
Cr_2O_3	0.01	0.00	0.11	0.12	0.00	0.00	0.00	0.00
FeO	0.04	0.04	0.00	0.00	0.00	0.00	0.05	0.15
MnO	0.00	0.03	0.05	0.00	0.00	0.01	0.04	0.01
MgO	0.02	0.00	0.00	0.00	0.02	0.02	0.00	0.01
CaO	1.39	1.74	1.90	2.08	1.01	1.29	1.55	1.79
Na_2O	10.67	10.20	9.74	9.46	11.00	10.44	10.28	9.93
K_2O	0.13	0.17	0.14	0.11	0.08	0.18	0.24	0.08
TOTAL	100.82	100.91	99.10	98.49	100.16	100.21	100.06	97.03
Structural formulae based on 8 O								
Si	3.00	2.98	2.98	2.97	2.98	2.96	2.93	2.98
Ti	0.00	0.00	0.00	0.00	0.00	0.00	0.00	0.00
Al	1.03	1.06	1.07	1.10	1.03	1.08	1.10	1.04
Cr	0.00	0.00	0.00	0.00	0.00	0.00	0.00	0.00
Fe^{3+}	0.00	0.00	0.00	0.00	0.00	0.00	0.00	0.00
Fe^{2+}	0.00	0.00	0.00	0.00	0.00	0.00	0.00	0.01
Mn	0.00	0.00	0.00	0.00	0.00	0.00	0.00	0.00
Mg	0.00	0.00	0.00	0.00	0.00	0.00	0.00	0.00
Ca	0.07	0.08	0.09	0.10	0.05	0.06	0.07	0.09
Ba	0.00	0.00	0.00	0.00	0.00	0.00	0.00	0.00
Na	0.90	0.87	0.84	0.82	0.93	0.89	0.88	0.88
K	0.01	0.01	0.01	0.01	0.00	0.01	0.01	0.00
An	6.68	8.52	9.63	10.77	4.80	6.30	7.57	9.02
Ab	92.56	90.49	89.50	88.58	94.72	92.67	91.06	90.50
Or	0.76	0.99	0.86	0.65	0.47	1.03	1.37	0.49

Table A4 – Representative electron microprobe analyses of K - Feldspar from Quipapá pluton.

SAMPLE	CG05A4	CG05B12	CG17C11	CG094	CG094	CG05B11	CG05B41	CG05A1
SiO_2	63.83	64.23	63.52	66.19	65.88	65.21	63.38	66.23
TiO_2	0.01	0.08	0.05	0.00	0.02	0.04	0.02	0.07
$Al2O_3$	17.15	18.75	18.44	18.04	18.02	18.58	18.70	17.83
Cr_2O_3	0.00	0.00	0.00	0.00	0.00	0.01	0.00	0.00
FeO_t	0.00	0.01	0.00	0.00	0.07	0.06	0.00	0.04
MnO	0.01	0.00	0.01	0.00	0.00	0.02	0.00	0.05
MgO	0.00	0.02	0.00	0.01	0.00	0.01	0.01	0.01
CaO	0.04	0.06	0.06	0.01	0.00	0.16	0.03	0.03
Na_2O	0.49	0.32	0.63	0.40	0.30	0.32	0.68	0.47
K_2O	15.50	16.10	15.99	15.34	15.67	16.18	15.50	15.30
TOTAL	97.01	99.57	98.70	99.98	99.96	100.58	98.31	100.03
Structural formulae based on 8 O								
Si	3.07	3.05	3.06	3.07	3.00	2.98	2.97	2.97
Ti	0.00	0.00	0.00	0.00	0.00	0.00	0.00	0.00
Al	0.97	0.96	0.99	0.99	1.01	1.03	1.03	1.02
Cr	0.00	0.00	0.00	0.00	0.00	0.00	0.00	0.00
Fe^{3+}	0	0	0	0	0	0	0	0
Fe^{2+}	0	0	0	0	0	0	0	0
Mn	0	0	0	0	0	0	0	0
Mg	0	0	0	0	0	0	0	0
Ca	0	0	0	0	0	0	0	0
Ba	0	0	0	0	0	0	0	0
Na	0.04	0.04	0.03	0.04	0.03	0.03	0.06	0.06
K	0.90	0.94	0.93	0.91	0.95	0.95	0.93	0.95
An	0.18	0.18	0.00	0.03	0.78	0.28	0.16	0.29
Ab	4.45	4.53	2.84	3.82	2.90	2.93	6.22	5.67
Or	95.37	95.29	97.16	96.15	96.32	96.79	93.61	94.05

Table A5 – Representative electron microprobe analyses of ilmenite from Quipapá pluton.

SAMPLES	CG05B31	CG05B51	CG1711	CG1712	CG1721	CG1722	CG1723	CG1751
Cr_2O_3	0.00	0.00	0.00	0.03	0.05	0.03	0.00	0.04
Al_2O_3	0.00	0.01	0.00	0.00	0.00	0.00	0.00	0.00
TiO2	52.16	52.39	50.59	49.08	52.10	52.15	51.36	51.60
FeO	41.43	39.28	44.72	45.29	43.68	42.80	43.06	44.37
MgO	0.02	0.02	0.05	0.02	0.01	0.03	0.02	0.05
MnO	7.77	8.07	4.82	4.89	5.11	5.39	5.24	4.65
NiO	0.00	0.04	0.00	0.09	0.10	0.00	0.00	0.00
V_2O_5	0.27	0.23	0.31	0.19	0.30	0.28	0.33	0.27
Total	101.64	99.80	100.17	99.39	101.06	100.40	99.69	100.71
Formula units based on 24 oxygens and Fe^{2+}/Fe^{3+} assuming full site occupancy								
Cr	0.00	0.00	0.00	0.00	0.01	0.01	0.00	0.01
Al	0.00	0.00	0.00	0.00	0.00	0.00	0.00	0.00
Ti	7.78	7.95	7.63	7.46	7.80	7.86	7.79	7.75
Fe^{3+}	0.33	0.01	0.62	0.98	0.28	0.16	0.29	0.39
Fe^{2+}	6.55	6.62	6.89	6.69	7.00	7.01	6.98	7.02
Mg	0.00	0.01	0.01	0.01	0.00	0.01	0.01	0.01
Mn	1.31	1.38	0.82	0.84	0.86	0.91	0.90	0.79
Ni	0.00	0.01	0.00	0.02	0.02	0.00	0.00	0.00
V	0.04	0.03	0.04	0.03	0.04	0.04	0.04	0.04

Table A6 – Summary of LA-ICP-MS U-Th-Pb zircon data for sample GUS-102

												Apparent Ages (Ma)						
SPOTS	U (ppm)	Th (ppm)	Th/ U	$^{206}Pb/^{204}Pb$	$^{207}Pb/^{206}Pb$	1s (%)	$^{207}Pb/^{235}U$	1s (%)	$^{206}Pb/^{238}U$	1s (%)	Rho	$^{207}Pb/^{206}Pb$ age	1s (Ma)	$^{207}Pb/^{235}U$ age	1s (Ma)	$^{206}Pb/^{238}U$ age	1s (Ma)	Conc. (%)
22-Z13	1561	156	0.10	39986	0.0586	1.8488	0.7470	3.6645	0.0924	3.1602	0.86	554	39.84	566	15.79	570	17	102.84
06- Z04	617	196	0.32	4919	0.0592	2.2871	0.7623	2.9145	0.0934	1.7999	0.73	574	48.97	575	12.72	576	9.94	100.18
57-Z35	832	370	0.44	1767	0.0598	0.9953	0.7906	2.0220	0.0958	1.7424	0.86	598	21	591	9.02	590	9.91	98.68
12-Z08	580	122	0.21	7543	0.0592	0.8814	0.8129	1.4312	0.0995	1.1250	0.90	576	19	604	6.50	612	6.58	106.25
23-Z14	782	249	0.32	8442	0.0597	1.3219	0.8509	2.2408	0.1033	1.8055	0.80	594	28	625	10.41	634	10.91	106.79
06-Z04r	275	229	0.83	1843	0.0621	1.7824	0.8631	2.4008	0.1007	1.6084	0.87	679	38	632	11.29	619	9.49	91.17
53-Z33	738	209	0.28	13322	0.0607	1.4375	0.8759	2.2667	0.1046	1.7503	0.77	629	30.68	639	10.69	642	10.69	102.03
17-Z11	190	144	0.76	12272	0.0603	2.0487	0.8898	2.7769	0.1071	1.8747	0.67	613	44	646	13.28	656	11.69	106.96
27-Z16	407	124	0.31	19727	0.0611	1.0059	0.8926	2.0147	0.1060	1.7441	0.86	642	21.48	648	9.60	649	10.77	101.09
54-Z34	685	304	0.44	1480	0.0623	1.6706	0.9034	1.9448	0.1052	0.9958	0.73	683	35.67	654	9.37	645	6.11	94.47
23-Z14	1240	397	0.32	5056	0.0628	0.6080	0.9648	1.0554	0.1115	0.8626	0.80	700	12.95	686	5	681	5.58	97.29
46-Z28	2375	1159	0.49	6066	0.0629	0.4412	1.0340	0.8239	0.1192	0.6958	0.82	704	9	721	4.25	726	4.78	103.01
52 Z32	75	77	1.02	63909	0.1131	8.3568	4.2070	9.3340	0.2698	4.1543	0.44	1850	143.89	1675	73.82	1540	56.70	83.23
45 Z27	390	75	0.19	83856	0.1142	0.7031	4.9982	1.7014	0.3173	1.5491	0.91	1868	12.63	1819	14.29	1777	24.01	95.11
45-Z27r	441	194	0.44	18567	0.1183	0.4264	5.0947	1.0203	0.3125	0.9261	0.90	1930	7.62	1835	8.62	1753	14.21	90.82
41-Z25	201	71	0.35	163962	0.1206	0.5398	5.1362	1.6323	0.3088	1.5404	0.94	1965	9.60	1842	13.78	1735	23.39	88.28
42 Z26	616	238	0.39	71139	0.1167	1.5671	5.1547	2.5555	0.3204	2.0181	0.81	1906	27.88	1845	21.50	1792	31.50	93.99
52-Z32	82	89	1.07	26025	0.1035	2.2170	5.2169	2.4863	0.3655	1.1256	0.44	1688	40.90	1855	21.18	2008	19.42	118.96
29-Z18	325	50	0.15	303473	0.1265	0.4999	5.4042	2.1438	0.3099	2.0846	0.97	2049	8.80	1885	18.20	1740	31.72	84.91
41-Z25	252	37	0.15	64446	0.1208	1.2622	5.5112	2.7910	0.3310	2.4887	0.89	1967	22	1902	23.71	1843	39.78	93.67
42-Z26	816	464	0.57	12838	0.1231	1.3163	5.9920	2.0450	0.3531	1.5631	0.90	2001	23	1975	17.64	1949	26.27	97.41
48-Z30	195	72	0.37	63586	0.1257	1.4928	7.3343	2.2505	0.4231	1.6841	0.76	2038	26	2153	20	2275	32.28	111.56
48-Z30r	143	93	0.65	107136	0.1307	0.7426	7.7272	1.3223	0.4289	1.0941	0.91	2106	13	2200	11.89	2301	21.17	109.22

Table A7 – Major and trace elements for two mica granites from Quipapá and Jurema plutons.

TWO MICA GRANITES																
	QUIPAPÁ										JUREMA					
SAMPLES	**LMC51**	**LMC53**	**LMC61**	**CG05A**	**CG05B**	**CG09**	**CG13A**	**CG16**	**CG17**	**CG30**	**CG45A**	**ISA11A**	**ISA13**	**ISA14**	**GUS116**	**GUS111**
SiO2	71.1	73.9	71.2	74.3	73.8	74.2	74.7	75	70.8	71.9	73.6	72.93	72.76	73.74	71.37	71.95
Al2O3	14.25	14.4	14.25	14.2	14.45	14.5	14.3	14.25	14.4	14.45	13.9	13.81	14.5	14.28	14.68	14.27
FeOt	1.8	1.4	2.14	1.45	1.61	1.89	1.63	1.41	2.12	2.35	1.96	2.17	1.86	1.8	1.85	1.81
MnO	0.02	0.02	0.03	0.03	0.03	0.03	0.02	0.02	0.05	0.03	0.03	0.02	0.02	0.03	0.02	0.02
MgO	0.35	0.25	0.53	0.24	0.25	0.39	0.32	0.2	0.46	0.55	0.33	0.3	0.25	0.25	0.38	0.35
CaO	0.9	0.81	1.04	0.76	0.78	0.84	0.7	0.61	1.09	1.43	0.98	0.63	0.52	0.63	1.04	1.08
Na2O	3.31	3.86	3.06	3.4	3.27	3.29	3.33	3.22	3.44	3.38	2.88	2.71	2.46	2.89	2.76	2.96
K2O	5.64	5.27	5.32	5.03	4.93	5.08	5.11	5.13	5.38	5.4	5.9	6.18	5.4	5.41	6.5	5.95
TiO2	0.23	0.14	0.29	0.11	0.16	0.23	0.17	0.16	0.29	0.38	0.27	0.27	0.22	0.2	0.29	0.23
P2O5	0.18	0.2	0.19	0.21	0.19	0.23	0.15	0.16	0.21	0.2	0.14	0.1	0.127	0.143	0.18	0.12
LOI	1.01	0.97	0.82	0.96	1.33	1.22	1.16	1.32	1.66	1.44	0.94	0.7	1.7	0.5	0.7	1
TOTAL	98.79	101.22	98.87	100.69	100.8	101.9	101.59	101.48	99.9	101.51	100.93	99.82	99.817	99.873	99.77	99.74
TRACE ELEMENTS (ppm)																
Ba	550	299	578	285	222	374	373	215	570	647	443	540	326	270	633	421
Sr	121	85.5	122.5	81.1	59.8	99.6	96.1	61.3	123.5	175.5	112.5	129.1	77.9	71.2	166	119
Rb	304	292	335	323	369	323	300	334	390	369	347	327.6	408.6	418.2	305	333
Cs	5.19	9.32	5.91	7.73	7.04	11.4	9.09	9.78	6.65	5.96	6.02	4.7	6.2	8.8	4.3	9.7
Ga	23	21.4	24	21.4	28.4	25.4	23.1	26.8	25.9	27.3	24.3	20.7	24.9	23.9	22.4	22.6
Hf	4.7	2.5	6.9	3	3.1	4.3	3.7	3	6.5	7.6	5.6	6	4.1	3.7	5.7	5.6
Zr	167	81	229	95	98	136	138	90	232	282	189	186.1	121.7	112.1	183	201
Nb	18	15.2	20.1	18	26.5	21	20.4	29.4	24.8	20.1	24.7	21.6	28.8	27.9	18	22.1
Ta	1.2	1.7	1.2	1.6	1.5	1.7	1.8	2.3	1.5	1.5	1.7	1.9	1.9	2.1	1.3	1.7
Th	36.5	13.95	52.8	19.9	16.9	26.4	31	16.65	72.3	76.8	53.5	47.8	36.2	32	55.7	61.4
U	6.52	12.85	10.95	8.37	25.4	7.1	10.65	3.45	8.54	5.59	3.07	5.8	10.2	4	3.2	3.2
Y	9.7	5.6	9.5	10	9.4	8.8	13.2	6.7	14.8	11.5	17.5	11.4	13.7	14.1	13.8	17.5
La	58.5	20.6	77.8	28.6	23.1	47.5	59.1	24.6	95.5	92.6	64	47.5	42.1	35.2	80	78.1
Ce	129.5	44.8	173.5	60.9	52.5	102	122	54.3	217	204	139	104.6	85.5	76.4	167.6	160.3
Pr	14.05	5.13	20.7	6.45	5.78	12.25	13.25	6.15	25.6	24	15.75	11.98	10.14	9.06	18.6	18.5
Nd	47.2	17.4	71.6	21.9	21	41.9	44.2	20.4	88.7	81.9	54.1	43.7	37	32.1	64.3	62.2

Sm	8.34	3.97	11.3	4.93	4.83	8.06	7.88	4.4	14.25	12.6	10.25	8.12	6.42	6.23	11.4	11.8
Eu	0.86	0.57	1.09	0.62	0.45	0.88	0.81	0.53	1.7	1.09	0.68	0.67	0.45	0.44	0.9	0.8
Gd	4.73	3.01	5.52	3.88	3.41	5.2	4.9	3.23	7.73	5.5	6	5.22	4.54	4.29	5.34	5.8
Tb	0.53	0.36	0.53	0.51	0.48	0.66	0.58	0.4	0.89	0.56	0.8	0.6	0.62	0.6	0.74	0.76
Dy	2.33	1.38	2.08	2.15	2.08	2.53	2.78	1.6	3.4	2.59	3.72	2.59	3	3.01	2.55	3.66
Ho	0.33	0.19	0.34	0.36	0.33	0.35	0.45	0.23	0.54	0.39	0.6	0.39	0.48	0.47	0.4	0.53
Er	0.82	0.37	0.65	0.85	0.83	0.69	1.12	0.48	1.04	0.96	1.31	0.9	1.26	1.17	1	1.39
Tm	0.14	0.06	0.12	0.14	0.14	0.14	0.17	0.09	0.19	0.18	0.26	0.16	0.19	0.19	0.15	0.23
Yb	0.58	0.27	0.53	0.57	0.46	0.38	0.79	0.44	0.97	0.81	1.14	0.96	1	1.15	0.85	1.21
Lu	0.07	0.04	0.08	0.1	0.1	0.08	0.16	0.04	0.12	0.11	0.18	0.16	0.17	0.16	0.13	0.21
Z. Sat. (°C)	747.6	677.5	788.2	704.3	712.4	740.9	743.5	705.7	779.2	794.0	762.9	768.2	750.1	728.6	757.5	767.0
A. Sat. (°C)	671.6	736.7	621.1	628.7	576.9	621.0	569.9	560.5	714.9	828.8	654.5	549.1	469.3	530.3	657.5	628.8

Table A8 – Major and trace elements composition data for representative samples of Mamanguape pluton.

SAMPLES	GB-103	GB-104	GB-105	GB-105B	GB-125
SiO_2	72.7	73.7	73.1	74.4	72.8
Al_2O_3	13.85	13.6	13.45	14.15	14.15
Fe_2O_3	1.9	1.98	1.65	1.99	1.93
CaO	0.89	1.01	0.6	0.98	1.01
MgO	0.3	0.33	0.27	0.34	0.32
Na_2O	3.54	3.32	2.6	3.09	3.4
K_2O	4.85	4.96	6.59	5.56	5.57
Cr_2O_3	0.03	0.027	0.022	0.027	0.028
TiO_2	0.17	0.21	0.18	0.21	0.2
MnO	0.04	0.03	0.02	0.02	0.03
P_2O_5	0.13	0.13	0.18	0.13	0.15
SrO	<0.01	0.01	<0.01	0.01	0.01
BaO	0.03	0.04	0.03	0.06	0.05
LOI	0.91	0.75	0.73	0.83	0.77
Total	99.34	100.1	99.42	101.8	100.42
	TRACE ELEMENTS (PPM)				
Ba	272	331	252	464	431
Sr	75.2	92.5	81.4	113	106
Rb	330	279	401	288	286
Cs	15.65	11.95	7.67	10.6	10.15
Ga	22.6	21.4	20.7	20.6	21.6
Hf	3.9	5.1	4.5	4.2	4.4
Zr	114	154	125	135	141
Nb	21.4	20.1	16	18.1	18.3
Ta	2.5	1.9	1.1	1.5	1.7
Th	25	29.1	17.6	26.9	28
U	14.6	9.93	11.25	7.4	4.32
Y	25.6	26.1	19.8	22.7	23.7
V	34	6	25	15	32
W	14	13	11	12	13
Cr	230	200	200	200	210
Sn	12	8	6	7	7
La	39.4	47.3	27.1	44.2	46.6
Ce	86.3	103.5	63.6	97.2	100
Pr	9.57	11.85	7.35	10.85	11.4
Nd	32.7	39.1	25.2	36.6	38
Sm	6.84	7.45	6.55	7.2	7.79
Eu	0.52	0.42	0.37	0.48	0.46
Gd	5.83	6.36	5.84	5.83	6.13
Tb	0.93	0.96	0.96	0.97	0.98

Continuation					
Dy	5.12	4.77	4.64	4.35	4.88
Ho	0.88	0.96	0.66	0.83	0.88
Er	2.28	2.18	1.52	1.86	2.22
Yb	1.83	1.98	1.07	1.93	1.61
Lu	0.31	0.24	0.14	0.22	0.24
Zr. Sat. (°C)	714	742.5	721.9	731.8	727.4
Ap. Sat. (°C)	617.1	650.7	691	615	719
Eu/Eu*	0.25	0.19	0.18	0.23	0.2
(Ce/Yb)N	11.9	13.29	15.12	12.81	15.8

Table A9 – Summary of LA-ICP-MS U-Pb zircon data from sample GB-105 of the Mamanguape pluton.

SPOTS	ISOTOPIC RATIOS											APPARENT AGES								
	U (ppm)	Th (ppm)	Th/U	$^{206}Pb/^{204}Pb$	$^{207}Pb/^{206}Pb$	2*s* (%)	$^{207}Pb/^{235}U$	2*s* (%)	$^{206}Pb/^{238}U$	2*s* (%)	Rho	$^{207}Pb/^{206}Pb$	2*s* abs	$^{206}Pb/^{238}U$	2*s* abs	$^{207}Pb/^{235}U$	2*s* abs	$^{208}Pb/^{232}Th$	2*s* abs	Conc. (%)
1.sSMPABC108*	1180.9	53.9	0.046	242.197	0.060	2.555	0.757	2.929	0.092	1.432	0.489	587	55.4	569	7.8	572	12.9	392.8	29.8	100.6
1.sSMPABC109*	360.9	208.1	0.577	6673.441	0.059	3.186	0.742	3.585	0.091	1.644	0.459	567	69.4	563	8.9	564	15.6	71.9	7.3	100.2
1.sSMPABC110*	263.3	203.7	0.774	89.418	0.059	5.147	0.736	5.913	0.091	2.912	0.492	564	112.1	559	15.6	560	25.8	119.2	19.8	100.2
1.sSMPABC111*	445.5	36.1	0.081	132.597	0.059	2.728	0.765	3.115	0.093	1.504	0.483	584	59.2	575	8.3	577	13.8	478.2	40.9	100.3
1.sSMPABC115*	1633.8	211.3	0.129	164.770	0.060	2.527	0.777	2.909	0.095	1.440	0.495	586	54.8	583	8.0	584	13.0	427.6	33.9	100.1
1.sSMPABC118*	1586.1	272.8	0.172	123.826	0.060	2.202	0.768	2.624	0.093	1.426	0.544	589	47.8	576	7.9	578	11.6	320.1	15.0	100.5
1.sSMPABC119*	1049.8	193.3	0.184	1015.560	0.060	2.547	0.777	2.926	0.094	1.441	0.493	592	55.2	581	8.0	584	13.1	349.5	25.8	100.4
1.sSMPABC132*	2344.4	1132.6	0.483	45070.565	0.060	3.218	0.772	3.632	0.094	1.684	0.464	591	69.8	578	9.3	581	16.2	415.3	57.3	100.5
1.sSMPABC136*	1655.2	192.9	0.117	282.674	0.059	2.609	0.761	3.001	0.093	1.482	0.494	572	56.7	575	8.2	575	13.3	459.4	43.4	99.9
1.sSMPABC138*	3870.3	759.5	0.196	290.819	0.060	2.589	0.757	3.015	0.092	1.546	0.513	589	56.2	568	8.4	572	13.3	368.5	33.9	100.8
1.sSMPABC139*	1854.9	429.0	0.231	290.193	0.059	2.291	0.766	2.693	0.093	1.415	0.526	584	49.7	576	7.8	578	11.9	349	22.7	100.3
1.sSMPABC152*	2111.7	894.1	0.423	126.474	0.060	3.461	0.777	3.891	0.094	1.778	0.457	598	75.0	580	9.9	583	17.4	268	48.0	100.6
1.sSMPABC153*	2338.4	1272.2	0.544	398.900	0.060	2.402	0.781	2.812	0.094	1.462	0.520	602	52.0	582	8.1	586	12.6	454.7	36.2	100.7
1.sSMPABC160*	1354.4	249.4	0.184	25250.390	0.059	2.433	0.748	2.861	0.092	1.505	0.526	574	52.9	566	8.2	567	12.5	292.6	22.0	100.3
1.sSMPABC113**	990.9	158.9	0.160	130.467	0.060	11.585	0.830	12.652	0.100	5.086	0.402	613	250.3	614	29.8	613	60.0	0	818.6	99.9
1.sSMPABC131**	1903.3	643.6	0.338	164.683	0.060	2.487	0.827	2.931	0.099	1.551	0.529	616	53.7	611	9.0	612	13.6	128.8	9.0	100.1
1.sSMPABC149**	862.0	187.4	0.217	73.950	0.062	4.363	0.912	4.847	0.107	2.111	0.436	666	93.4	656	13.2	658	23.8	413.3	93.4	100.3
1.sSMPABC150**	2170.5	546.6	0.252	269.258	0.061	3.422	0.851	3.826	0.102	1.713	0.448	632	73.7	624	10.2	625	18.0	435.5	76.6	100.2
1.sSMPABC112***	366.3	63.5	0.173	65.758	0.059	2.484	0.706	2.874	0.087	1.446	0.503	559	54.2	539	7.5	542	12.2	256.2	15.6	100.7
1.sSMPABC114***	1740.9	904.9	0.520	89.061	0.066	2.320	0.869	2.709	0.096	1.399	0.516	793	48.7	591	7.9	635	12.9	247.3	14.7	107.3
1.sSMPABC117***	784.3	180.9	0.231	39.822	0.065	2.422	0.862	2.873	0.096	1.545	0.538	775	51.0	592	8.7	631	13.6	370.2	17.1	106.6
1.sSMPABC120***	2321.4	523.8	0.226	156.830	0.060	2.293	0.781	2.690	0.095	1.407	0.523	597	49.7	583	7.9	586	12.1	301.8	18.1	100.4
1.sSMPABC128***	1763.1	545.7	0.310	56.005	0.064	2.380	0.875	2.842	0.099	1.554	0.547	740	50.3	610	9.0	638	13.6	164	8.7	104.6
1.sSMPABC129***	1812.0	377.2	0.208	563.881	0.059	2.181	0.700	2.624	0.086	1.458	0.556	556	47.6	534	7.5	539	11.0	117.5	5.5	100.7
1.sSMPABC130***	730.4	316.7	0.434	30.206	0.065	2.777	1.004	3.184	0.112	1.557	0.489	773	58.4	685	10.1	706	16.3	140.3	12.5	103.0

Continuation.																				
1.sSMPABC133***	435.2	42.2	0.097	11881.821	0.064	2.769	1.096	3.159	0.124	1.521	0.481	751	58.5	751	10.8	751	16.9	481.9	46.1	99.9
1.sSMPABC134***	1297.0	970.0	0.748	63.506	0.073	2.597	1.028	3.009	0.102	1.519	0.505	1018	52.6	626	9.1	718	15.6	0	12.4	114.7
1.sSMPABC135***	1400.7	351.0	0.251	74.745	0.066	2.455	0.893	2.864	0.099	1.475	0.515	794	51.5	607	8.5	648	13.8	354.4	25.5	106.7
1.sSMPABC137***	644.9	176.9	0.274	232.465	0.065	3.979	0.911	4.671	0.102	2.447	0.524	775	83.7	624	14.6	658	22.9	227.3	18.1	105.3
1.sSMPABC140***	2279.1	1459.5	0.640	95.316	0.065	2.632	0.727	3.034	0.080	1.509	0.497	790	55.2	499	7.2	555	13.0	145.7	14.0	111.1
1.sSMPABC151***	1631.5	1081.1	0.663	46.467	0.072	2.505	1.003	2.955	0.101	1.568	0.531	978	51.0	623	9.3	705	15.1	0	135.0	113.2
1.sSMPABC154***	3581.0	1566.5	0.437	143.345	0.060	2.338	0.654	2.766	0.079	1.479	0.534	608	50.6	490	7.0	511	11.2	288.8	20.0	104.3
1.sSMPABC155***	2093.6	351.9	0.168	215.179	0.061	2.282	0.829	2.715	0.099	1.473	0.542	624	49.2	610	8.6	613	12.6	218.6	12.9	100.4
1.sSMPABC156***	1909.4	532.0	0.279	127.488	0.064	2.628	0.815	3.038	0.092	1.523	0.501	756	55.5	566	8.3	605	13.9	370.9	37.5	106.9
1.sSMPABC157***	1502.9	217.3	0.145	47.983	0.075	2.647	0.939	3.168	0.090	1.741	0.549	1080	53.1	557	9.3	673	15.7	0	78.1	120.6
1.sSMPABC158***	1475.8	296.2	0.201	52.686	0.068	2.959	0.972	3.390	0.104	1.654	0.488	863	61.4	637	10.0	689	17.1	473.6	57.3	108.1
1.sSMPABC159***	1927.5	504.7	0.262	33.861	0.070	3.066	0.937	3.653	0.097	1.987	0.544	924	63.0	599	11.4	671	18.1	161.8	12.3	112.1

Table A10 – Lu-Hf isotopic data from the sample GB-105 of the Mamanguape pluton

SPOTS	$^{176}Lu/^{177}Hf$	±2s	$^{176}Hf/^{177}Hf$	±2s	$^{176}Hf/^{177}Hf_{(t)}$	eHf(t)	T_{DM}
1.sSMPABC108	0.000898	0.000005	0.282348	0.000020	0.282338	-3.0	1.6
1.sSMPABC109	0.000369	0.000002	0.282323	0.000028	0.282319	-3.7	1.7
1.sSMPABC112	0.000763	0.000006	0.282265	0.000022	0.282257	-5.9	1.8
074seq.dat	0.002292	0.000020	0.282096	0.000018	0.282071	-12.4	2.1
1.sSMPABC118	0.002212	0.000015	0.282059	0.000018	0.282035	-13.7	2.2
1.sSMPABC119	0.002555	0.000021	0.282101	0.000020	0.282073	-12.4	2.1
1.sSMPABC132	0.002624	0.000016	0.282117	0.000019	0.282089	-11.8	2.1
1.sSMPABC160	0.001918	0.000012	0.282072	0.000021	0.282051	-13.2	2.2
1.sSMPABC137	0.001891	0.000012	0.282486	0.000025	0.282466	1.5	1.4

Table A11 – Sm-Nd isotopic data from the sample GB-105 of the Mamanguape pluton

AMOSTRA	$^{147}Sm/^{144}Nd$	$^{143}Nd/^{144}Nd$	Age(Ga)	$\varepsilon Nd_{(0)}$	$\varepsilon Nd_{(t)}$
CG-45A	0,1139	0,511742	0,63	-17,48	-10,83
CG-17	0,0969	0,511492	0,63	-22,35	-14,34
CG-30	0,0941	0,511496	0,63	-22,28	-14,04
GB-105	0,1542	0,511911	0,574	-14,18	-11,08

CG-45A e CG-30 (pluton Jurema), CG-17 (pluton Quipapá) e GB-105 (pluton Mamanguape)

Table A12 – Summary of petrological and geochronological data of peraluminous leucogranites from Borborema Province

CENTRAL SUBPROVINCE	PETROGRAPHIC CHARACTERIZATION	LIQUIDUS TEMPERATUTE	METHOD	AGE	Reference
Mamanguape Pluton	Two-mica syenogranites, with enclaves of metasedimentary rocks	713 to 742 °C	U-Pb zircon, LA-ICP-MS	574 ± 2 Ma	This work
			U-Pb zircon, SHRIMP	564 ± 5 Ma	Ferreira et al. (2006)
SOUTHERN SUBPROVINCE					
Quipapá Pluton	Syenogranite, hosting enclaves of metasedimentary rocks and rare mafic enclaves. Flat-lying foliation recorded locally	677 to 794 °C	U-Pb zircon, LA-ICP-MS	641 ± 5 Ma	Brainer et al. (2021)
			U-Pb zircon, SHRIMP	630 ± 5 Ma	Silva Filho et al. (2021)
Cabanas Pluton	Monzogranites with enclaves of high-T mylonites. Crystallization associated to transcurrence.	685 to 801 °C	U-Pb zircon, LA-ICP-MS	573 ± 4 Ma	Neves et al. (2008)
Chã Grande Pluton	Two – mica leucogranites.	706 to 830°C	U-Pb Monazite LA-ICP-MS	566 ± 5 Ma	Neves et al. (2020)
Gravatá Pluton	Biotite granites.	653 to 816 °C	U-Pb zircon, LA-ICP-MS	562 ± 7 Ma	Neves et al. (2020)
Poço Redondo	Two-mica leucogranites with migmatite xenoliths.	609 to 801 °C	U-Pb zircon, SHRIMP	623 ± 7 Ma	Oliveira et al. (2015)
Xingó Dykes	Biotite monzogranites. Flat-lying magmatic foliation. Metasedimentary enclaves. Muscovite is rare.	611 to 702 °C	Whole rock Rb-Sr	609 ± 1 Ma	Guimarães et al. (1992)
Glória Sul Pluton	Leucogranites varying from monzogranites to syenogranites with microgranular mafic enclaves and magmatic foliation.	644 to 744 °C	U-Pb zircon, LA-ICP-MS	627 ± 7 Ma	Conceição et al. (2016)
Angico Pluton	Two-mica leucogranites with mafic enclaves.		Titanite ID-TIMS	584 ± 9 Ma	Bueno et al. (2009)
Jupi orthogneiss.	Syenogranitic composition with paragneiss enclaves. Flat-lying foliation.	–	U-Pb zircon, LA-ICP-MS	606 ± 8 Ma	Neves et al. (2008)
NORTHERN SUBPROVINCE					
Banabuiú Pluton	Monzogranites with angular enclaves of hosting rocks. Subertical foliation on margins.	644 to 803 °C	U-Pb zircon, LA-ICP-MS	578 ± 6 Ma	Lima et al., (2010)
Dona Inês Pluton		650 to 831°C	U-Pb zircon, LA-ICP-MS	582 ± 5 Ma	Guimarães et al., (2017)

ANEXO A – CARTA DE ACEITE 1° ARTIGO

Decision on submission to Journal of South American Earth Sciences
1 mensagem

Journal of South American Earth Sciences <em@editorialmanager.com> 3 de agosto de 2021 15:46
Responder a: Journal of South American Earth Sciences <support@elsevier.com>
Para: CAIO CEZAR GARNIER BRAINER <caiocgbrainer@gmail.com>

Manuscript Number: SAMES-D-21-00195R1

EARLY EDIACARAN TWO-MICA GRANITES MARKING THE CONTRACTIONAL STAGE OF THE BRASILIANO OROGENY IN THE PERNAMBUCO-ALAGOAS DOMAIN, NE BRAZIL

Dear Mr. BRAINER,

Thank you for submitting your manuscript to Journal of South American Earth Sciences.

I am pleased to inform you that your manuscript has been accepted for publication.

My comments, and any reviewer comments, are below.
Your accepted manuscript will now be transferred to our production department. We will create a proof which you will be asked to check, and you will also be asked to complete a number of online forms required for publication. If we need additional information from you during the production process, we will contact you directly.

We appreciate you submitting your manuscript to Journal of South American Earth Sciences and hope you will consider us again for future submissions.

Kind regards,
andres folguera
Editor-in-Chief

Journal of South American Earth Sciences

Editor and Reviewer comments:

ANEXO B – CARTA DE SUBMISSÃO 2° ARTIGO

Brazilian Journal of Geology - Manuscript ID BJGEO-2021-0047

1 mensagem

Tatiana Alonso <onbehalfof@manuscriptcentral.com> 21 de junho de 2021 13:36
Responder a: secretaria@zeppelini.com.br
Para: caiocgbrainer@gmail.com
Cc: caiocgbrainer@gmail.com, ignez@ufpe.br, afsf@ufpe.br, jefferson1901@hotmail.com, cristianodeclana@gmail.com

21-Jun-2021

Dear Mr. Brainer:

Your manuscript entitled "PETROGENESIS OF EDIACARAN LEUCOGRANITES IN THE BORBOREMA PROVINCE, NE BRAZIL: U-Pb ZIRCON GEOCHRONOLOGICAL, GEOCHEMICAL AND Lu-Hf ISOTOPIC DATA CONSTRAINTS" has been received by the Editorial Office of the Brazilian Journal of Geology.

Please note that this message is not a confirmation of submission, which will only be given once your manuscript is considered to be within the scope and of interest to the journal.

Your manuscript ID is BJGEO-2021-0047.

Please mention the above manuscript ID in all future correspondence or when calling the office for questions. If there are any changes in your street address or e-mail address, please log in to ScholarOne Manuscripts at https://mc04.manuscriptcentral.com/bjgeo-scielo and edit your user information as appropriate.

You can also view the status of your manuscript at any time by checking your Author Center after logging in to https://mc04.manuscriptcentral.com/bjgeo-scielo.

Thank you for submitting your manuscript to the Brazilian Journal of Geology.

Sincerely,
Brazilian Journal of Geology Editorial Office